REGULATION OF VASCULAR TONE IN CEREBRAL AND CORONARY ARTERIES BY APELIN/APJ RECEPTOR MECHANISMS

A Dissertation
Submitted to the Graduate Faculty
of the
North Dakota State University
of Agriculture and Applied Science

By

Amreen Mughal

In Partial Fulfillment of the Requirements
for the Degree of
DOCTOR OF PHILOSOPHY

Major Department:
Pharmaceutical Sciences

March 2018

Fargo, North Dakota

North Dakota State University
Graduate School

Title

Regulation of Vascular Tone in Cerebral and Coronary Arteries by Apelin/APJ Receptor Mechanisms

By

Amreen Mughal

The Supervisory Committee certifies that this ***disquisition*** complies with North Dakota State University's regulations and meets the accepted standards for the degree of

DOCTOR OF PHILOSOPHY

SUPERVISORY COMMITTEE:

Dr. Stephen T. O'Rourke
Chair

Dr. Chengwen Sun

Dr. Yagna Jarajapu

Dr. Kimberly Vonnahme

Approved:

03/08/2018
Date

Dr. Jagdish Singh
Department Chair

ABSTRACT

The peptide, apelin, is expressed in fat cells, endothelial cells, and CNS neurons. Increasing evidence (e.g. inotropic and vasomotor effects) supports a role for apelin in the regulation of the cardiovascular system. This research aimed to understand vascular effects of apelin and bridge gaps in the knowledge about apelin-induced effects on different vascular beds i.e. cerebral and coronary arteries. My first objective was to assess apelin-induced vascular effects in cerebral arteries. Based on current data, one could conclude that apelin by itself has no effects on vasomotor tone of cerebral arteries, but it does impair nitric oxide dependent relaxations of cerebral arteries, possibly by inhibiting functions of large conductance calcium activated potassium (BK_{Ca}) channels.

Apelin increases coronary blood flow; however, the involved mechanism(s) has not yet been elucidated. Hence, my next aim was to determine the mechanism(s) involved in apelin-induced vascular effects. The results suggest that apelin causes endothelium APJ receptor dependent relaxation of coronary arteries, which is possibly mediated by nitric oxide dependent direct activation of BK_{Ca} channels. Interestingly, my results also suggest that pathways involved in apelin-induced coronary arteries relaxation are markedly different from another endothelium dependent vasodilator, acetylcholine. This research is the first to report that nitric oxide, generated in response to different stimuli, can likely activate more than one signaling pathways in coronary arteries.

In my final aim, I determined effects of apelin on smooth muscle BK_{Ca} channel functions in coronary arteries. My data suggest that functionally active apelin-APJ signaling has no inhibitory effects on BK_{Ca} channel functions and does not inhibit nitric oxide-induced relaxations of coronary arteries. Possible reasons for difference in apelin response between cerebral and

coronary arteries could be associated with differences in activation of G-proteins and PI3K signaling pathways between these two vascular beds.

Altogether, this research provides an improved understanding about apelin-induced vascular effects in cerebral and coronary arteries, and highlights some key mechanistic differences in apelin-induced vascular effects between these two blood vessels. Moreover, this knowledge may have important therapeutic implications in future design and development of apelin analogs for treatment of cardiovascular diseases.

ACKNOWLEDGEMENTS

I started my PhD program at NDSU, Department of Pharmaceutical Sciences in June 2013 and have been fortunate to surround by eminent scientists. The positive and collaborative environment of the department allowed me to complete my research in timely manner. At the outset, I would like to express my sincere gratitude to Dr. Stephen O'Rourke, my advisor, whose continuous guidance, unwavering motivation and support allowed me to complete this research and dissertation successfully. Dr. O'Rourke helped me to learn and develop critical analytical outlook towards scientific questions. With his guidance, I developed 'out of box' thinking, and ability to analyze and confirm novel findings in science. He also supported my professional development that helped me to receive several accolades.

I am thankful to my thesis advisory committee: Drs. Chengwen Sun, Yagna Jarajapu and Kimberly Vonnahme for their advice and insightful suggestions during my preliminary defense and individual interactions with them. I would also like to thank Dr. Kristian Agmund Haanes, Dr. Pawel Borowicz, Jordan Flaten, Dr. Steven Vetter, Dr. Sathish Venkatachalem, Dr. Swapnil Sonkusare and Dr. Nancy Rusch for their help and suggestions on different aspects of my research.

I would like to express my gratitude to Dr. Jagdish Singh, Chair, Department of Pharmaceutical Sciences for his motivation and providing excellent research facilities in the department. On similar note, I also appreciate all faculty, staff and graduate students from College of Health Professions. I learned many things from them, which I applied during my PhD and would definitely use them in future as well.

My special thanks goes to Dr. Stephanie Watts, Professor at Michigan State University for her excellent mentorship, motivation and positive outlook that helped me to grow at professional and personal levels. I would also like appreciate Dr. Mukta Sane, my previous lab mate and a very

good friend, for all her professional help and enriching my experience with Fargo and NDSU with many wonderful and pleasurable memories. My special thanks also goes to Dr. Sapana Kushwah for her constant motivation, encouragement and emotional support that allowed me to continue my research with a positive attitude. I also want to acknowledge ASPET, PEO and Honor society of Phi Kappa Phi for extending their support by providing fellowships and travel awards to attend several national level conferences.

I would like to express my heartfelt appreciation to super-scientists of my life, my family. Their unconditional love, motivation and unwavering confidence, allowed me to complete my research and dissertation with many accomplishments. At the end, I thank almighty Allah for this opportunity to accomplish my dream, and all the strength and grace that made my journey easier.

DEDICATION

To Almighty Allah and My Lovely Family

TABLE OF CONTENTS

ABSTRACT iii

ACKNOWLEDGEMENTS v

DEDICATION vii

LIST OF FIGURES x

LIST OF ABBREVIATIONS xii

LIST OF APPENDIX FIGURES xiv

CHAPTER 1. INTRODUCTION 1

Apelin and Other Analogs 2

APJ Receptor 3

Vascular Effects of Apelin 5

Role of Apelinergic System in Vasodilation 5

Role of Apelinergic System in Vasoconstriction 7

Research Gaps 8

CHAPTER 2. APELIN IMPAIRS NITRIC OXIDE-INDUCED RELAXATION OF CEREBRAL ARTERIES BY INHIBITING ACTIVATION OF LARGE CONDUCTANCE, CALCIUM-ACTIVATED K CHANNELS 11

Introduction 11

Material and Methods 12

Results 18

APJ Receptor Expression in Cerebral Arteries 18

Vascular Relaxation Studies 19

Electrophysiology Studies 25

Cyclic GMP Measurements 27

Discussion 27

CHAPTER 3. VASCULAR EFFECTS OF APELIN IN CORONARY ARTERIES: COMPARISON WITH ANOTHER NITRIC OXIDE DEPENDENT VASODILATOR, ACETYLCHOLINE 33

Introduction 33

Materials and Methods 34

Results 41

APJ Receptor Expression and Localization 41

Vascular Relaxation Studies 42

Intracellular NO and Cyclic GMP Measurement 47

Electrophysiology Studies 49

Discussion 50

CHAPTER 4. EFFECT OF APELIN ON BK_{Ca} CHANNELS AND NITRIC OXIDE-INDUCED RELAXATION IN CORONARY ARTERIES: COMPARISON WITH CEREBRAL ARTERIES 55

Introduction 55

Materials and Methods 56

Results 62

Electrophysiology Studies 62

Functionality of APJ receptor 65

Vascular Relaxation Studies 66

Expression of Apelin 68

Effect of Apelin on PI3K/Akt Signaling Pathway 69

Discussion 70

CHAPTER 5. SUMMARY AND CONCLUSIONS 74

REFERENCES 78

APPENDIX 98

LIST OF FIGURES

Figure		Page
1.	Schematic representation for synthesis of apelin	3
2.	Expression and localization of APJ receptors.	19
3	Lack of direct effect of apelin on rat isolated cerebral arteries.	20
4.	DEA NONOate-induced relaxation of isolated cerebral arteries is inhibited by apelin and iberiotoxin.	21
5.	The APJ receptor antagonist, F13A, inhibits the effect of apelin on cerebral artery relaxation induced by DEA NONOate.	21
6.	Bradykinin-induced, endothelium-dependent relaxation of isolated cerebral arteries is inhibited by apelin and iberiotoxin.	22
7.	Bradykinin-induced, endothelium-dependent relaxation of isolated cerebral arteries is inhibited by apelin and iberiotoxin.	23
8.	The APJ receptor antagonist, F13A, inhibits the effect of apelin on cerebral artery relaxation induced by bradykinin.	23
9.	Effect of combined treatment with apelin plus iberiotoxin on cerebral artery relaxation to DEA NONOate and bradykinin.	24
10.	Apelin selectively inhibits relaxation of cerebral arteries in response to BK_{Ca} channel activators	24
11.	Apelin inhibits DEA NONOate-induced increase in whole cell BK_{Ca} currents.	25
12.	F13A abolishes apelin-induced inhibitory effects on whole cell BK_{Ca} currents.	26
13.	Apelin inhibits NS1619-induced whole cell BK_{Ca} currents	26
14.	Lack of effect of apelin on DEA NONOate- and bradykinin-induced increases in intracellular cyclic GMP levels.	27
15.	Expression and localization of APJ receptors.	42
16.	Apelin causes endothelium APJ receptor dependent relaxation of isolated coronary arteries	43
17.	Apelin-induced response in dependent on nitric oxide, but not on cGMP or Protein Kinase G.	44

18. NO-cGMP pathways in coronary arteries mediate acetylcholine-induced response. 45

19. Apelin and acetylcholine-induced nitric oxide activates BK_{Ca} channels to relax coronary arteries. 45

20. Apelin-induced relaxation requires activation of smooth muscle K^+ channels. 46

21. Apelin-induced response is not dependent on K_{ATP} channels, SERCA and hydrogen peroxide. 47

22. Apelin increases intracellular NO production, similar to acetylcholine. 48

23. Acetylcholine, but not apelin increases intracellular cGMP production in coronary arteries. 48

24. DEA NONOate-induced increase in whole cell BK_{Ca} currents were not inhibited by ODQ, but by iberiotoxin. 49

25. Sodium nitroprusside-induced increase in whole cell BK_{Ca} currents are not inhibited by ODQ. 50

26. Apelin does not inhibit BK_{Ca} channels currents in coronary arterial smooth muscle cells. 63

27. Apelin has no inhibitory effects on BK_{Ca} channel currents-induced by NS1619. 64

28. Apelin inhibits BK_{Ca} channels currents in cerebral arterial smooth muscle cells. 64

29. Smooth muscle APJ receptor are functionally active. 65

30. Apelin does not inhibit nitric oxide donors-induced relaxations of coronary arteries. 66

31. Apelin does not impair acetylcholine-induced relaxation, but exacerbate 5-HT contractile response. 67

32. Apelin impairs forskolin-induced relaxation of cerebral, but not of coronary arteries. 68

33. Expression and localization of apelin. 69

34. Effect of apelin on PI3-kinase activity in coronary and cerebral arteries. 70

35. Effect of hypoxia on apelin gene expression in primary cultured cells from cerebral arteries. 77

LIST OF ABBREVIATIONS

ACh	acetylcholine
ACE-2	angiotensin converting enzyme-2
APJR	apelin receptor
APS	ammonium persulfate
BSA	bovine serum albumin
BK_{Ca}	large conductance Ca2+-activated potassium channels
Ca^{2+}	calcium
cAMP	cyclic adenosine mono phosphate
cGMP	cyclic guanosine mono phosphate
CHO	Chinese hamster ovary
CNS	central nervous system
CPA	cyclopiazonic acid
DEA	diethylamine
GPCR	G-protein coupled receptor
DMSO	dimethylsulfoxide
EC_{50}	concentration required to produced 50% of maximal response
eNOS	endothelial nitric oxide synthase
F13A	H-Gln-Arg-Pro-Arg-Leu-Ser-His-Lys-Gly-Pro-Met-Pro-Ala-OH
HETE	hydroxyeicosatetraenoic acid
HEPES	4-(2-hydroxyethyl)-1-piperazineethanesulfonic acid
IACUC	institutional Animal Care and Use Committee
IBTx	iberiotoxin

K^+	potassium
K_{ATP}	ATP sensitive potassium channels
MAP	mean arterial pressure
MLC	myosin light chain
NO	nitric oxide
NLA	ω-Nitro-L-Arginine
ODQ	1H-[1,2,4]Oxadiazolo[4,3-a]quinoxalin-1-one
PI3K	phosphoinositide-3-kinase
PKC	protein kinase C
PSS	physiological salt solution
PVDF	polyvinylidene difluoride
SDS-PAGE	sodium dodecyl sulfate-polyacrylamide gel electrophoresis
SERCA	sarcoplasmic/endoplasmic reticulum calcium ATPase
sGC	soluble Guanylyl cyclase
SEM	standard error of mean
SNP	sodium nitroprusside
TEMED	N,N,N′,N′-Tetramethylethylenediamine

LIST OF APPENDIX FIGURES

Figure Page

A1. Representative tracings from normalization protocol 98

A2. Representative tracings for concentration response curves of bradykinin and acetylcholine 98

A3. Representative tracings for concentration response curves of DEA NONOate and sodium nitroprusside. 99

CHAPTER 1. INTRODUCTION

Cardiovascular diseases are leading cause of death with ~17.3 million deaths per year; predicated to reach ~23.6 million by 2030 (1). Cardiovascular diseases are complex multifactorial disorders and underlying pathology varies from inflammation, endothelial dysfunction to blood vessels damage. There is steady decrease in clinical trials for cardiovascular diseases in past two decades and new interventions are only providing small benefits over existing molecules (2). The disease burden is major cause of concern and calls for better therapeutic strategies. Apelin is considered as one of the novel therapeutic target in cardiovascular research due to its protective actions (3).

APJ signaling is modulated in many diseases including cardiovascular, HIV, neurodegenerative and metabolic to name a few. From the time of discovery, enormous information is gathered about APJ signaling and their modulation during cardiovascular diseases. Scientists have identified many novel and characteristic details about APJ signaling that involves diverse intracellular mechanism(s). Apelin and APJ receptor are ubiquitously expressed in mammalian central and peripheral system (4, 5). This expression pattern along with multiple roles in physiology has continuously attracting the scientific community for evaluating potential roles of apelinergic system in cardiovascular diseases (3, 6). Currently, several on-going clinical trials are evaluating vascular effects of apelin in health and disease states. Besides, growing body of knowledge is bringing several new updates about apelinergic system, including new ligands (Apela/ELABELA/Toddler) (7, 8), synthesis analogs (E339-3D6, ML-233) (9, 10) and antagonist (F13A, ML221) (11, 12). Many reports are now showing previously unidentified or novel mechanistic role(s) of apelinergic system (13, 14). From the time of discovery, researchers are focused to identify apelin-induced vascular effects. Until now, many intracellular mediators i.e.

endothelial nitric oxide synthase (eNOS), phosphoinositol-3 kinase (PI3K), protein kinase C (PKC) and many others are shown to be involved in vascular effects of apelin. However, we still lack a comprehensive understanding about regulatory role of apelin on vasomotor tone.

Apelin and Other Analogs

Discovered in 1998, apelin was initially considered as a sole endogenous ligand for APJ receptor (15), until the recent discovery of another peptide, apela/Toddler/Elabela (7, 8). Apelin gene is located on band q25-26.1 of the chromosome X and is highly expressed in lungs, mammary gland, heart and vascular endothelial cells (16-18). Apelin-77 (Pre-pro-apelin) is the precursor of various pharmacological active apelin isoforms (apelin-12, -13, -17 and -36), and shares a 75-95% sequence homology among various species including rat, mice and bovine (19). N-terminal residues of apelin-77 are post-transnationally modified by endopeptidase to form pro-apelin-55, which is further cleaved to apelin-36, -17, -13 and -12 **(Figure 1)**. All these fragments have a conserved C-terminal region, which is essential for APJ receptor binding and functional activity (20). Additionally, post-translationally modification of N-terminal residue of apelin-13 with a cyclized glutamine forms [Pyr]-apelin-13 that evades enzymatic degradation and results into a longer biological effects (21). These different apelin isoforms (apelin-12, -13, -17 and -36) have variable potency, but apelin-13 and [Pyr]-apelin-13 are identified as more predominate and potent isoforms in cardiovascular system (15, 22). Based on the essential role of C-terminal, Lee et al. has designed a functional antagonist; F13A by synthetic replacement of C-terminal phenylalanine residue with alanine, which inhibited apelin induced hypotensive effects (11).

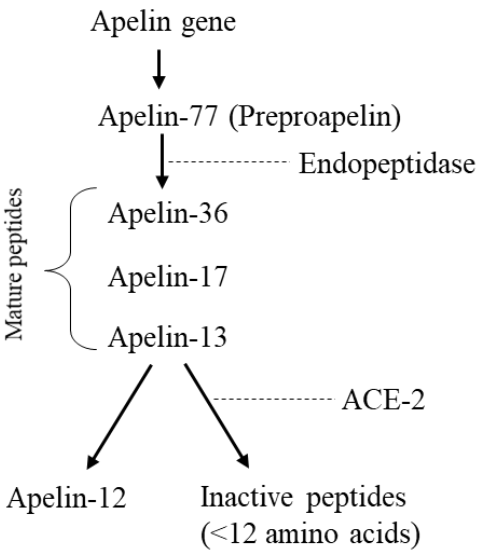

Fig. 1. Schematic representation for synthesis of apelin.

Although apelin has potent vascular effects, but its shorter biological life (19), and lack of complete information about its degradation pathways makes design and development of synthetic apelin analogs a challenging process. A few studies have shown role of angiotensin converting enzyme type-2 (ACE-2), a zinc-containing carboxy monopeptidase is partially responsible for the metabolism of apelin (23-25). Wang et al. showed that [Pyr]-apelin-13 is more susceptible towards ACE-2 degradation than apelin-17, and resulted metabolites i.e. [Pyr]-apelin-12 and apelin-16 respectively have reduced functional activity (23). Another recent report showed that ACE-2 metabolizes [Pyr]-apelin-13 to biologically active [Pyr]-apelin-13 (1-12), suggesting beneficial effect of increased ACE-2 expression during cardiovascular diseases (24). Researchers are continuously trying to develop biologically stable analogs of apelin (26, 27), and information related to metabolism and degradation can further support the development.

APJ Receptor

APJ receptor is a G-protein coupled receptor (GPCR) located in chromosome 11 and composed of an intron-less (*APLNR*) gene, which is conserved in many species including human,

monkey, chimpanzee, mice and rat (20). APJ receptor was first discovered by O'Dowd et al. in 1993 during their search for vasopressin receptor (28). APJ receptor has a 380 amino acid sequence with G-protein characteristic including seven transmembrane domains and post-translation modification sites for phosphorylation, palmitoylation and glycosylation along with association site for β-arrestin (28). Moreover, APJ receptor shares ~34% sequence homology with AT-1 receptor, but does not have binding affinity for angiotensin II (28).

APJ receptors are associate with heterotrimeric G-protein and multiple G-subunits are associated with apelin-induced effects. Initial work suggested involvement of pertussis toxin sensitive $G_{\alpha i/o}$ subunits that inhibits forskolin induced cAMP formation in CHO cells (15). These findings were later strengthened by apelin-induced inhibition of intracellular Ca^{2+} mobilization in CHO cell lines expressing APJ receptor (29). We have also shown that apelin-inhibits BK_{Ca} channel currents in cerebral vascular smooth muscle cells via pertussis toxin sensitive $G_{\alpha i/o}$-subunit (30). However, apelin was also found to increase Ca^{2+} mobilization in neuronal cells (31), indicating involvement of other G-subunits. In subsequent research, apelin induced cardiac and smooth muscle contractile response were attenuated by phospholipase C and protein kinase C inhibitors, adding $G_{\alpha q/11}$ subunit to APJ receptor (32, 33). In addition to these two subunits, functional role of $G_{\alpha 13}$ subunit has been deciphered in apelin-induced cytoplasmic translocation of histone deacetylase during cardiac and vascular development (34).

Central and peripheral expression of APJ receptor makes it an attractive target for cardiovascular regulation (16). Similarly, both membranous and nuclear expression of APJ receptor in hypothalamus and blood vessels indicates involvement of apelinergic system in signal transduction and gene regulation (35). Moreover, central versus peripheral administered apelin is shown to have different effects of hemodynamics and energy metabolism (36, 37). These previous

studies were focused on neurohormonal effects of apelin, but it is essential to understand vascular effects of central and peripheral administered apelin.

Vascular Effects of Apelin

Apelin has complex vasomotor effects as it can cause either vasodilation or vasoconstriction depending on the vascular bed and underlying conditions. These dual actions are attributed to the presence of APJ receptor on endothelial and smooth muscle cell layers of blood vessels. The following sections summarizes the current available information about vasoactive effects of apelin.

Role of Apelinergic System in Vasodilation

Apelin has multiple mechanisms to control vascular tone, possibly involving nitric oxide and prostanoids (22, 38). Interestingly, apelin can reduce both pre- and after-load due to its arterial and venodilation abilities (39). Researchers are continuously reporting role of nitric oxide in vascular effects of apelin (3, 40-43), however majority of these experiments were done using indirect approach i.e. with eNOS inhibitors, which cannot specifically differentiate between NO and other reactive nitrogen species (44, 45). Further, the downstream signaling mechanism(s) activated in response to apelin and nitric oxide signaling have not studied thus far. Intracellular nitric oxide can relax vascular smooth muscle cells by various mechanisms including well established cGMP dependent pathways (46, 47) or by other mechanisms like direct activation of BK_{Ca} channels (48, 49), activation of SERCA pump (50) and by inhibiting effects of vasoconstrictive mediators i.e. 20-HETE (51). Major body of current knowledge focuses on role of nitric oxide in apelin-induced vasodilation and hypotensive effects (18, 40, 41, 43, 52), but further studies are required to determine downstream mediators activated in response to apelin-

induced nitric oxide and this knowledge will possibly provide a paradigm-shift in apelinergic signaling cascade.

Not only the mediators, but apelin-induced hypotensive effects are also under critical scrutiny. Charles et. al observed a biphasic hemodynamic response with bolus apelin treatment in conscious sheep, where transient fall in arterial pressure was followed by a rise in arterial pressure (53). Likewise, in conscious rats, peripheral administration of apelin failed to produce a depressor response, but caused a pressor response (54). These reports suggest that apelin-induced response is mediated by complex intracellular events involving multiple mediator(s), which may not be dissected using isolated preparations and demands for a better correlation using in-vitro and in-vivo studies. Moreover, various apelin isoforms are also shown to have different potency in different experimental models. For example, Tatemato et al. reported that apelin-12 is more potent in reducing mean arterial pressure (MAP) in comparison to apelin-13 and -36 in anesthetized normotensive rats (55). However, apelin-17 is shown to cause higher depressor response as compared to [Pyr]-apelin-13 and apelin-15 in normotensive rats (56). Whereas, Lee et al. suggested that apelin-13 has higher potency in comparison to apelin-12 using spontaneous hypertensive rats (11). These differences can also be attributed to differences in apelin response between central and peripheral systems (54, 57).

Cardiovascular regulatory regions of brain controls the peripheral vascular resistance and tone, and apelinergic system is highly expressed in cardiovascular regulatory regions i.e. hypothalamus and brain stem (58). Moreover, apelin induced central response is suggested to be different from peripheral vasodilation (59, 60). Our previous report also suggests that apelin inhibits BK_{Ca} channels currents in cerebral arterial smooth muscle cells (30). Potassium channels including BK_{Ca} channels are highly expressed on cerebral arteries and are responsible for

maintaining membrane potential (61). Functional inhibition of BK_{Ca} channels can alter vascular tone; resulting into vasospasm and ischemia (62). These findings raised questions about differences in vasoactive response mediated by apelin in cerebral and peripheral system.

Role of Apelinergic System in Vasoconstriction

Vasoconstriction is known to be regulated by calcium release (63), myosin like chain (MLC) phosphorylation (64) and ion channels (65). Hashimoto et al. showed that apelin causes vasoconstriction in mice thoracic aorta by increasing phosphorylation of MLC via $G_{\alpha i/o}$ dependent activation of PKC and Na^{+}-Ca^{2+} exchanger dependent pathways (33). Moreover, apelin is shown to permeate through dysfunctional endothelial cells (66), to cause vasoconstriction by phosphorylation of MLC (67). Likewise, Maguire et al. also reported [Pyr]-Apelin-13 induced vasocontractile response in human endothelial denuded saphenous vein and mammary arteries (22). Interestingly, most of smooth muscle dependent effects of apelin are derived either from endothelial denuded or dysfunctional blood vessels or from in-vitro cell culture studies. Nevertheless, we need answers for biphasic hemodynamic changes observed during in-vivo conditions (53), which requires an advanced technical approach to characterize these changes at the level of endothelial as well as smooth muscle cell individually.

Regulation of apelin-APJ receptor during endothelial dysfunction and cardiovascular disease remains controversial. On one hand, increased apelin/APJ receptor expression and bioavailability produced beneficial vascular effects in the conditions with endothelial dysfunction like end-stage heart failure (68), atherosclerosis (69) and obesity (41), while others have also shown apelinergic signaling can be a mediator for atherosclerosis (70), indeed up-regulated apelin gene is localized in atherosclerosis plaques (18) and stenotic aortic valve (71). It is important to

know that whether this increased expression of apelin has a role in progression of disease or is involved in compensatory feedback mechanism (69).

Higher expression of both apelin and APJ receptor on cardiovascular regulatory regions of brain (58), suggest involvement of apelin signaling in hemodynamic regulation. Previous studies showed site specific delivery of apelin to brain stem regions i.e. nucleus tractus solitarius (NTS) and rostral ventrolateral medulla (RVLM) caused a sustained increase in arterial pressure (57), possibly by mitogen activated protein kinase dependent pathway (72). Similarly, our previous reports suggested apelin microinjection into RVLM elevates blood pressure and sympathetic nerve activity, via NAPDH oxidase derived superoxide(s) (59, 60). Moreover, we showed that upregulation of apelin gene in normotensive rats can cause chronic increase in blood pressure, similar to hypertensive rats (59). Similarly, intracerebroventricular injection of [Pyr]-apelin-13 increased mean arterial pressure and heart rate by increasing c-fos expression in paraventricular nucleus (PVN) region of hypothalamus (54). Most of these studies were focused on estimating neurohormonal mechanism(s) involved in regulation of peripheral resistance and vascular tone, but involvement of apelin in cerebral vascular tone and blood flow still needs evaluation.

Research Gaps

Apelin is an endogenous peptide, which activates APJ receptor. Apelin is involved in cardiovascular homeostasis due to its vasodilation and positive inotropic actions (73). However, apelin-induced vasoactive effects are determined in very limited blood vessels, which do not include cerebral and coronary arteries. Apelin is synthesized in vascular endothelial cells and adipose tissues (4), and found to mediate autocrine and paracrine effects on vasculature (74). It has been reported that apelin induces hypotensive effects (19) by activating APJ receptor (75) and through nitric oxide dependent pathways (43, 55). Moreover, apelin causes vasoconstriction in

endothelium denuded/dysfunctional blood vessels (66, 67). Previous data suggested that apelin inhibits BK_{Ca} channel currents in cerebral arteries smooth muscle cells (30). Nonetheless, whether this inhibition of BK_{Ca} channels has negative impact on nitric oxide dependent relaxation and in turn on vasomotor tone has yet to be determined. It is also important to note that apelin is shown to increase forearm blood flow (52, 76) and can cause vasodilation in peripheral arteries (22). However, mediators and pathways involved in apelin-induced relaxation of coronary arteries have not been studied thus far. Apelin and its analogs are currently under clinical trials, evaluating their therapeutic benefits in pulmonary hypertension and myocardial infraction (https://clinicaltrials.gov/). Considering its enormous therapeutic potential, it is timely to evaluate apelin-induced vasoactive response in cerebral and coronary arteries.

The central hypothesis of this research is that activation of apelin-APJ axis inhibits nitric oxide-induced relaxations in cerebral arteries by inhibiting BK_{Ca} channel functions. Further, apelin relaxes coronary arteries by nitric oxide dependent activation of smooth muscle BK_{Ca} channels. The proposed research will significantly reduce critical gaps in the knowledge about apelin-induced effects on cerebral and coronary arteries.

I set the following specific aims to test my central underlying hypothesis and accomplish the overall objective of this research.

Specific Aim 1: Determine vascular effects of apelin on nitric oxide dependent relaxation of cerebral arteries. Previous data demonstrated that apelin inhibits BK_{Ca} channel currents in cerebral arteries (30). BK_{Ca} channels are key mediators for maintaining membrane potential and are involved in endothelium nitric oxide dependent relaxation. Hence, the aim is to evaluate effects of apelin on nitric oxide-induced relaxation of cerebral arteries.

Specific Aim 2: Determine vascular effects of apelin in coronary arteries. Previous studies demonstrated that apelin increases coronary blood flow and has beneficial effects during heart failure (42, 52). In a few peripheral arteries, apelin is shown to induce nitric oxide dependent vasodilation (22). However, effects of apelin on coronary arterial vasoactive tone has not been evaluated thus far. Therefore, the present aim is to evaluate effects of apelin on coronary arterial vasomotor tone and understand involved downstream signaling mechanisms.

Specific Aim 3: Determine effects of apelin on BK_{Ca} channel functions in coronary arteries and compare the similarities/differences in signaling mechanisms with cerebral arteries. Apelin is shown to cause vasoconstriction in endothelium denuded or dysfunctional blood vessels (33, 67). Vasoconstriction can be regulated by protein or ion channels. Thus, the present aim is to determine effects of apelin on BK_{Ca} channel currents and functions in coronary arteries. Further, I aim to compare possible signaling events activated in response to apelin in coronary arterial smooth muscle cells, with cerebral arteries.

This research has a marked impact on current and on-going clinical trials, and drug development process. This research provides a comprehensive understanding about vasoactive role(s) of apelin in cerebral (central) and coronary (peripheral) arteries, which will help in devising apelin-based therapies with higher beneficial effects and lesser-associated risks. It is essential to understand the risks associated with conditions with higher plasma apelin levels like diabetes and obesity, before bringing apelin from bench-to-bedside. Apelin has multifaceted roles in diabetes, cancer, and neurodegenerative disorders; therefore, this research will have broader implications, by enhancing our understanding about the apelinergic system in health and disease.

CHAPTER 2. APELIN IMPAIRS NITRIC OXIDE-INDUCED RELAXATION OF CEREBRAL ARTERIES BY INHIBITING ACTIVATION OF LARGE CONDUCTANCE, CALCIUM-ACTIVATED K CHANNELS

Introduction

Apelin is an endogenous peptide that is emerging as an important signaling molecule in several organ systems, including the cardiovascular system (77). Apelin binds to a single G-protein-coupled receptor, termed APJ, which is widely expressed in peripheral organs and tissues as well as the central nervous system (28, 78). With respect to the cardiovascular system, APJ receptors are found in heart (5, 79), blood vessels (5, 18), and cardiovascular regulatory centers in the brain (58, 78, 80).

A growing body of evidence supports a role for the apelin/APJ receptor signaling system in the regulation of blood vessel diameter. Studies indicate that apelin is a powerful vasodilator with an efficacy that exceeds that of hydralazine or nitrates (39, 42). This action, along with its inotropic effects on the heart, has led to the proposition that modulating the apelin/APJ system may offer a novel and rational therapeutic strategy for treating certain cardiovascular disorders, including myocardial ischemia, pulmonary arterial hypertension, and heart failure (42, 81).

A confounding factor, however, is that the effect of APJ receptor activation on vascular tone is dependent on the particular vascular bed being studied. While APJ receptor stimulation leads to endothelium- and NO-dependent vasodilation in several blood vessels (22, 38), it can also result in vascular smooth muscle contraction in others (22, 67). These divergent vasomotor effects of apelin are consistent with the widely recognized heterogeneity that exists among blood vessels from different origins in terms of their reactivity to vasoactive agents (82). Therefore, whereas

systemic administration of apelin may have an overall beneficial hypotensive effect, it could also result in dangerous vasoconstriction in specific vascular beds.

Our knowledge of the vasomotor actions of apelin in specific blood vessels is rather limited at the present time. One important vascular bed that has not been rigorously investigated with respect to the apelin/APJ system is the cerebral vasculature; however, a potential vasoconstrictor role for apelin in the regulation of cerebral arterial tone is suggested by our recent finding that apelin inhibits large conductance, calcium-activated K (BK_{Ca}) channel currents evoked by voltage-dependent increases in membrane potential in cerebral artery smooth muscle cells (30). Thus, in cerebral arteries the net effect of apelin on blood vessel diameter could be the result of the ability of APJ receptor activation on the endothelium to evoke NO-dependent relaxations on one hand versus the effect of APJ receptor activation on the smooth muscle to inhibit relaxation via interference with NO-induced increases in BK_{Ca} currents. In the present study, I assessed the question of the net effect of apelin in cerebral arteries, as well as the hypothesis that the actions of apelin in cerebral arteries are indeed secondary to stimulation of APJ receptors.

Material and Methods

Animals and Tissue Preparation: Experiments were performed on tissues isolated from 12-week-old male Sprague-Dawley rats (Envigo RMS, Indianapolis, IN). Rats were housed at 22 ± 2°C on a 12 h-12 h light-dark cycle and provided with food and water ad libitum. All animal protocols were approved by the North Dakota State University Institutional Animal Care and Use Committee. Brains were isolated from animals anesthetized with isoflurane and placed into ice-cold physiological salt solution (PSS) with the following composition (in mM): NaCl 119mM, $NaHCO_3$ 15mM, KCl 4.6mM, $MgCl_2$ 1.2mM, NaH_2PO_4 1.2mM, $CaCl_2$ 1.5mM and glucose 5.5mM. Middle cerebral arteries were dissected and cleaned of surrounding tissue.

Western Immunoblotting: After collection, cerebral arteries were immediately frozen in liquid nitrogen. Tissues were homogenized in lysis buffer and supplemented with a protease and phosphatase inhibitor cocktail (Santa Cruz Biotechnology Inc., Santa Cruz, CA) at 4°C using an IKA Ultra-Turrax T8 homogenizer (IKA Works Inc., Wilmington, NC). Tissue homogenates were kept on ice for 10 min and then centrifuged at 10000g for 10 min. Supernatant was collected and protein determination was performed using a Pierce BCA protein estimation kit (ThermoFisher Scientific, Waltham, MA). Aliquots of supernatant containing equal amounts of protein (40 μg) were separated on 7.5-10% polyacrylamide gel by SDS-polyacrylamide gel electrophoresis, and proteins were electroblotted onto a polyvinylidene difluoride membrane (Bio-Rad Laboratories, Hercules, CA). Blots were blocked with 5% nonfat dry milk in Tris-buffered saline (TBS, pH 7.4) and incubated overnight at 4°C with a primary antibody specific for APJ receptors using a dilution of (1:200) (Santa Cruz Biotechnology Inc.). Membranes were washed three times for 10 min using TBS-Tween 20 and incubated with a horseradish peroxidase-linked secondary antibody (Santa Cruz Biotechnology Inc.). To ensure equal loading, the blots were analyzed for β-actin expression using an anti-actin antibody (Santa Cruz Biotechnology Inc.). Immuno-detection was performed using an enhanced chemiluminescence light detection kit (ThermoFisher Scientific).

RT- qPCR: Freshly isolated arteries were immediately frozen in liquid nitrogen and total RNA was isolated using an RNeasy Mini kit according to the manufacturer's protocol (Qiagen, Germantown, MD). The concentration and purity of RNA was determined using a spectrophotometer (Nanodrop Technologies, Wilmington, DE). cDNA was synthesized using 50 ng of RNA and an iScript cDNA synthesis kit (Bio-Rad). A Sybr Green expression assay was used to determine expression of APJ receptors, with β-actin used as a housekeeping gene (Bio-Rad). The following primers (synthesized by Invitrogen, Carlsbad, CA) were used:

APJ receptor – forward: 5'-ACAAGACATGTGCCATTGGA-3'; reverse: 5'-TCTCCCAGAAGCCTCCTACA-3'; β-actin – forward: 5'-GTCGTACCACTGGCATTGTG-3'; reverse: 5'-TCTCAGCTGTGGTGGTGAAG-3'. Real-time RT-PCR reaction conditions were 95°C for 10 min, followed by 40 cycles of 95°C for 10 s, 60°C for 20 s, and 72°C for 30 s.

Immunofluorescence Microscopy: Freshly isolated cerebral arteries were fixed in 10% formalin solution, processed and embedded in paraffin blocks. Paraffin blocks were sectioned at 5 μm and mounted onto ProbeOn Plus microscopic slides (ThermoFisher Scientific). Sections were fixed by heating at 60°C for 30 min. Nonspecific antibody binding was blocked with normal serum [10% w/v; in TBS] for 1 h at room temperature. Sections were incubated overnight at 4°C in 1% serum containing a primary antibody against APJ receptors (Abcam, Cambridge, MA) and/or smooth muscle actin (Santa Cruz Biotechnology) or isotype control (Abcam). For co-localization of APJ receptor with smooth muscle actin, double immunofluorescent staining was performed by incubating the tissue sections with more than one primary antibody at the same time. Detection of the primary antibodies against the APJ receptor and smooth muscle actin was accomplished using Texas red-conjugated (goat anti-rabbit IgG; Invitrogen, Carlsbad, CA) and Alexa Fluor-488 (goat anti-mouse IgG; Santa Cruz Biotechnology) secondary antibodies, respectively. Rat lung tissue was used as positive control for APJ receptor detection (58). All negative controls were incubated overnight at 4°C with either 1% serum and/or an isotype control antibody for APJ receptors, followed by secondary antibodies. All dilutions and thorough washes between stages were performed using TBS containing Triton X-100 [0.3% (v/v)] unless otherwise stated. Sections were drained by blotting with filter paper, and a drop of mounting medium containing an anti-fade reagent (Vector Laboratories, Burlingame, CA) was added to the slides. Images of the sections

were obtained using an Olympus confocal laser-scanning microscope (Olympus, Tokyo, Japan). The images were generated using Olympus FluoView FV300 (v. 4.3) confocal software.

Vascular Function Studies: Arterial rings (80-100 μm; 1.2 mm in length) were suspended in wire myographs (DMT, Aarhus, Denmark) for isometric tension recording. The myograph chambers were filled with PSS (5 ml), which was continuously aerated with 95% O_2/5% CO_2 and maintained at 37°C throughout the experiment. The vessel rings were stretched to an initial tension of 1.2 mN and allowed to stabilize for 7 minutes, followed by another stretch to 2.4 mN with stabilization for 7 minutes. At end of stretching, vessels were allowed to equilibrate for 30-40 min with intermittent washings. Vessel reactivity was confirmed by evoking a response to KCl (60 mM) (83). In some vessels, the endothelium was removed by gently rubbing the intimal surface with a human hair. The presence or absence of endothelium was confirmed by measuring relaxation in response to the endothelium-dependent vasodilator, bradykinin (10^{-7} M). Responses to the vasodilators used in this study were obtained in arterial rings contracted with 5-HT (10^{-7} M). Inhibitors were added to the myograph chamber 20 min prior to contraction with 5-HT, with the exception of apelin (10^{-7} M), which was added 5 min after the contraction had stabilized in order to minimize desensitization of APJ receptors. This concentration of apelin was selected because in previous studies it produced the greatest inhibitory effect on BK_{Ca} channel currents in rat cerebral smooth muscle cells (30). After addition to the myograph chamber, the inhibitors remained in contact with the tissues for the remainder of the experiment. Experiments with inhibitors were conducted in parallel with untreated control rings taken from the same animal.

Cerebral Artery Smooth Muscle Cell Isolation: Enzymatic isolation of single vascular smooth muscle cells was carried out as described previously, with brief modification (84). Arteries were placed in cell isolation solution of the following composition (in mM): 60 NaCl, 80 Na-

glutamate, 5 KCl, 2 $MgCl_2$, 10 glucose, and 10 HEPES (pH 7.2). Arterial segments were initially incubated in 1.2 mg/ml papain (Worthington) and 2.0 mg/ml dithioerythritol (Sigma Aldrich) for 17 min at 37°C and then in 0.8 mg/ml type II collagenase (Worthington) for 12 min at 37°C. The digested segments were washed three times in ice-cold cell isolation solution and incubated on ice for 30 min. After this incubation period, vessels were triturated to liberate smooth muscle cells and stored in ice-cold cell isolation solution for use. Smooth muscle cells were studied within 6 h following isolation.

Electrophysiological Recording: Isolated smooth muscle cells were placed into a recording chamber (Warner Instruments, Hamden, CT) and allowed to adhere for 20 min at room temperature. Whole cell currents were recorded using an AxoPatch 200B amplifier equipped with an Axon CV 203BU headstage (Molecular Devices). Current data were collected and analyzed with pCLAMP 10.0 software (Molecular Devices, Sunnywale, CA). The patch electrodes (3-4 MΩ) were fabricated from 1.5-mm borosilicate glass capillaries. Smooth muscle cells were superfused at a rate of 2.0 ml/min with a solution containing (in mM) 145 NaCl, 5.4 KCl, 1.8 $CaCl_2$, 1 $MgCl_2$, 5 HEPES, 10 glucose; pH 7.4 (NaOH). Patch pipettes were filled with internal pipette solution containing (in mM) 145 KCl, 5 NaCl, 0.37 $CaCl_2$, 2 $MgCl_2$, 10 HEPES, 1 EGTA, 7.5 Glucose; pH 7.2 (KOH). All drugs were diluted in fresh bath solution and perfused into the experimental chamber. Voltage-activated currents were filtered at 2 kHz and digitized at 10 kHz, and capacitative and leakage currents were subtracted digitally. Series resistance and total cell capacitance were calculated from uncompensated capacitive transients in response to 10 ms hyperpolarizing step pulses (5 mV), or obtained by adjusting series resistance and whole-cell capacitance using the Axopatch 200B amplifier control system. Standard recording conditions for

BK_{Ca} currents were achieved by stepping in 10 mV increments from a holding potential of -60 to +80 mV. BK_{Ca} currents were expressed as current density (current divided by its capacitance).

Cyclic GMP Estimation: A competitive ELISA method was used to measure cyclic GMP levels in cerebral arteries. Arterial segments were equilibrated in PSS for at least 20 min at 37°C. After the equilibration period, arterial segments were treated with bradykinin (10^{-7} M, 5 min) or DEA NONOate (DEA; 10^{-6} M, 5 min). In some experiments, arterial segments were pretreated with apelin (10^{-7} M) for 5 min, before being exposed to bradykinin or DEA NONOate. After drug treatments, segments were immediately frozen in liquid nitrogen and homogenized with an IKA Ultra, Turrax-T8 homogenizer (IKA Works) at 4°C in 0.1 M hydrochloric acid. Tissue homogenates were centrifuged for 10 min at ≥600 g. Cyclic GMP and total protein content were determined in the supernatant as described in the direct cyclic GMP enzyme immunoassay kit (Assay Design, Ann Arbor, MI) and Pierce BCA protein assay kit (ThermoFisher Scientific), respectively. Cyclic GMP levels were expressed as picomoles per microgram of protein.

Drugs: The following drugs were used: bradykinin, diethylamine NONOate (DEA NONOate), diltiazem, 5-hydroxytryptamine (5-HT), indomethacin, levcromakalim, NS1619, and nitro-l-arginine (NLA) (Sigma Chemical, St. Louis, MO); BMS 191011, iberiotoxin, and 1H-[1,2,4] oxadiazolo[4,3-a]quinoxalin-1-one (ODQ) (Tocris, Ellisville, MO); apelin-13, and F13A (H-Gln-Arg-Pro-Arg-Leu-Ser-His-Lys-Gly-Pro-Met-Pro-Ala-OH trifluoroacetate salt) (Bachem, Torrance, CA). Drug solutions were prepared fresh daily, kept on ice, and protected from light until used. All drugs were dissolved in double-distilled water with the exception of ODQ, BMS 191011, and NS1619, which were dissolved initially in DMSO, and indomethacin, which was dissolved initially in 1 mM sodium carbonate, prior to further dilution in double-

distilled water. Drugs were added to the myograph chambers in volumes not greater than 0.02 ml. Drug concentrations are reported as final molar concentrations in the myograph chamber.

Data Analysis: Relaxation responses are expressed as a percent of the initial tension induced by 5-HT (10^{-7} M). EC_{50} values (drug concentration that produced 50% of its own maximal response) were determined, converted to their negative logarithm, and expressed as -log molar EC_{50} (pD_2). RT-qPCR data were analyzed to quantify relative gene expression by ΔCt relative to β-actin. Results are expressed as means ± SEM, and n refers to the number of animals from which blood vessels were taken, unless otherwise stated. Values were compared by Student's t-test or one-way ANOVA using Tukey's test as post-hoc analysis for paired or unpaired observations, as appropriate, to determine significance between groups. Values were considered significantly different when $p<0.05$.

Results

APJ Receptor Expression in Cerebral Arteries

RT-qPCR and immunoblot analyses were used to evaluate APJ receptor mRNA and protein expression, respectively. **Figure 2** shows that APJ receptor protein **(Figure 2A)** and mRNA transcripts **(Figure 2B)** are expressed in cerebral arteries; similar results were demonstrated for rat lung, which was used as a positive control for APJ receptor expression (58). In immunofluorescence studies using confocal microscopy, APJ receptor protein was detected in cerebral arteries and localized to the smooth muscle cell layer, as well as endothelium **(Figure 2C.1-C.3)**. An isotype negative control antibody demonstrated a lack of non-specific binding of secondary antibody in the absence of primary APJ receptor antibody **(Figure 2C.5)**. Rat lung tissue (positive control) demonstrated staining for APJ receptors on bronchial epithelium **(Figure 2C.6)**.

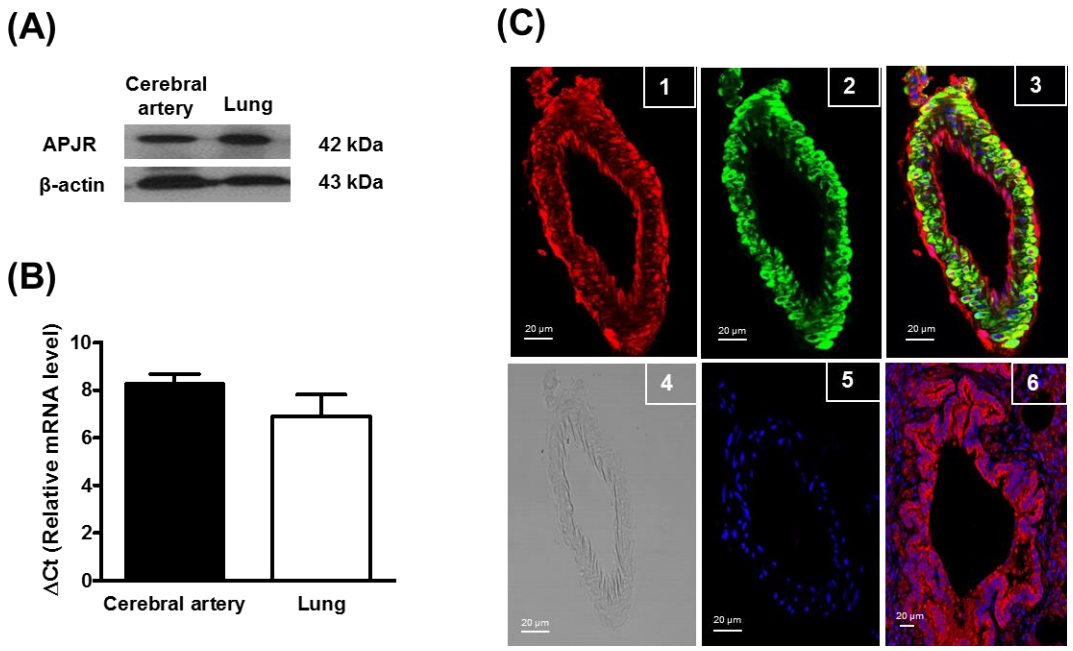

Fig. 2. Expression and localization of APJ receptors.
(A) Representative immunoblot showing expression of APJ receptor (APJR) protein in homogenates from rat cerebral arteries (Lane 1) and lung tissue (Lane 2); β-actin was used as a loading control. The immunoblots shown are representative of data obtained from five different animals. (B) Bar graph showing relative mRNA expression of APJ receptor, represented as ΔCt values relative to β-actin. Data are presented as mean ± SEM (n=3). (C) Representative immunofluorescence images of: (1) APJ receptors (red fluorescence), (2) smooth muscle cell actin (green fluorescence), (3) merged image showing co-localized areas in smooth muscle cells (yellow fluorescence) and endothelium (red fluorescence) in rat cerebral artery; (4) differential interference contrast image of rat cerebral artery; (5) isotype negative control for APJ receptor antibody with nuclear staining (blue fluorescence); and (6) APJ receptors (red fluorescence) with nuclear staining (blue fluorescence) in rat bronchial epithelium (positive control). The images are representative of those obtained from three different animals. Scale bar, 20 μm.

Vascular Relaxation Studies

In cerebral arteries contracted with 5-HT (10^{-7} M), addition of increasing concentrations of apelin (10^{-8} - 3 x 10^{-6} M) to the preparations had no effect on vasomotor tone in rings with or without endothelium **(Figure 3)**. Likewise, these concentrations of apelin had no effect on resting tone in quiescent cerebral arterial rings (data not shown).

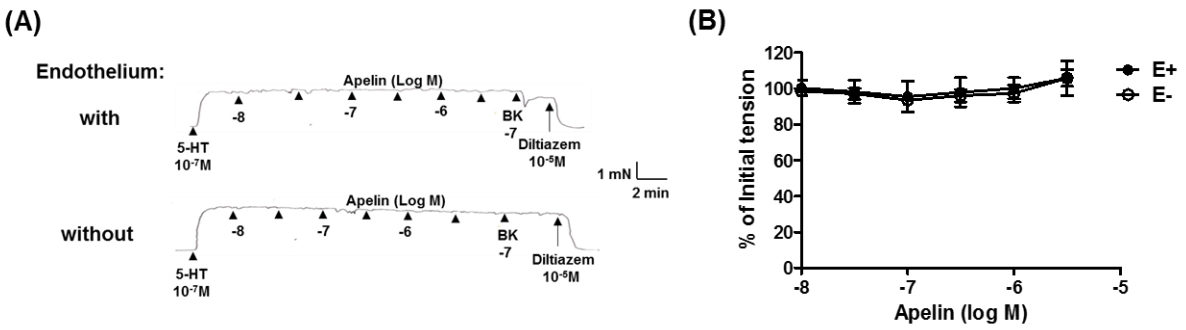

Fig. 3. Lack of direct effect of apelin on rat isolated cerebral arteries.
(A) Representative original tracings of isometric tension recordings from rat isolated cerebral arteries (with and without endothelium) in response to cumulative addition of increasing concentrations of apelin, followed by bradykinin (BK; 10^{-7} M) and diltiazem (10^{-5} M). (B) Mean data demonstrating a lack of vasomotor effect of apelin on cerebral arteries with (E+) and without (E-) endothelium. Data are expressed as a percentage of the initial increase in tension induced by 5-HT (10^{-7} M). Each point represents the mean ± S.E.M. (n=5).

The NO-donor, DEA NONOate (10^{-9} - 10^{-5} M), caused concentration-dependent relaxation of endothelium-denuded cerebral arteries contracted with 5-HT (10^{-7} M) **(Figure 4)**. The concentration-response curve to DEA NONOate was inhibited in the presence of apelin (10^{-7} M) **(Figure 4A)**; the pD_2 values for the responses to DEA NONOate shown in Figure 3A were 6.92 ± 0.20 vs. 6.13 ± 0.08, in the absence and presence of apelin, respectively ($p<0.05$). The BK_{Ca} channel blocker, iberiotoxin (10^{-7} M), had an inhibitory effect on the response to DEA NONOate that was similar to that observed with apelin **(Figure 4B)**. The corresponding pD_2 values for DEA NONOate were 6.98 ± 0.21 vs. 6.14 ± 0.13, without and with iberiotoxin, respectively ($p<0.05$). Treatment with a combination of apelin (10^{-7} M) plus iberiotoxin (10^{-7} M) had no greater inhibitory effect on DEA NONOate-induced relaxation of isolated cerebral arteries (pD_2 = 6.19 ± 0.07; n=6) than apelin or iberiotoxin alone **(Figure 9A)**.

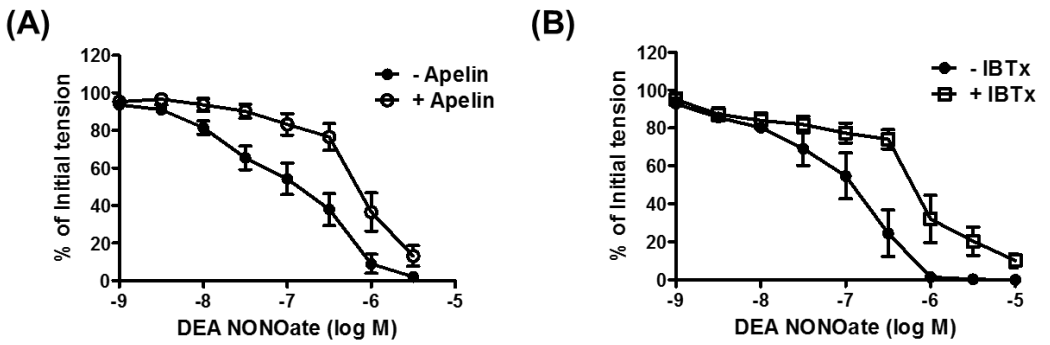

Fig. 4. DEA NONOate-induced relaxation of isolated cerebral arteries is inhibited by apelin and iberiotoxin.
Log concentration-response curves for DEA NONOate in producing relaxation of endothelium-denuded cerebral arteries, in the absence and presence of: (A) apelin (10^{-7} M); $pD_2 = 6.92 \pm 0.20$ vs. 6.13 ± 0.08, in the absence and presence of apelin, respectively ($p<0.05$); and (B) iberiotoxin (IBTx; 10^{-7} M); $pD_2 = 6.98 \pm 0.21$ vs. 6.14 ± 0.13, without and with IBTx, respectively ($p<0.05$). Data are expressed as a percentage of the initial increase in tension induced by 5-HT (10^{-7} M). Each point represents the mean ± S.E.M. (n=5-10).

The APJ receptor antagonist, F13A (10^{-7} M), which had no effect of its own on the response to DEA NONOate, abolished the inhibitory effect of apelin on DEA NONOate-induced relaxation **(Figure 5)**.

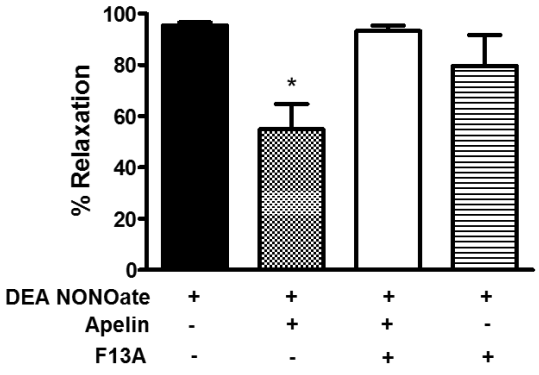

Fig. 5. The APJ receptor antagonist, F13A, inhibits the effect of apelin on cerebral artery relaxation induced by DEA NONOate.
Bar graph representing the effect of apelin (10^{-7} M) and F13A (10^{-7} M), alone or in combination, on DEA NONOate (10^{-6} M)-induced relaxation of cerebral arteries. Experiments with inhibitors were conducted in parallel with untreated control rings taken from the same animal. Each point represents the mean ± S.E.M. (n=6), * $p<0.05$ vs. DEA NONOate alone.

Experiments were then performed in order to determine the effect of apelin on cerebral arterial relaxations evoked by endogenous NO. The endothelium-dependent vasodilator, bradykinin, was used in these experiments since bradykinin-induced relaxation of rat cerebral arteries is mediated by endothelium-derived NO **(Figure 6)** (85, 86).

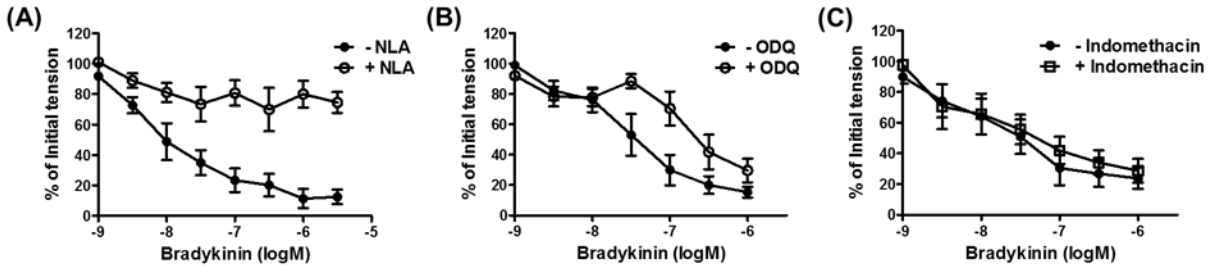

Fig. 6. Bradykinin-induced, endothelium-dependent relaxation of isolated cerebral arteries is inhibited by apelin and iberiotoxin.
Log concentration-response curves for bradykinin in producing relaxation of endothelium-intact cerebral arteries, in the absence and presence of: (A) nitro-l-arginine (NLA; 3 x 10^{-5} M); (B) ODQ (10^{-5} M); and (D) indomethacin (10^{-5} M). Data are expressed as a percentage of the initial increase in tension induced by 5-HT (10^{-7} M). Each point represents the mean ± S.E.M. (n=6).

The results of these experiments are shown in **Figure 7**, which demonstrates that bradykinin-induced relaxation of endothelium-intact cerebral arteries was inhibited in the presence of apelin (10^{-7} M), as evidenced by a significant difference in pD_2 values for bradykinin (7.76 ± 0.20 vs. 7.03 ± 0.12, in the absence and presence of apelin, respectively; $p<0.05$) and a reduction in the maximal relaxation response **(Figure 7A)**. Iberiotoxin (10^{-7} M) had an inhibitory effect on the bradykinin concentration-response curve that was similar to that observed with apelin; the pD_2 values for bradykinin were 8.02 ± 0.21 vs. 7.19 ± 0.22 in the absence and presence of iberiotoxin, respectively ($p<0.05$). The effect of combined treatment with apelin (10^{-7} M) plus iberiotoxin (10^{-7} M) on bradykinin-induced relaxation of isolated cerebral arteries was similar to that observed with either inhibitor alone (pD_2 = 7.15 ± 0.17; n=6) **(Figure 9B)**.

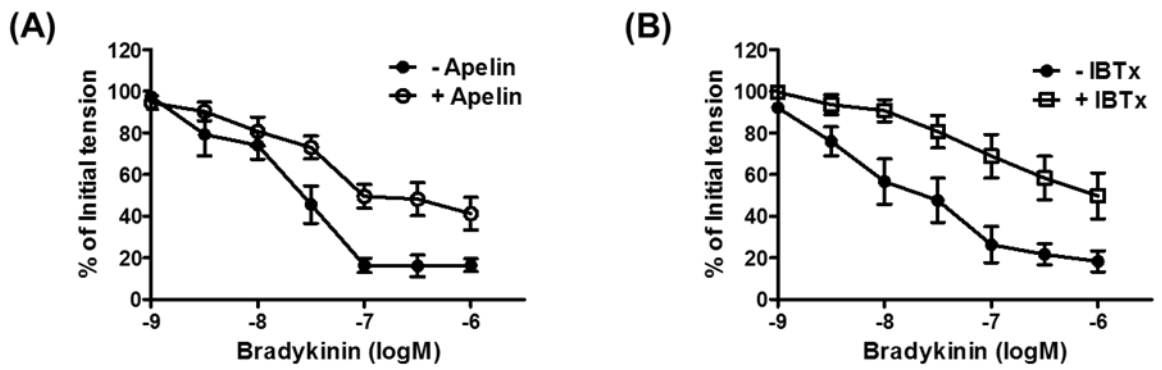

Fig. 7. Bradykinin-induced, endothelium-dependent relaxation of isolated cerebral arteries is inhibited by apelin and iberiotoxin.
Log concentration-response curves for bradykinin in producing relaxation of endothelium-intact cerebral arteries, in the absence and presence of: (A) apelin (10^{-7} M); $pD_2 = 7.76 \pm 0.20$ vs. 7.03 ± 0.12, in the absence and presence of apelin, respectively ($p<0.05$); and (B) iberiotoxin (IBTx; 10^{-7} M); $pD_2 = 8.02 \pm 0.21$ vs. 7.19 ± 0.22, in the absence and presence of IBTx, respectively ($p<0.05$). Data are expressed as a percentage of the initial increase in tension induced by 5-HT (10^{-7} M). Each point represents the mean ± S.E.M. (n=6-7).

As observed in the experiments with DEA NONOate, F13A (10^{-7} M) had no effect on the response to bradykinin, but abolished the inhibitory effect of apelin on bradykinin-induced relaxation **(Figure 8)**.

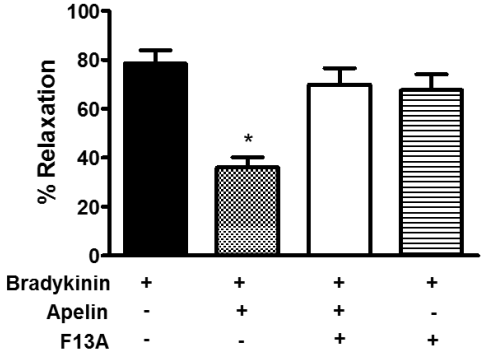

Fig. 8. The APJ receptor antagonist, F13A, inhibits the effect of apelin on cerebral artery relaxation induced by bradykinin.
Bar graph representing the effect of apelin (10^{-7} M) and F13A (10^{-7} M), alone or in combination, on bradykinin (10^{-6} M)-induced relaxation of cerebral arteries. Experiments with inhibitors were conducted in parallel with untreated control rings taken from the same animal. Each point represents the mean ± S.E.M. (n=6-12), * $p<0.05$ vs. Bradykinin alone.

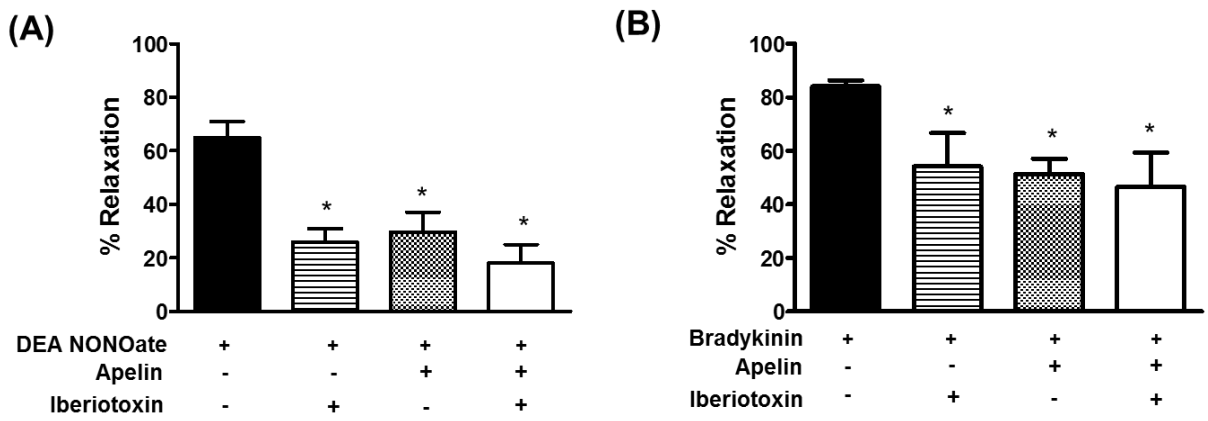

Fig. 9. Effect of combined treatment with apelin plus iberiotoxin on cerebral artery relaxation to DEA NONOate and bradykinin.
Bar graph representing effects of apelin (10^{-7} M) and iberiotoxin (10^{-7} M), alone or in combination, on (A) DEA NONOate (3 x 10^{-7} M) and (B) bradykinin (10^{-6} M)-induced relaxation of cerebral arteries. Each point represents the mean ± S.E.M. (n=5-8), *p<0.05 vs. DEA NONOate or bradykinin alone.

The effects of apelin on relaxations induced by the BK_{Ca} channel openers, NS1619 and BMS 191011 (87), and the K_{ATP} channel opener, levcromakalim (88), were also determined. At equieffective concentrations of the K channel openers, apelin inhibited the responses to NS1619 and BMS 191011 **(Figure 10A and 10B)**, but had no effect on levcromakalim-induced relaxation of endothelium-denuded cerebral arteries **(Figure 10C)**.

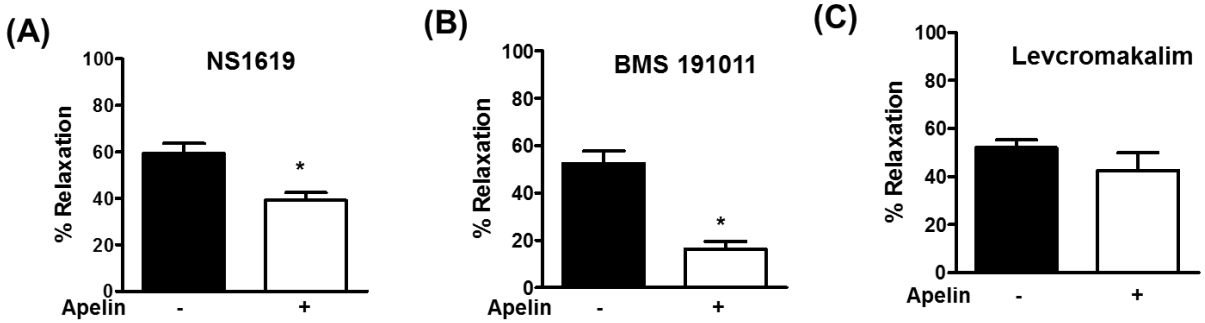

Fig. 10. Apelin selectively inhibits relaxation of cerebral arteries in response to BK_{Ca} channel activators.
Bar graph representing the effects of apelin (10^{-7} M) on relaxation of cerebral arteries in response to: (A) NS1619 (10^{-6} M); (B) BMS 191011 (3 x 10^{-6} M); and (C) levcromakalim (3 x 10^{-6} M). Each point represents the mean ± S.E.M. (n=6), *p<0.05 vs. NS1619 or BMS 191011 in the absence of apelin.

Electrophysiology Studies

DEA NONOate (10^{-5} M) caused a significant increase in whole-cell BK_{Ca} channel current measured in freshly isolated cerebral arterial smooth muscle cells **(Figure 11)**. The DEA NONOate-induced increase in BK_{Ca} channel current was nearly abolished by apelin (10^{-7} M) **(Figure 11A-E)**. As was observed in the vascular relaxation studies, the inhibitory effect of apelin on the response to DEA NONOate was mimicked by iberiotoxin (10^{-7} M) **(Figure 11F)**. In the presence of F13A (10^{-7} M), apelin (10^{-7} M) had no effect on the DEA NONOate-induced increase in BK_{Ca} channel current (peak current density (+80 mV) = 79.3 $\pm$ 7.2 with DEA NONOate alone versus 77.7 $\pm$ 5.5 pA/pF with DEA NONOate in the presence of apelin plus F13A; $p>0.05$; n=6) **(Figure 12)**

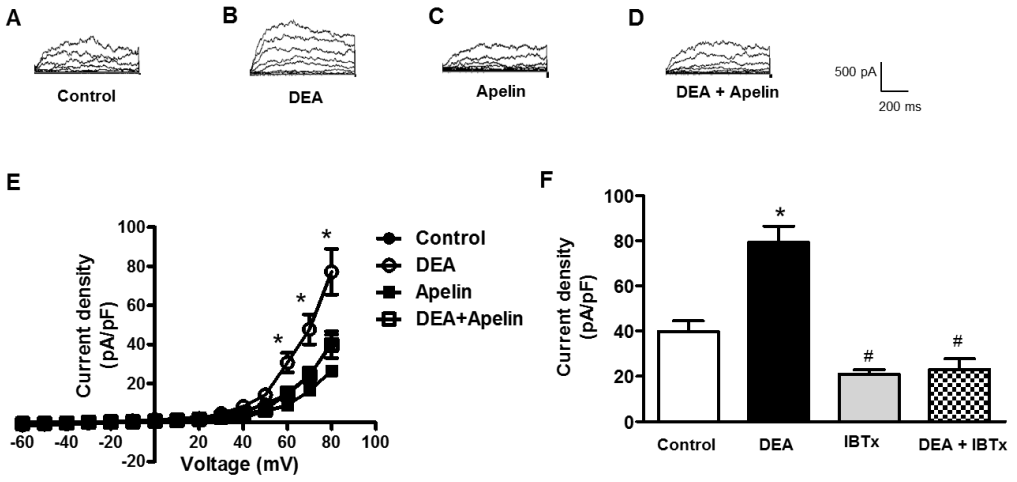

Fig. 11. Apelin inhibits DEA NONOate-induced increase in whole cell BK_{Ca} currents.
Whole cell BK_{Ca} currents were recorded in freshly isolated vascular smooth muscle cells in response to successive voltage pulses of 800 ms duration, increasing in 10 mV increments from -60 mV to +80 mV before and after treatment with DEA NONOate (DEA, 10^{-5} M) with and without apelin (10^{-7} M) or Iberiotoxin (IBTx, 10^{-7} M). **A-D:** Representative tracings depicting the sequential current recordings from a single smooth muscle cell in **(A)** control conditions followed by **(B)** DEA (10^{-5} M, 2 min); **(C)** apelin (10^{-7} M, 5 min) and **(D)** combination of DEA (10^{-5} M) and apelin (10^{-7} M). **E:** Summary I-V curve plot of BK_{Ca} currents at baseline and after treatment with DEA (10^{-5} M), with or without apelin (10^{-7} M). **F:** Bar graph summarizing the effect of Iberiotoxin (10^{-7} M, 5 min) on DEA (10^{-5} M)-induced average current density (pA/pF) at +80mV. Values are represented as mean ± SEM (n=6). *$p<0.05$ vs control current density; $^{\#}p<0.05$ vs DEA NONOate-induced current density.

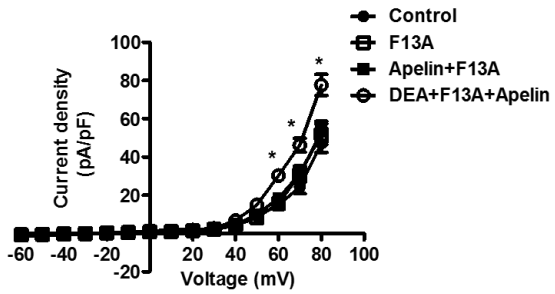

Fig. 12. F13A abolishes apelin-induced inhibitory effects on whole cell BK_{Ca} currents.
Whole cell BK_{Ca} currents were recorded in freshly isolated vascular smooth muscle cells in response to successive voltage pulses of 800 ms duration, increasing in 10 mV increments from -60 mV to +80 mV before and after treatment with DEA NONOate (DEA, 10^{-5} M) with and without alone or combined presence of apelin (10^{-7} M) and F13A (10^{-7}M). Values are represented as mean ± SEM (n=6). *p<0.05 vs control current density.

Likewise, apelin (10^{-7} M) also suppressed the NS1619-induced increase in BK_{Ca} channel current in isolated cerebral arterial smooth muscle cells **(Figure 13)**.

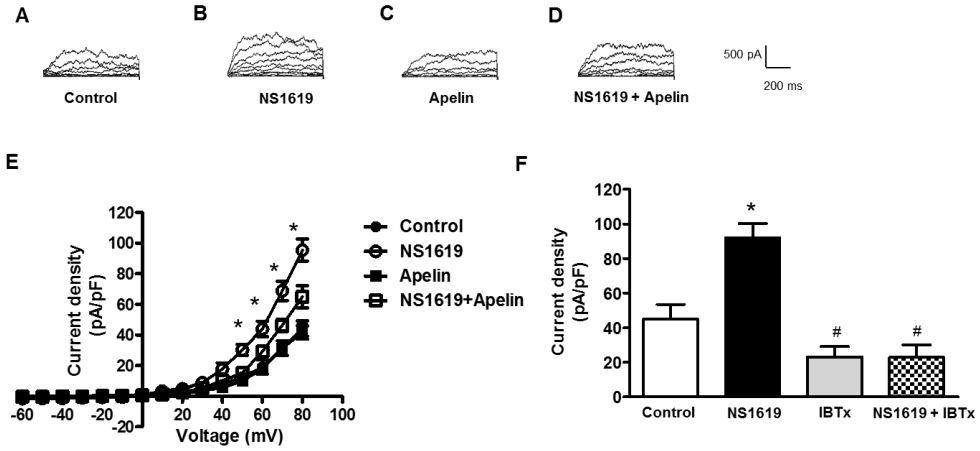

Fig. 13. Apelin inhibits NS1619-induced whole cell BK_{Ca} currents.
Whole cell BK_{Ca} currents were recorded in freshly isolated vascular smooth muscle cells in response to successive voltage pulses of 800 ms duration, increasing in 10 mV increments from -60 mV to +80 mV before and after the treatment with NS1619 (10^{-5} M), with and without apelin (10^{-7} M) or Iberiotoxin (IBTx, 10^{-7} M). **A-D:** Representative tracings depicting the sequential current recordings from a single smooth muscle cell in **(A)** control conditions followed by **(B)** NS1619 (10^{-5} M, 2 min); **(C)** apelin (10^{-7} M, 5 min) and **(D)** combination of NS1619 (10^{-5} M) and apelin (10^{-7} M). **E:** Summary I-V curve plot of BK_{Ca} currents at baseline and after treatment with NS1619 (10^{-5} M), with or without apelin (10^{-7} M). **F:** Bar graph summarizing the effect of Iberiotoxin (10^{-7} M, 5 min) on NS1619 (10^{-5} M)-induced average current density (pA/pF) at +80mV. Values are represented as mean ± SEM (n=6). *p<0.05 vs control current density; $^{\#}$p<0.05 vs DEA-induced current density.

Cyclic GMP Measurements

DEA NONOate (10^{-6} M) and bradykinin (10^{-6} M) each caused a significant increase in intracellular cyclic GMP levels in cerebral arteries **(Figure 14)**. Incubation of cerebral arteries with apelin (10^{-7} M) had no effect on the increases in cyclic GMP levels evoked by either DEA NONOate **(Figure 14A)** or bradykinin **(Figure 14B)**.

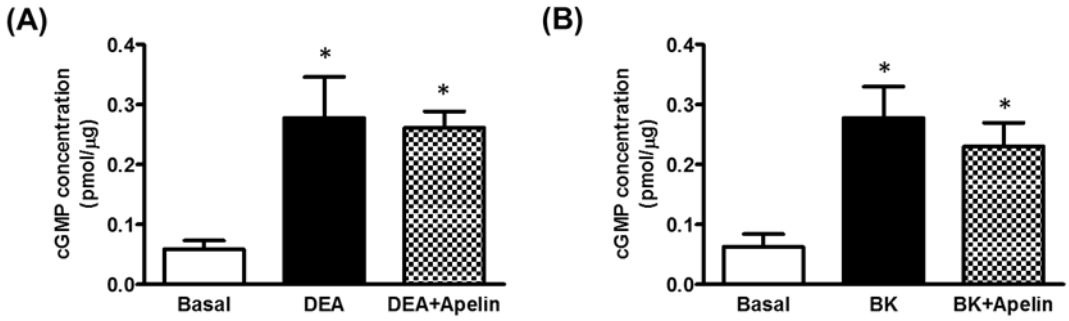

Fig. 14. Lack of effect of apelin on DEA NONOate- and bradykinin-induced increases in intracellular cyclic GMP levels.
Bar graphs representing the effects of apelin (10^{-7} M) on the increase in cyclic GMP levels in response to: (A) DEA NONOate (10^{-6} M) (DEA), and (B) bradykinin (10^{-6} M) (BK). Values are represented as mean ± SEM (DEA n=6; BK n=5). *$p<0.05$ vs basal levels.

Discussion

The major finding of the present study is that receptors for apelin (i.e. APJ receptors) are expressed in cerebral arteries and that activation of these receptors on vascular smooth muscle cells inhibits NO-induced relaxation. This conclusion, which identifies a previously unrecognized, novel action of apelin in blood vessels, is based on the findings that: 1) APJ receptor mRNA and protein are expressed in cerebral arteries; 2) APJ receptor protein co-localizes with smooth muscle cell actin in the arterial wall; 3) apelin inhibits relaxation of cerebral arteries in response to endothelium-derived NO, as well as an NO-donor; and 4) the inhibitory effects of apelin on NO-induced relaxation of cerebral arteries are abolished by an APJ receptor antagonist. Moreover, the findings indicate that apelin inhibits relaxation of cerebral arteries to NO by attenuating NO-

induced increases in BK_{Ca} current in the arterial smooth muscle cells. When taken together with the observation that apelin failed to cause relaxation in cerebral arteries, these actions of apelin could be expected to result in a net increase in cerebral vasomotor tone.

APJ receptors have been identified in several blood vessels throughout the cardiovascular system. For example, immunocytochemical and autoradiographic studies have detected APJ receptors in human saphenous vein, as well as coronary, internal mammary, radial, and pulmonary arteries, and in rat aorta, coronary, and pulmonary arteries (5, 18, 79). The results of the present study add to the current body of knowledge by demonstrating for the first time that APJ receptor gene transcripts and proteins are expressed in cerebral arteries. Moreover, immunofluorescence co-localization studies indicate that APJ receptors are present on both vascular smooth muscle and endothelial cells in the cerebral arterial wall, suggesting the possibility that APJ receptors may be involved in the local regulation of cerebral artery vasomotor tone.

An increasing body of evidence from both *in vivo* and *in vitro* studies supports a functional role for APJ receptors in regulating vascular tone. Intravenous administration of exogenous apelin has been shown to cause both an increase and a decrease in mean arterial blood pressure (39, 54, 75), as well as a decrease in preload consistent with a venodilator effect (39, 89). Apelin also increases forearm blood flow and coronary blood flow in humans (52, 76). In isolated arterial rings from several sources, apelin causes endothelium-dependent relaxations under normal conditions (22, 38), whereas vascular smooth muscle contraction is observed in blood vessels in which the endothelium has been removed or damaged (22, 67). Nonetheless, apelin itself failed to cause either contraction or relaxation of isolated cerebral arteries, regardless of the status of the endothelium and despite the presence of APJ receptors on vascular smooth muscle and endothelial cells in these arteries. These results demonstrate that apelin itself does not directly alter vasomotor

tone in cerebral arteries, in contrast to its actions reported in other arteries studied thus far; however, the lack of a direct effect does not preclude the possibility that apelin could indirectly regulate vasomotor tone by modulating the actions of other vasoactive substances (e.g. NO), or perhaps play a role in other functions of vascular cells in the arterial wall (e.g. proliferation, permeability).

A key finding of the present study is that despite having no measurable direct effect on cerebrovascular tone, apelin inhibited relaxations in response to bradykinin, an endothelium-dependent vasodilator that acts via the release of NO from endothelial cells in cerebral arteries (85, 86), and to DEA NONOate, an exogenous NO-donor (90). Since APJ receptors are expressed on cerebral artery endothelial cells, one potential site of action for apelin, at least with regard to endogenously produced NO, could be inhibition of endothelial nitric oxide synthase (eNOS); however, the only published reports regarding the regulation of eNOS by apelin indicate that the peptide increases, rather than inhibits, eNOS activity (40, 43). Although an effect of apelin on eNOS in cerebral arteries cannot be ruled out by the present study, the observation that apelin also inhibits NO-induced relaxation in response to DEA NONOate, which acts independently of the endothelium, suggests a site of action other than or in addition to eNOS. These results, together with data from the molecular studies indicating that cerebral arterial smooth muscle cells express APJ receptors, are consistent with an inhibitory effect of apelin at the level of the vascular smooth muscle, which is the primary site of action for the relaxing effect of NO (91, 92). Moreover, that the inhibitory effects of apelin on both the functional and electrophysiological responses to NO were blocked by pharmacologic inhibition with F13A, an APJ receptor antagonist (11), strongly suggests that activation of APJ receptors on smooth muscle cells mediates this effect of apelin in cerebral arteries.

The molecular mechanism by which APJ receptor activation by apelin causes impaired relaxation to NO likely involves inhibition of NO-induced increases in BK_{Ca} channel current in cerebral smooth muscle cells. Activation of BK_{Ca} channels leads to vascular smooth muscle cell hyperpolarization and relaxation (93, 94) and BK_{Ca} channels are abundantly expressed in cerebral arterial smooth muscle cells (61), where they play a pivotal role in regulating vascular tone (95). In cerebral arteries of the rat, NO-induced relaxation is mediated in part by increased BK_{Ca} channel activity and in part by increased formation of intracellular cyclic GMP resulting from activation of soluble guanylyl cyclase (51, 96, 97). Since apelin had no effect on the increase in cyclic GMP levels evoked by either bradykinin or DEA NONOate it is unlikely that inhibition of guanylyl cyclase underlies the ability of apelin to impair NO-induced relaxation in cerebral arteries. On the other hand, a role for BK_{Ca} channels in the effect of apelin on NO-induced relaxation is supported by several pieces of evidence, including: 1) apelin inhibited the increases in BK_{Ca} current induced by the NO-donor, DEA NONOate, and the synthetic BK_{Ca} channel activator, NS1619, in cerebral arterial smooth muscle cells; 2) the effects of apelin on both the functional and electrophysiological responses to NO were mimicked by iberiotoxin, a potent and selective BK_{Ca} channel blocker (98); 3) combined treatment with apelin plus iberiotoxin had no greater effect on NO-induced relaxation than either inhibitor alone, consistent with a shared mechanism of action for apelin and iberiotoxin; and 4) apelin inhibited relaxation of endothelium-denuded cerebral arteries in response to the BK_{Ca} channel activators, BMS 191011 and NS1619 (87, 99). With regard to the latter findings, it has been reported that in addition to activating BK_{Ca} channels, NS1619 also inhibits plasma membrane L-type calcium channels (100); however, in the present study this potential limitation was minimized by using two chemically distinct BK_{Ca} channel activators, as well as a concentration of NS1619 that has little effect on calcium currents and is known to relax cerebral arteries in a manner

that is nearly entirely due to BK_{Ca} channel activation (100, 101). Moreover, apelin had no effect on relaxation to the selective K_{ATP} channel opener, levcromakalim, thus providing further support for the view that apelin selectively inhibits responses that are mediated via BK_{Ca} channels in cerebral arterial smooth muscle cells. Taken together, the data indicate that the effect of apelin on BK_{Ca} channels is sufficient to meaningfully impair cerebral arterial relaxation evoked by NO as well as other BK_{Ca} channel-activating molecules.

The finding that apelin inhibits NO-induced relaxation in cerebral arteries is in contrast to its putative beneficial vasodilator effects reported in several peripheral arteries. Given the considerable heterogeneity known to exist among blood vessels from different origins in terms of their reactivity to vasoactive agents it is not necessarily surprising that cerebral arteries may differ from peripheral arteries in their response to apelin. In the rat, for example, the pineal hormone, melatonin, is a potent vasoconstrictor in isolated cerebral arteries (101) but causes relaxation of isolated aorta and caudal artery (102, 103). The reason(s) for the divergent responses to apelin among different blood vessels are not yet readily apparent, but possible explanations could include: 1) differences in the subtype of APJ receptor expressed in smooth muscle of cerebral vs peripheral arteries; however, it should be noted that there are no reports in the literature of multiple APJ receptor subtypes; 2) differences in the intracellular signaling pathways coupled to APJ receptor activation in cerebral versus peripheral arteries; and 3) differences in the role of BK_{Ca} channels in NO-induced relaxation among blood vessels.

The apelin/APJ receptor-signaling axis is generally considered to play a protective role in the cardiovascular system, with suggested benefits in disorders such as ischemia-reperfusion injury, heart failure, and pulmonary hypertension (42, 81, 104). Although apelin may have protective vasodilator effects in certain arteries (e.g. pulmonary vascular bed), it is evident from

the present study that, in cerebral arteries, the net effect of APJ receptor activation could adversely affect cerebrovascular function. This may present an important caveat when exploring the cardiovascular efficacy of systemically administered APJ receptor agonists. Indeed, apelin-like analogs are now in preclinical development as potential therapeutic agents for myocardial infarction and ischemia-reperfusion injury (47), and apelin itself is currently being administered to patients in clinical trials because of its putative beneficial effects on cardiac function and the pulmonary circulation (76, 105). The cerebrovascular consequences of such drugs may be particularly significant in certain patients, inasmuch as a single nucleotide polymorphism in the gene encoding the human APJ receptor, which results in increased apelin/APJ receptor signaling, has recently been identified and is associated with an increased risk of brain infarction (106). Since impaired vasodilation is a hallmark characteristic of the vascular dysfunction that occurs in many forms of cardiovascular disease (92), it is interesting to note that endogenous apelin levels are elevated in conditions such as obesity and diabetes (107-109), which are major risk factors for stroke and other cerebrovascular disorders (110).

In summary, apelin activates APJ receptors in cerebral arterial smooth muscle cells, resulting in inhibition of BK_{Ca} currents and impaired relaxation to endogenous and exogenous NO in cerebral arteries. Whether the ability of apelin to regulate vasomotor tone by inhibiting NO-induced relaxation is unique to the cerebral circulation is not yet clear, but given the pivotal role of NO in controlling vascular function, it will be important to determine if this novel effect of apelin is observed in other blood vessels. The potential for adverse effects on the cerebral circulation to occur with the use of APJ receptor-activating drugs may merit further consideration in future studies.

CHAPTER 3. VASCULAR EFFECTS OF APELIN IN CORONARY ARTERIES: COMPARISON WITH ANOTHER NITRIC OXIDE DEPENDENT VASODILATOR, ACETYLCHOLINE

Introduction

Apelin and APJ receptor are widely expressed in cardiovascular system including cardiomyocytes (4) and vasculature (5, 18), and can regulate vascular tone through both autocrine and paracrine mechanisms (74). APJ receptors are detected on endothelial and vascular smooth muscle cells within many blood vessel walls (5, 18) and this vascular distribution propose involvement of apelin-APJ axis in the regulation of vascular tone by endothelium dependent vasodilation (38, 43) and/or endothelium independent vasoconstriction (67). Apelin increases coronary blood flow and vascular functions of apelin are preserved during heart failure (76), suggesting enormous potential of apelin in restoring vascular functions during coronary artery diseases. Further, intravenous infusion of apelin increases preload consistent with a vasodilator effect (39, 89). Although pathophysiological alterations in apelin signaling during cardiovascular diseases are still under investigation (111, 112), but exogenous apelin is shown to improve hemodynamic and vascular functions during cardiovascular and metabolic diseases (41, 113-115).

Apelin causes vasodilation in most of the peripheral arteries, studied thus far, in part by nitric oxide dependent pathways (22, 38). Moreover, apelin increases forearm blood flow (52) and decreases mean arterial pressure (19, 55) via nitric oxide dependent pathways. Although current body of the knowledge demonstrates involvement of nitric oxide in apelin-induced vasoactive effects, the possible downstream signaling mechanism(s) is yet to be identified.

Endothelial nitric oxide is an important regulator of vascular tone and can activates multiple mediators including soluble guanylate cyclase to synthesize cGMP (91, 116), SERCA

(50, 117) and BK_{Ca} channels (48, 49). The ultimate endpoint for all signaling mechanism(s) is relaxation of vascular smooth muscle and vasodilation. However, a better understanding of relaxation pathways can provide better opportunities and models for apelin based therapeutic strategies for treatment of cardiovascular diseases. Thus to reduce critical gaps in the knowledge, the present study was aimed to identify possible mediators involved in apelin-induced relaxation in coronary arteries and compare it with a known endothelium dependent vasodilator, acetylcholine.

The present results demonstrate that apelin by activating endothelial APJ receptors can cause nitric oxide dependent relaxation of coronary arteries, likely through direct activation of smooth muscle BK_{Ca} channels. Moreover, different physiological stimuli i.e. apelin and acetylcholine can increase endothelial nitric oxide formation to activate different downstream mediators to relax coronary arteries.

Materials and Methods

Animals and Tissue Preparation: Experiments were performed on tissues isolated from 12-week-old male Sprague-Dawley rats (Envigo RMS, Indianapolis, IN). Rats were housed at 22 ± 2°C on a 12 h-12 h light-dark cycle and provided with food and water ad libitum. All animal protocols were approved by the North Dakota State University Institutional Animal Care and Use Committee. Rat hearts were isolated from animals anesthetized with isoflurane and placed into ice-cold physiological salt solution (PSS) with the following composition (in mM): 118.9 NaCl; 4.7 KCl; 2.5 $CaCl_2$; 1.2 $MgSO_4.7H_2O$; 1.2 KH_2PO_4; 25.0 $NaHCO_3$; 5.5 glucose and 0.03 EDTA. Epicardial coronary arteries were dissected and cleaned of surrounding tissues.

Western Immunoblotting: After collection, coronary arteries were immediately frozen in liquid nitrogen. Tissues were homogenized in lysis buffer and supplemented with a protease and

phosphatase inhibitor cocktail (FabGennix International, Frisco, TX) at 4°C using an IKA Ultra-Turrax T8 homogenizer (IKA Works Inc., Wilmington, NC). Tissue homogenates were kept on ice for 10 min and then centrifuged at 10000g for 10 min. Supernatant was collected, and protein determination was performed using a Pierce BCA protein estimation kit (ThermoFisher Scientific, Waltham, MA). Aliquots of supernatant containing equal amounts of protein (40 μg) were separated on 7.5-10% polyacrylamide gel by SDS-polyacrylamide gel electrophoresis, and proteins were electroblotted onto a polyvinylidene difluoride membrane (Bio-Rad Laboratories, Hercules, CA). Blots were blocked with 5% nonfat dry milk in Tris-buffered saline (TBS, pH 7.4) and incubated overnight at 4°C with a primary antibody specific for APJ receptors using a dilution of (1:200) (Santa Cruz Biotechnology Inc.). Membranes were washed three times for 10 min using TBS-Tween 20 and incubated with a horseradish peroxidase-linked secondary antibody (Santa Cruz Biotechnology Inc.). To ensure equal loading, the blots were analyzed for β-actin expression using an anti-actin antibody (Santa Cruz Biotechnology Inc.). Immuno-detection was performed using an enhanced chemiluminescence light detection kit (ThermoFisher Scientific).

RT-qPCR: Freshly isolated arteries were immediately frozen in liquid nitrogen and total RNA was isolated using an RNeasy Mini kit, according to the manufacturer's protocol (Qiagen, Germantown, MD). The concentration and purity of RNA was determined using a spectrophotometer (Nanodrop Technologies, Wilmington, DE). cDNA was synthesized using 50 ng of RNA and an iScript cDNA synthesis kit (Bio-Rad). A Sybr Green expression assay was used to determine expression of APJ receptors, with β-actin used as a housekeeping gene (Bio-Rad). The following primers (synthesized by Invitrogen, Carlsbad, CA) were used:

APJ receptor – forward: 5'-ACAAGACATGTGCCATTGGA-3'; reverse: 5'-TCTCCCAGAAGCCTCCTACA-3'; β-actin – forward: 5'-GTCGTACCACTGGCATTGTG-3';

reverse: 5'-TCTCAGCTGTGGTGGTGAAG-3'. Real-time RT-PCR reaction conditions were 95°C for 10 min, followed by 40 cycles of 95°C for 10 s, 60°C for 20 s, and 72°C for 30 s.

Immunofluorescence microscopy: Freshly isolated coronary arteries were fixed in 10% formalin solution, processed and embedded in paraffin blocks. Paraffin blocks were sectioned at 5 μm and mounted onto ProbeOn Plus microscopic slides (ThermoFisher Scientific). Sections were fixed by heating at 60°C for 30 min. Nonspecific antibody binding was blocked with normal serum [10% w/v; in TBS] for 1 h at room temperature. Sections were incubated overnight at 4°C in 1% serum containing a primary antibody against APJ receptors (Abcam, Cambridge, MA), smooth muscle actin (Santa Cruz Biotechnology) and/or PECAM-1 (Santa Cruz Biotechnology). For co-localization, double immunofluorescent staining was performed by incubating the tissue sections with more than one primary antibody at the same time. Detection of the primary antibodies against the APJ receptor, smooth muscle actin and PECAM-1 was accomplished using Texas red-conjugated (goat anti-rabbit IgG; Invitrogen, Carlsbad, CA), Alexa Fluor-488 (donkey anti-mouse IgG; Santa Cruz Biotechnology) and Alexa Fluor-555 (donkey anti-goat IgG; Santa Cruz Biotechnology) secondary antibodies, respectively. Rat lung tissue was used as positive control for APJ receptor detection (58). All negative controls were incubated with 1% serum solution overnight followed by secondary antibodies. All dilutions and thorough washes between stages were performed using TBS containing Triton X-100 [0.3% (v/v)] unless otherwise stated. Sections were drained by blotting with filter paper, and a drop of mounting medium containing an anti-fade reagent (Vector Laboratories, Burlingame, CA) was added to the slides. Images of the sections were obtained using an Olympus confocal laser-scanning microscope (Olympus, Tokyo, Japan). The images were generated using Olympus FluoView FV300 (v. 4.3) confocal software.

Vascular Functional Studies: Arterial rings (120-150 μm; 1.2 mm in length) were suspended in wire myographs (DMT, Aarhus, Denmark) for isometric tension recording. The myograph chambers were filled with PSS (5 ml), which was continuously aerated with 95% O_2/5% CO_2 and maintained at 37°C throughout the experiment. The vessels were stretched to using DMT normalization guide, where arteries were stretched up to 6 mN by a sequential stretching of 1.5 mN for 5 min (until 6 mN). Then vessels were allowed to stabilize for 30-40 min with intermittent washings. Vessel reactivity was confirmed by evoking a response to KCl (60 mM). In some vessels, the endothelium was removed by gently rubbing the intimal surface with a human hair. The presence or absence of endothelium was confirmed by measuring relaxation in response to the endothelium-dependent vasodilator, acetylcholine (10^{-6} M). Responses to the vasodilators used in this study were obtained in arterial rings contracted with 5-HT (10^{-7} M). Inhibitors were added to the myograph chamber 20 min prior to contraction with 5-HT and the inhibitors remained in contact with the tissues for the remainder of the experiment. Experiments with inhibitors were conducted in parallel with control rings taken from the same animal.

Coronary Endothelial Cells (ECs) Isolation: Endothelial cells were isolated from coronary arteries as previously described (118) with minor modifications. Briefly, coronary arteries were digested in dissociation solution (55 mM NaCl, 80 mM Na-glutamate, 6 mM KCl, 2 mM $MgCl_2$, 0.1 mM $CaCl_2$, 10 mM glucose, 10 mM HEPES, pH 7.3) containing Worthington neutral protease (0.5 mg/mL) and elastase (0.5 mg/mL) for 60 minutes at 37°C. Then, Collagenase (Worthington type II, 0.5 mg/mL) was added to the same enzyme solution and digestion was continued for 2 minutes. The artery was removed and placed back in the dissociation solution without enzymes for an additional 10 min before trituration with a polished Pasteur pipette to yield single endothelial cells suspension.

Real-Time NO Imaging: Freshly isolated ECs were allowed to attach in eight well LabTek chambers (Thermo Fisher Scientific, Waltham, MA) for 3-4 hours. The cells were then loaded with NO-sensitive fluorescent dye 4,5-diaminofluorescein diacetate (DAF-2 DA; Thermo Fisher Scientific, Waltham, MA; 5 μM; 60 min at room temperature). The real time imaging was performed using an Olympus confocal laser-scanning microscope (Olympus, Tokyo, Japan) with a 40x numerical aperture oil immersion lens (with excitation at 488 nm and emission at 515 nm). All experiments were carried out at room temperature in HBSS. The effect of various agonists and inhibitors on intracellular NO level was obtained in paired experiments. In experiments with inhibitors, NLA (3×10^{-5} M) or F13A (10^{-7} M) was added to the chamber for 10 min before addition of apelin (10^{-7} M) or acetylcholine (10^{-6} M). ECs were isolated from 4-6 animals (each animal on different day) and 2-3 cells were analyzed for each treatment from each animal.

Cyclic GMP Estimation: Competitive ELISA method was used to measure cGMP levels in coronary arteries. Arterial segments were equilibrated in PSS for at least 30 min at 37°C. After the equilibration period, arterial segments were treated with apelin (10^{-7} M, 5 min) or acetylcholine (ACh; 10^{-6} M, 5 min). In some experiments, arterial segments were pretreated for 20 min with NLA (3×10^{-5} M) or ODQ (10^{-5} M), before being exposed to agonists. After drug treatments, segments were immediately frozen in liquid nitrogen and homogenized with an IKA Ultra, Turrax-T8 homogenizer (IKA Works) at 4°C in 0.1 M hydrochloric acid. Tissue homogenates were centrifuged for 10 min at ≥600 g. cGMP and total protein content were determined in the supernatant as per the direct cGMP enzyme immunoassay kit (Assay Design, Ann Arbor, MI) and Pierce BCA protein assay kit (ThermoFisher Scientific) respectively. cGMP levels are expressed as picomoles per microgram of protein.

Coronary Smooth Muscle Cell Isolation: Enzymatic isolation of single vascular smooth muscle cells was carried out as described previously, with brief modification (30). Arteries were placed in cell isolation solution of the following composition (in mM): 60 NaCl, 80 Na-glutamate, 5 KCl, 2 $MgCl_2$, 10 glucose, and 10 HEPES (pH 7.2). Arterial segments were initially incubated in 1.2 mg/ml papain (Worthington) and 1.0 mg/ml dithioerythritol (Sigma Aldrich) for 17 min at 37°C and then in 1.2 mg/ml type II collagenase (Worthington) and 0.5 mg/ml elastase (Worthington) for 12 min at 37°C. The digested segments were washed three times in ice-cold cell isolation solution and incubated on ice for 30 min. After this incubation period, vessels were triturated to liberate smooth muscle cells and stored in ice-cold cell isolation solution for use. Smooth muscle cells were studied within 6 h following isolation.

Electrophysiological Recording: Isolated smooth muscle cells were placed into a recording chamber (Warner Instruments, Hamden, CT) and allowed to adhere for 20 min at room temperature. Whole cell currents were recorded using an AxoPatch 200B amplifier equipped with an Axon CV 203BU headstage (Molecular Devices). Current data were collected and analyzed with pCLAMP 10.0 software (Molecular Devices, Sunnywale, CA). The patch electrodes (3-4 MΩ) were fabricated from 1.5-mm borosilicate glass capillaries. Smooth muscle cells were superfused at a rate of 2.0 ml/min with a solution containing (in mM) 145 NaCl, 5.4 KCl, 1.8 $CaCl_2$, 1 $MgCl_2$, 5 HEPES, 10 glucose; pH 7.4 (NaOH). Patch pipettes were filled with internal pipette solution contained (in mM) 145 KCl, 5 NaCl, 0.37 $CaCl_2$, 2 $MgCl_2$, 10 HEPES, 1 EGTA, 7.5 Glucose; pH 7.2 (KOH). All drugs were diluted in fresh bath solution and perfused into the experimental chamber. Voltage-activated currents were filtered at 2 kHz and digitized at 10 kHz, and capacitative and leakage currents were subtracted digitally. Series resistance and total cell capacitance were calculated from uncompensated capacitive transients in response to 10 ms

hyperpolarizing step pulses (5 mV), or obtained by adjusting series resistance and whole-cell capacitance using the Axopatch 200B amplifier control system. Standard recording conditions for BK_{Ca} were achieved by stepping in 10 mV increments from a holding potential of -60 to +80 mV. BK_{Ca} currents were expressed as current density (current divided by its capacitance).

Drugs: The following drugs were used: acetylcholine, diethylamine NONOate (DEA NONOate), sodium nitroprusside (SNP), diltiazem, 5-hydroxytryptamine (5-HT), indomethacin, PEG-catalase, DT-2 trifluoroacetate salt, nitro-l-arginine (NLA) and glyburide (Sigma Chemical, St. Louis, MO); iberiotoxin, and 1H-[1,2,4] oxadiazolo[4,3-a]quinoxalin-1-one (ODQ) (Tocris, Ellisville, MO); apelin-13, and F13A (H-Gln-Arg-Pro-Arg-Leu-Ser-His-Lys-Gly-Pro-Met-Pro-Ala-OH trifluoroacetate salt) (Bachem, Torrance, CA) and cyclopiazonic acid (Abcam, Cambridge, MA). Drug solutions were prepared fresh daily, kept on ice, and protected from light until used. All drugs were dissolved in double-distilled water with the exception of ODQ and cyclopiazonic acid which were dissolved initially in DMSO, indomethacin, which was dissolved initially in 1 mM sodium carbonate, and glyburide, which was dissolved initially in 0.1 N NaOH prior to further dilution in double-distilled water. Drugs were added to the myograph chambers in volumes not greater than 0.02 ml. Drug concentrations are reported as final molar concentrations in the myograph chamber.

Data Analysis: Relaxation responses are expressed as a percent of the initial tension induced by 5-HT (10^{-7} M). EC_{50} values (drug concentration that produced 50% of its own maximal response) were determined, converted to their negative logarithm, and expressed as -log molar EC_{50} (pD_2). RT-qPCR data were analyzed to quantify relative gene expression by ΔCt relative to β-actin. For NO imaging, amplitude of DAF-2 fluorescence was calculated by subtracting peak fluorescence intensity from basal fluorescence intensity. Results are expressed as means ± SEM,

and n refers to the number of animals from which blood vessels were taken, unless otherwise stated. Values were compared by Student's t-test or one-way ANOVA using Tukey's test as post-hoc analysis for paired or unpaired observations, as appropriate, to determine significance between groups. Values were considered significantly different when $p<0.05$.

Results

APJ Receptor Expression and Localization

APJ receptor expression was analyzed using RT-qPCR and immunoblot analyses. Both protein **(Figure 15A)** and mRNA transcripts **(Figure 15B)** suggest APJ receptor are expressed in coronary arteries along with rat lung tissue, which was used as a positive control (58). Moreover, APJ receptor protein was localized in both endothelial and smooth muscle cells of coronary artery **(Figure 15C.1- C.3)** using immunofluorescence confocal microscopy. Rat lung tissue was used to demonstrate staining for APJ receptors on bronchial epithelium **(Positive control, Figure 15C.5)**; inset shows non-specific binding of the secondary antibody in the absence of primary antibody for APJ receptors.

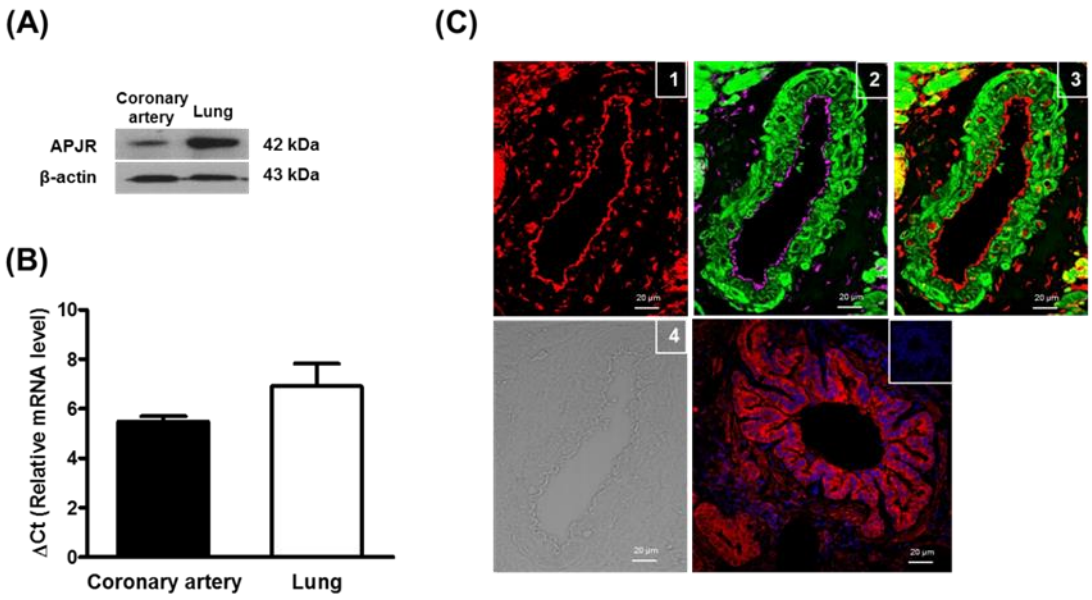

Fig. 15. Expression and localization of APJ receptors.
(A) Representative immunoblot showing expression of APJ receptor (APJR) protein in homogenates from rat coronary arteries (Lane 1) and lung tissue (Lane 2); β-actin was used as a loading control. The immunoblots shown are representative of data obtained from five different animals. (B) Bar graph showing relative mRNA expression of APJ receptor, represented as ΔCt values relative to β-actin. Data are presented as mean ± SEM (n=3). (C) Representative immunofluorescence images of: (1) APJ receptors (red fluorescence); (2) merged image showing endothelial cells (magenta fluorescence) with smooth muscle cells actin (green fluorescence); (3) merged image showing APJ receptor co-localized areas in smooth muscle cells (yellow fluorescence) and endothelium (red fluorescence) in rat coronary artery; (4) differential interference contrast image of rat coronary artery; and (5) APJ receptors (red fluorescence) with nuclear staining (blue fluorescence) in rat bronchial epithelium (positive control); inset demonstrates a lack of staining after incubation of tissue with serum followed by the secondary antibody (negative control). The images are representative of those obtained from three different animals. Scale bar, 20 μm.

Vascular Relaxation Studies

In coronary arteries contracted with 5-HT (10^{-7} M), increasing concentration of apelin (10^{-8} – 3 x 10^{-6} M) caused endothelium dependent relaxation, which was blunted with endothelium denudation (% Emax: 44.74 ± 6.56 vs. 15.54 ± 3.73 with and without endothelium respectively, $p<0.05$) **(Figure 16A)**. Similarly, an APJ receptor antagonist, F13A (10^{-7} M) abolished apelin-

induced relaxations **(Figure 16B)**, but had no effect on the response to acetylcholine (10^{-9} M – 3 x 10^{-6} M) **(Figure 16C)**.

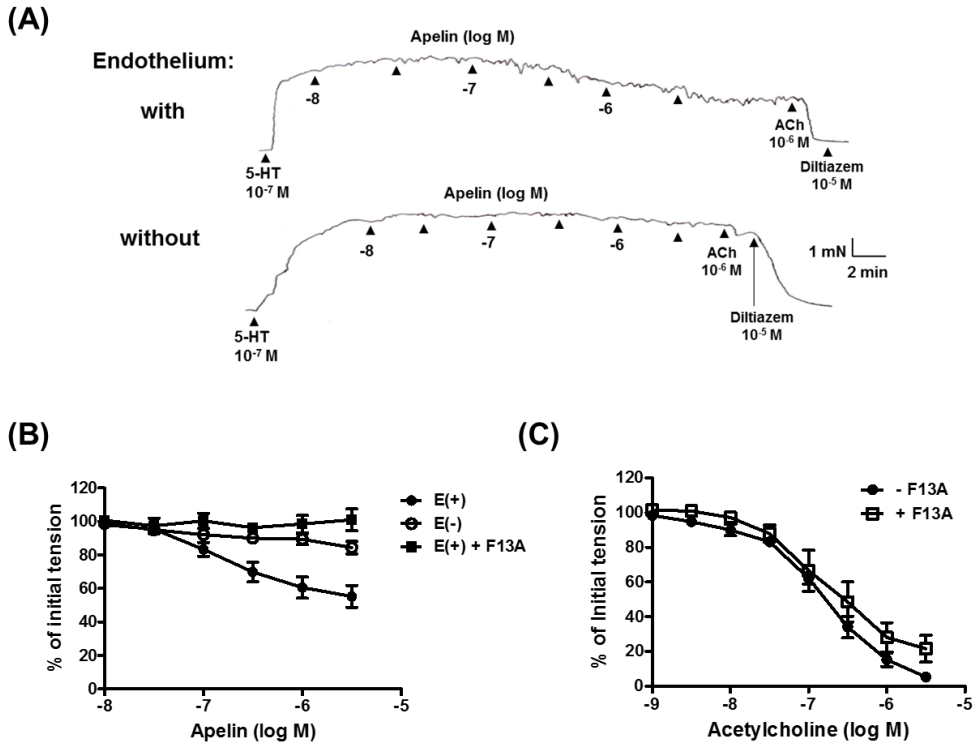

Fig. 16. Apelin causes endothelium APJ receptor dependent relaxation of isolated coronary arteries.
(A) Representative original tracings of isometric tension recordings from isolated coronary arteries (with and without endothelium) in response to cumulative addition of increasing concentrations of apelin, followed by acetylcholine (ACh; 10^{-6} M) and diltiazem (10^{-5} M). Log concentration-response curve for (B) apelin-induced relaxation in coronary arteries with endothelium (E+), which was abolished in the endothelium denuded (E-) segments or in the presence of F13A (10^{-7} M) and (C) acetylcholine in the absence and presence of F13A (10^{-7} M). Data are expressed as a percentage of the initial increase in tension induced by 5-HT (10^{-7} M). Each point represents the mean ± S.E.M. (n=5-9).

Experiments were then performed to evaluate the mediators involved in apelin-induced relaxation. Apelin-induced relaxations were significantly inhibited in the presence of the endothelial NO synthase inhibitor, NLA (3 x 10^{-5} M) **(Figure 17A)**, whereas guanylyl cyclase inhibitor, ODQ (10^{-5} M) was without effect (% Emax: 37.04 ± 4.68 vs. 41.98 ± 6.90 without and with ODQ respectively, $p>0.05$) **(Figure 17B)**. Likewise, protein kinase G inhibitor, DT-2 (10^{-6}

M) and cyclooxygenase inhibitor, indomethacin caused no change in the response to apelin **(Figure 17C and 17D)**.

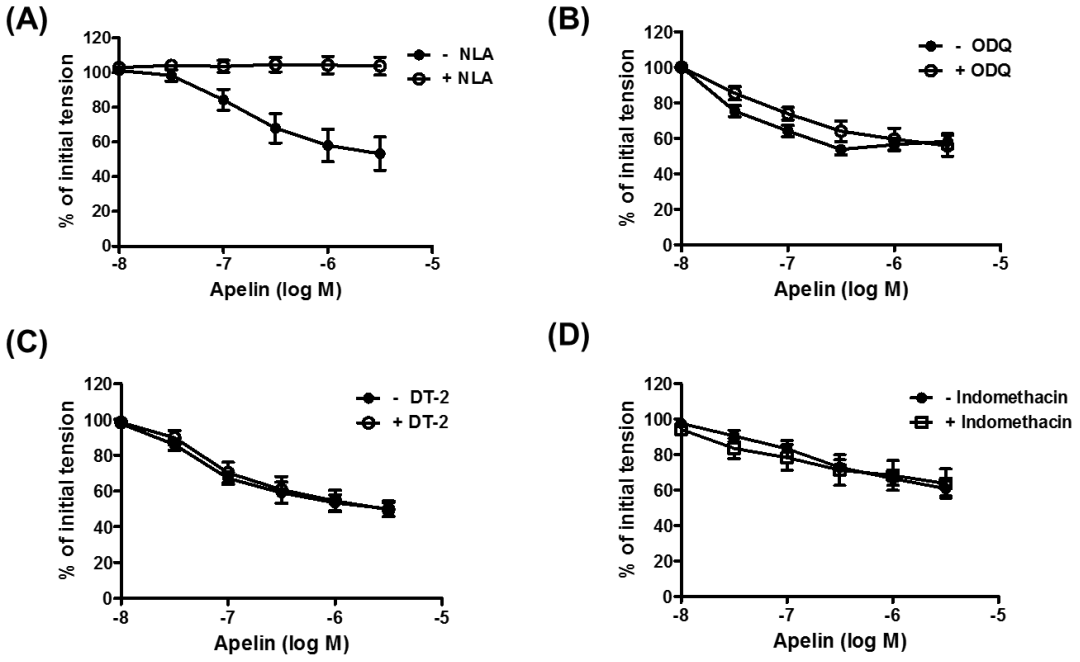

Fig. 17. Apelin-induced response in dependent on nitric oxide, but not on cGMP or Protein Kinase G.
Log concentration-response curves for apelin in producing relaxation of endothelium-intact coronary arteries in the absence and presence of (A) nitro-l-arginine (NLA; 3 x 10^{-5} M, n=6); (B) ODQ (10^{-5} M, n=5); (C) DT-2 (10^{-6} M, n=6); and (D) indomethacin (10^{-5} M, n=6). Data are expressed as a percentage of the initial increase in tension induced by 5-HT. Each point represents the mean ± S.E.M.

Vasoactive response of a known endothelium dependent vasodilator, acetylcholine (ACh) was also assessed in coronary arteries segments. ACh (10^{-9} M – 3 x 10^{-6} M)-induced relaxation was attenuated in the presence of NLA (% Emax: 97.24 ± 1.74 vs. 39.84 ± 10.44 without and with NLA respectively, $p<0.05$), and similarly by ODQ (10^{-5} M) or DT-2 (10^{-6} M) **(Figure 18A-C)**. However, cyclooxygenase inhibitor, indomethacin (10^{-5} M) caused no change in apelin or ACh-induced response **(Figure 18D)**.

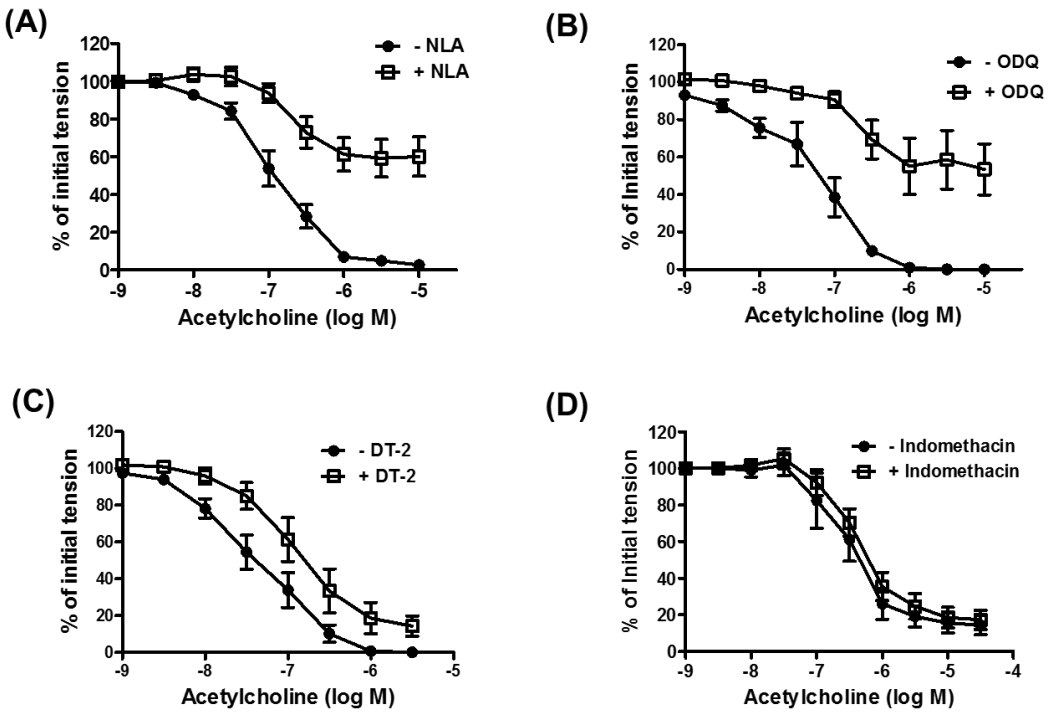

Fig. 18. NO-cGMP pathways in coronary arteries mediate acetylcholine-induced response.
Log concentration responses for acetylcholine in the absence and presence of (A) NLA (3 x 10^{-5} M, n=7); (B) ODQ (10^{-5} M, n=6); (C) DT-2 (10^{-6} M, n=6) and (D) indomethacin (10^{-5} M, n=7). Each point represents the mean ± S.E.M.

The BK_{Ca} channel blocker, iberiotoxin (IBTx; 10^{-7} M) inhibited apelin and acetylcholine-induced relaxation **(Figure 19A-B)**, whereas K_{ATP} channel blocker, glyburide (10^{-6} M), was without effects **(Figure 21A)**.

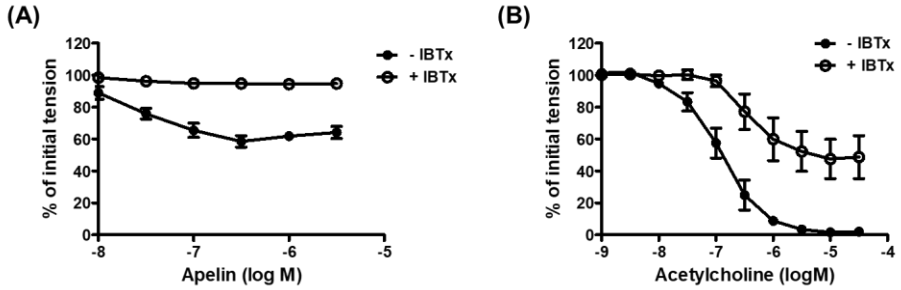

Fig. 19. Apelin and acetylcholine-induced nitric oxide activates BK_{Ca} channels to relax coronary arteries.
Log concentration-response curves for (A) apelin and (B) acetylcholine in producing relaxation of endothelium-intact coronary arteries in the absence and presence of iberiotoxin (10^{-7} M, n=6).

Role of BK_{Ca} channels in NO-induced relaxation was further evaluated in high potassium (40 mM K^+) contracted arterial segments. Apelin-induced endothelium dependent relaxation was completely abolished in the segments contracted with 40 mM K^+ **(Figure 20A)**, whereas ACh response had a rightward shift with inhibition of maximum relaxation (% Emax: 98.6 ± 1.40 vs. 75.50 ± 5.05 with 5-HT and 40 mM K^+ contractions respectively, $p<0.05$) **(Figure 20B)**.

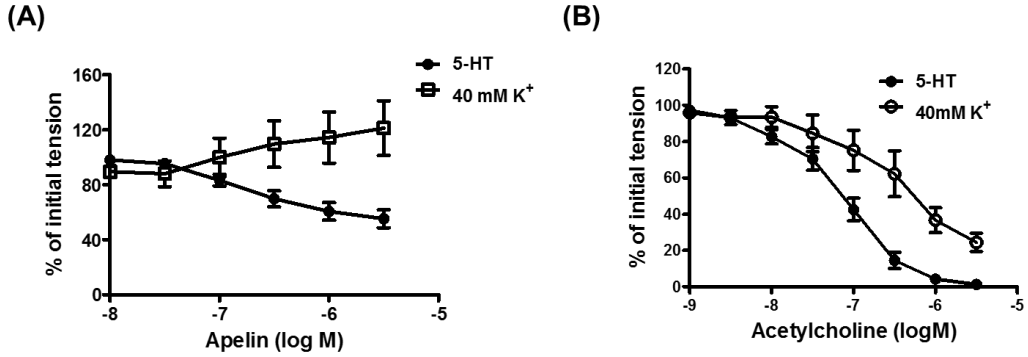

Fig. 20. Apelin-induced relaxation requires activation of smooth muscle K^+ channels.
Log concentration response curve for (A) apelin and (B) acetylcholine in producing relaxation of endothelium-intact coronary arteries contracted with 5-HT (10^{-7} M) and 40 mM K^+. Each point represents the mean ± S.E.M. (n=7-11).

Possible involvement of other pathways i.e. NO-induced activation of sarco/endoplasmic reticulum Ca^{2+}-ATPase (SERCA) pump and hydrogen peroxide (H_2O_2) were evaluated using SERCA inhibitor, cyclopiazonic acid (CPA, 2 x 10^{-5} M) and a well-known decomposer of H_2O_2, PEG-Catalase (P-Catalase, 500 U/ml) respectively. The presence of CPA had no effect on apelin-induced relaxations, whereas ACh-induced relaxation was inhibited (% Emax: 98.77 ± 1.22 vs. 51.44 ± 5.08 without and with CPA respectively, $p<0.05$) (**Figure 21B)**. Moreover, presence of P-catalase had no effect on either apelin or ACh-induced relaxations **(Figure 21C)**.

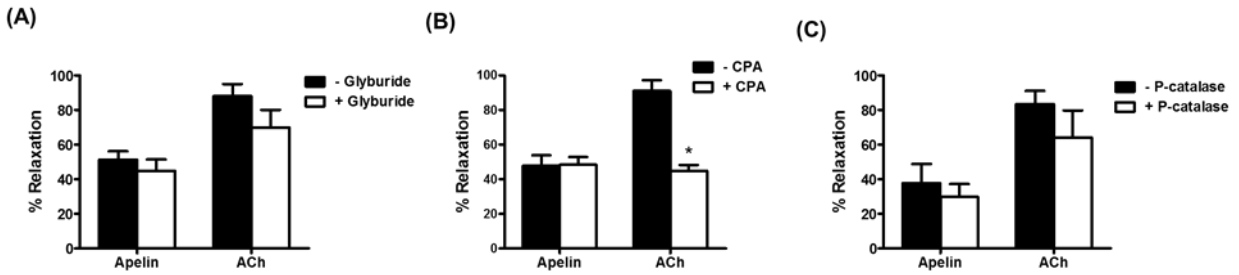

Fig. 21. Apelin-induced response is not dependent on K_{ATP} channels, SERCA and hydrogen peroxide.
Bar graph representing maximum relaxation response of apelin (3 x 10^{-6} M) and acetylcholine (10^{-6} M) in endothelium-intact coronary arteries in the absence and presence of (A) glyburide (10^{-6} M, n=6); (B) Cyclopiazonic acid (CPA, 2 x 10^{-5} M, n=6); and (C) PEG-catalase (P-catalase, 500u/ml, n=5). Each point represents the mean ± S.E.M. *p<0.05 vs. ACh alone.

Intracellular NO and Cyclic GMP Measurement

In freshly isolated endothelial cells, apelin (10^{-7} M) increased DAF-2 fluorescence, which was inhibited in the presence of NLA (3 x 10^{-5} M) or F13A (10^{-7} M) **(Figure 22A and 22B)**. Likewise, ACh (10^{-6} M) also increased DAF-2 fluorescence, which was abolished in the presence of NLA (3 x 10^{-5} M), whereas F13A (10^{-7} M) was without any effect **(Figure 22C)**.

Intracellular cGMP levels were measured by incubating freshly coronary arteries with apelin or ACh. Different concentration of apelin caused no change in basal cGMP levels **(Figure 23A)**, but ACh (10^{-6} M) caused a marked increase in intracellular cGMP, which was inhibited in the presence of NLA (3 x 10^{-5} M) or ODQ (10^{-5} M) **(Figure 23B)**.

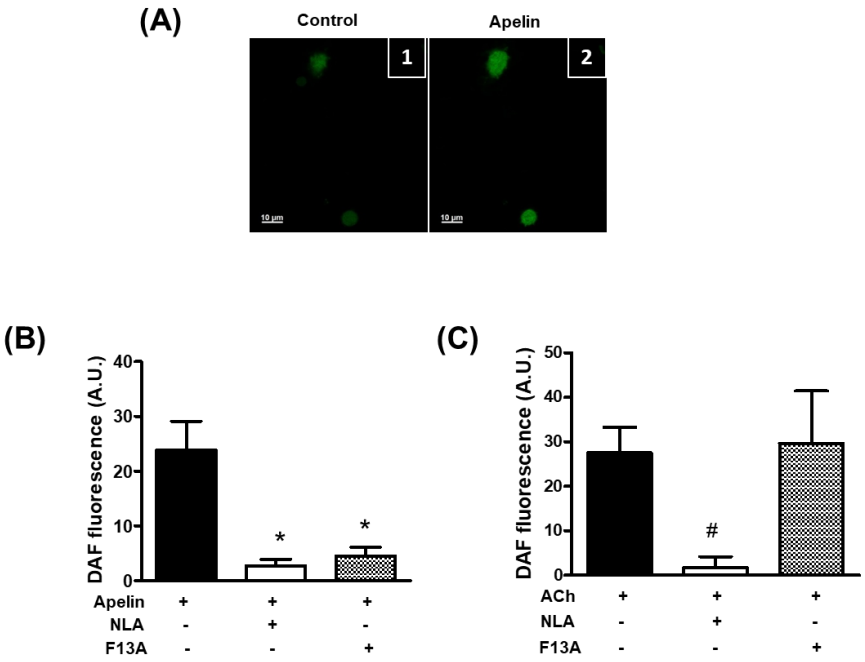

Fig. 22. Apelin increases intracellular NO production, similar to acetylcholine.
A) Representative images of DAF-2 (5 µM) loaded freshly isolated coronary ECs (1) before and (2) after apelin (10^{-7} M) treatment. Bar graph representing increase in DAF-2 fluorescence after exposure to (B) apelin (10^{-7} M) and (C) acetylcholine (10^{-6} M) in the absence and presence of NLA (3 x 10^{-5} M) or F13A (10^{-7} M). Amplitude of change in DAF fluorescence was calculated as the maximal fluorescence after agonist exposure corrected for baseline fluorescence. Values are represented as means ± S.E.M. (n = 4 - 6 animals, 9 - 18 total cells). * $p<0.05$ vs. apelin or acetylcholine alone as calculated by ANOVA using Tukey's test as post-hoc analysis.

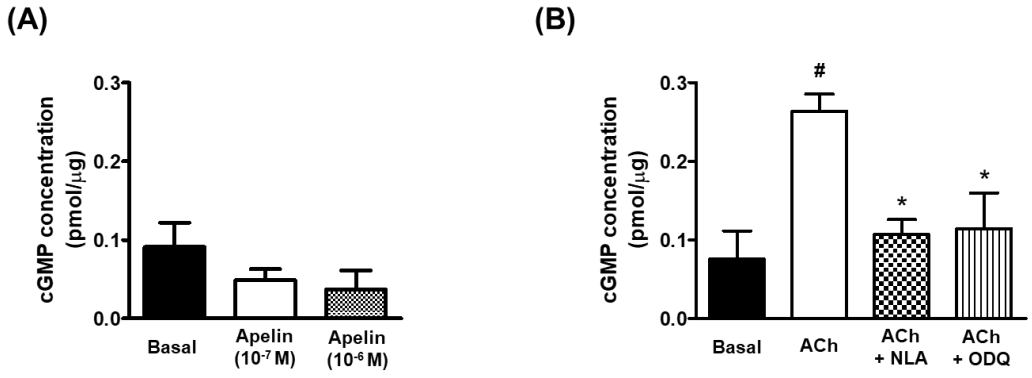

Fig. 23. Acetylcholine, but not apelin increases intracellular cGMP production in coronary arteries. Bar graph representing effect of (A) apelin and (B) acetylcholine (10^{-6} M) on intracellular cGMP levels in intact coronary arterial segments. Values are represented as means ± S.E.M. (n = 4). * $p<0.05$ vs. ACh; and $^{\#}$ $p<0.05$ vs. basal.

Electrophysiology Studies

Whole cell K^+ currents were increased in the presence of exogenous NO - donor DEA NONOate (DEA; 10^{-5} M) **(Figure 24A)**. The BK_{Ca} channel blocker, iberiotoxin (10^{-7} M) attenuated basal and DEA- induced whole cell K^+ currents **(Figure 24G)**, whereas ODQ (10^{-5} M) had no inhibitory effects on basal and NO – donors induced current density **(Figure 24A-F and 25)**.

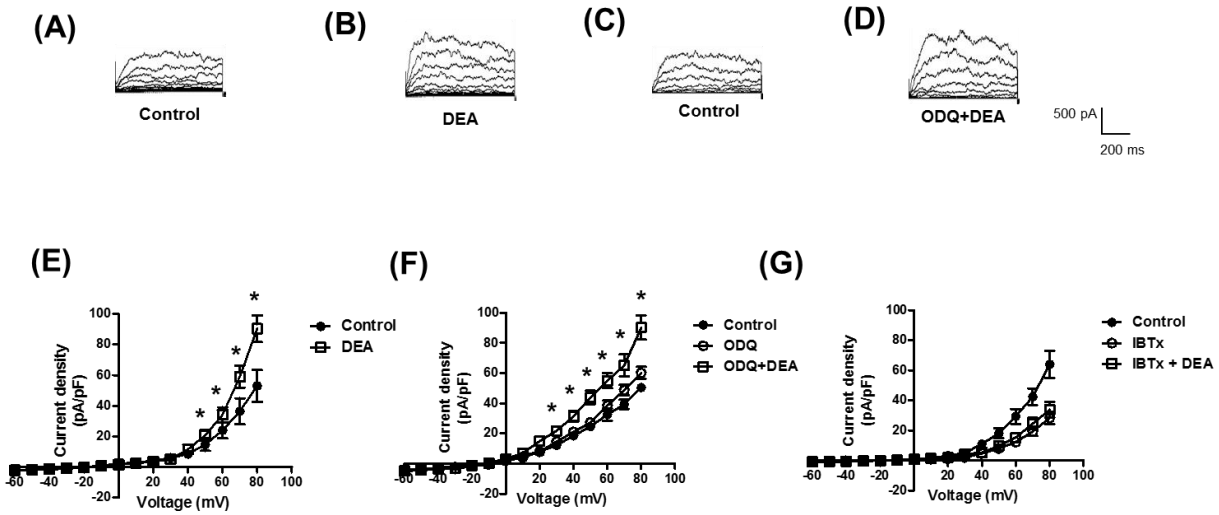

Fig. 24. DEA NONOate-induced increase in whole cell BK_{Ca} currents were not inhibited by ODQ, but by iberiotoxin.
Whole cell BK_{Ca} currents were recorded in freshly isolated vascular smooth muscle cells in response to successive voltage pulses of 800 ms duration, increasing in 10 mV increments from -60 mV to +80 mV before and after treatment with DEA NONOate (DEA, 10^{-5} M) with and without ODQ (10^{-5} M) or Iberiotoxin (IBTx, 10^{-7} M). A-D: Representative tracings depicting the sequential current recordings from a single smooth muscle cell (A and C) before and (B) after treatment of DEA (10^{-5} M, 2 min) alone or (D) in combined presence of ODQ (10^{-5} M, 5 min) and DEA (10^{-5} M, 2 min); E-G: Summary I-V curve plots of BK_{Ca} currents at baseline and after treatment with DEA (10^{-5} M), in the (E) absence and (F) presence of ODQ (10^{-5} M); or (G) Iberiotoxin (IBTx; 10^{-7} M). Values are represented as mean ± SEM (n=6). * $p<0.05$ vs. control current density.

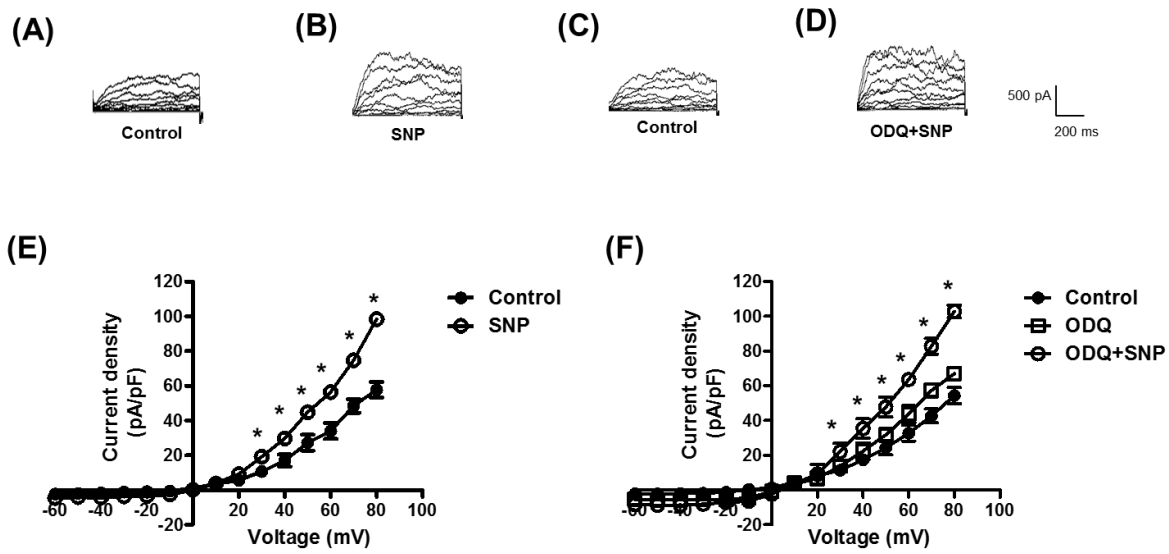

Fig. 25. Sodium nitroprusside-induced increase in whole cell BK_{Ca} currents are not inhibited by ODQ.
Whole cell BK_{Ca} currents were recorded in freshly isolated vascular smooth muscle cells in response to successive voltage pulses of 800 ms duration, increasing in 10 mV increments from -60 mV to +80 mV before and after treatment with sodium nitroprusside (SNP; 10^{-5} M) with and without ODQ (10^{-5} M). A-D: Representative tracings depicting the sequential current recordings from a single smooth muscle cell (A and B) before and (C) after treatment of SNP (10^{-5} M, 2 min) alone or (D) in combined presence of ODQ (10^{-5} M, 5 min) and SNP (10^{-5} M, 2 min); E-F: Summary I-V curve plots of BK_{Ca} currents at baseline and after treatment with SNP (10^{-5} M), in the absence (E) and presence of (F) ODQ (10^{-5} M). Values are represented as mean ± SEM (n=6). *$p<0.05$ vs control current density.

Discussion

There are two novel findings in this study. First, data show that apelin by binding to endothelial APJ receptors can cause NO mediated relaxation that does not require cGMP-PKG as mediators, but direct activation of smooth muscle BK_{Ca} channels. Second, both apelin and acetylcholine activate eNOS to form nitric oxide or reactive nitrogen species (RNS, ex. peroxynitrile or nitrate), but induced relaxations are mediated by different downstream mediators.

Our understanding about apelin-APJ axis in the regulation of vascular tone is continuously evolving, but the consensus is apelin causes nitric oxide dependent relaxation in the peripheral arteries. Much of the data, which examines vasodilation mechanism(s) of apelin, are limited to

involvement of nitric oxide, however the downstream mediators activated by apelin-induced nitric oxide are yet to be identified. Endogenous nitric oxide can activate diverse signaling pathways in different vascular beds, but the ability of nitric oxide to activate multiple pathways in same blood vessel is unknown. To my knowledge, this is the first report providing novel evidence that apelin and acetylcholine-induced NO can relax vascular smooth muscle cells by different downstream mediators. These results suggest possibilities of 1) nitric oxide itself can produce diverse response based on physiological stimuli i.e. apelin vs. acetylcholine; 2) eNOS activation generates multiple vasoactive RNS in coronary arteries to relax of vascular smooth muscle cells.

In agreement with the previous reports, APJ receptor were localized in both endothelial and smooth muscle cells of rat coronary arteries (5, 18, 79). APJ receptors are uniformly distributed on endothelial cell lining, whereas has a punctate appearance on smooth muscle cells of arterial wall. In line with APJ receptor expression, apelin-induced endothelium dependent relaxation under physiological conditions (22, 38), but in contrast to previous reports, we did not observe vasoconstriction in endothelium denuded arterial segments (22, 67). The observed differences in endothelium independent response can be attributed different arterial preparations and contractile agents used during different studies. Apelin-induced relaxations were blocked by APJ receptor antagonist, F13A (11), confirming apelin selectively activates endothelial APJ receptors to produce relaxation of coronary arteries.

Apelin increases human forearm blood flow via nitric oxide (52) and improves coronary blood flow and cardiac output in humans (76). Moreover, apelin decreases mean arterial pressure and produces protective vascular effects via endothelial nitric oxide (40, 43, 55, 75). In several isolated arterial preparations, apelin caused endothelium dependent relaxation, in part by nitric oxide dependent pathways (22, 38). Most of these studies have used endothelial nitric oxide

synthase (eNOS) inhibitor, nitro-L-arginine methyl ester (L-NAME) or other nitro-L-arginine analogs to decipher the role of nitric oxide. In agreement with previous results, eNOS inhibitor, NLA inhibited apelin-induced vascular response in endothelial intact coronary arteries, similar to a known endothelial nitric oxide dependent vasodilator, acetylcholine (119-121).

Nitric oxide can activate various downstream mediators to relax vascular smooth muscle cells including cGMP by activating soluble guanylate cyclase (sGC) (116), SERCA to increase intracellular Ca^{2+} re-uptake (50), smooth muscle potassium channels like BK_{Ca} to cause hyperpolarization (48, 49). Interestingly, apelin-induced relaxation was not inhibited in the presence sGC inhibitor, ODQ or protein kinase G inhibitor, DT-2 suggesting cGMP and/or PKG are not involved in apelin-induced relaxation. By contrast, response to acetylcholine was inhibited in the presence of ODQ and DT-2. Moreover, apelin had no effect on basal cGMP levels, whereas acetylcholine increased intracellular cGMP formation, which was inhibited by NLA or ODQ. These results suggest that apelin and acetylcholine-induced NO (or RNS) can activate different mediators to relax vascular smooth muscle of coronary arteries. However, nitro-L-arginine has an ability to inhibit effects of hydrogen peroxide (122). The possible involvement of hydrogen peroxide was precluded by experiments in the presence of PEG-Catalase (123, 124), which had no effect on both apelin or acetylcholine-induced relaxations. The functional role of nitric oxide was further confirmed by real time intracellular NO imaging using DAF-2DA. Apelin increased DAF-2DA fluorescence similar to acetylcholine, which was inhibited in the presence of NLA. DAF-2DA is widely used fluorometric tool to estimate intracellular nitric oxide levels, however its selectivity towards nitric oxide is still questionable. Previous reports suggest that DAF-2DA is more sensitive towards peroxynitrile than nitric oxide (125), and DAF fluorescence can be modulated in the presence of other reactive species and/or Ca^{2+} ions (126, 127). Although in the

present study, both apelin and acetylcholine-induced similar DAF fluorescence, the possible involvement of other RNS cannot be excluded (45).

Based on the involvement of nitric oxide, my next hypothesis was that apelin-induced nitric oxide can relax coronary arteries by direct activation of BK_{Ca} channels (48, 49). In here, apelin-induced relaxations were blocked by a selective and potent BK_{Ca} channel blocker, iberiotoxin. Likewise, acetylcholine-induced response was attenuated in the presence of iberiotoxin. Moreover, apelin-induced response was completely abolished in the presence of high K^+-induced contractile tone, however acetylcholine-induced response had a rightward shift with inhibition of maximum relaxation, establishing disparity in the extent of K^+ channels involvement in these two vasodilators-induced response. Additionally, NO donor - DEA NONOate increased whole cell K^+ currents, which were markedly attenuated by IBTx, but not in the presence of ODQ, further supporting the possibilities that nitric oxide can directly activate BK_{Ca} channels to relax the coronary arteries. These data questions the similarity between exogenous and intracellular NO. The electrophysiology data suggest similarities in NO donor and apelin-induced nitric oxide response, but also identifies that acetylcholine-induced NO differs from the ones generated by exogenous donors (44).

Moreover, apelin-induced relaxations were unchanged in presence of CPA, a potent SERCA inhibitor (128), provides further support for the view that apelin-induced NO can directly activate BK_{Ca} channels to relax coronary arteries. By contrast, CPA attenuated acetylcholine-induced relaxation confirming the possibilities of different vasoactive pathways activated by nitric oxide in the response to different physiological stimulus.

In summary, apelin and acetylcholine both cause endothelium nitric oxide dependent relaxation in coronary arteries by distinct mechanisms i.e. apelin-induced NO directly activates

BK_{Ca} channels, whereas acetylcholine increases NO-cGMP cascade to activate multiple pathways including BK_{Ca} channels and SERCA. These results indicate the possibilities of distinct physiological mechanism(s) involving nitric oxide activated in response to different vasodilators, to modulate the vascular tone of coronary arteries. This novel physiological response of apelin needs further evaluation in other vascular beds, to provide a comprehensive and advanced understanding about apelinergic system.

CHAPTER 4. EFFECT OF APELIN ON BK_{Ca} CHANNELS AND NITRIC OXIDE-INDUCED RELAXATION IN CORONARY ARTERIES: COMPARISON WITH CEREBRAL ARTERIES

Introduction

APJ receptor and its cognate ligand; apelin is continuously evaluated for their therapeutic potentials in cardiovascular regulation. Role of apelin-APJ signaling in vasomotor tone regulation is defined by their higher expression on vascular walls (4, 5, 20) and cardiovascular regulatory region i.e. hypothalamus and brain stem (58, 78, 80). Interestingly, apelin has different effects in central and peripheral system (54). Apelin is classified as a vasodilator based on its ability to relax peripheral arteries including aorta (40, 129), mesenteric and mammary arteries (22, 38, 79). However, central administration or increased gene expression of apelin in hypothalamus and other regulatory regions of brain are shown to cause vasopressor response (59, 60). Likewise, response to central administered apelin on fluid homeostasis and metabolism also differs, as intraperitoneal administered apelin increases energy expenditure and water intake, but intracerebroventricular injection has opposite effects (19, 36, 130). However, effects of apelin on cerebral and peripheral vascular system are still unknown. Our recent report is the first one to propose that vasoactive action of apelin on cerebral arteries may not be protective, like peripheral arteries (30). My previous data suggest that apelin by inhibiting BK_{Ca} channels can impair endothelium nitric oxide dependent relaxation. BK_{Ca} channels are highly localized on smooth muscle cells and has essential modulating role in maintaining membrane potential and vasodilation (94, 95) and impairment of BK_{Ca} channel functions can result into cerebral vasospasm.

Apelin is shown to have dual vascular effects in peripheral blood vessels as well, depending on underlying physiological or pathological conditions. Apelin causes endothelium dependent

vasodilation (38, 40, 43), but can also induce vasoconstriction in endothelium denuded or dysfunctional blood vessels (67, 79). It is important to note that this phenomenon is described in very limited vascular beds and in models with pathological conditions. Moreover, a limited amount of information is available about the possible mechanisms involved in apelin-induced vasoconstriction. The possible signaling events that are suggested to be involved include PKC dependent MLC phosphorylation (33, 67) and PI3K dependent inhibition of BK_{Ca} channels (30, 81).

Apelin has beneficial effects during ischemia reperfusion injury, myocardial infraction and heart failure (13, 76). However, higher expression of apelin in atherosclerotic plaques (18) and stenosis valve disease (71) has been associated with the progression of disease. Surprisingly, regulatory fuctions of apelin-APJ signaling in coronary arteries are not studied thus far. A well-defined role of coronary arteries in cardiovascular system and increasing evidence-supporting role of apelin in coronary blood flow (52, 76) warrants a careful examination of apelin-induced vascular effects in coronary arteries smooth muscle cells. Hence, the present study has two specific aims: 1. determine functional role of apelin-APJ signaling in coronary arterial smooth muscle cells; and 2. compare the signaling events activated in response to apelin between coronary and cerebral arteries.

Materials and Methods

Animals and Tissue Preparation: Experiments were performed on tissues isolated from 12-week-old male Sprague-Dawley rats (Envigo RMS, Indianapolis, IN). Rats were housed at 22 ± 2°C on a 12 h-12 h light-dark cycle and provided with food and water ad libitum. All animal protocols were approved by the North Dakota State University Institutional Animal Care and Use Committee. Rat hearts and brains were isolated from animals anesthetized with isoflurane and

placed into ice-cold physiological salt solution (PSS). Epicardial coronary and cerebral arteries were dissected and cleaned of surrounding tissues.

Smooth Muscle Cell Isolation: Enzymatic isolation of single vascular smooth muscle cells was carried out as described previously, with brief modification (Gonzales et al., 2010). Arteries were placed in cell isolation solution of the following composition (in mM): 60 NaCl, 80 Na-glutamate, 5 KCl, 2 MgCl2, 10 glucose, and 10 HEPES (pH 7.2). Arterial segments were initially incubated in 1.2 mg/ml papain (Worthington, Lakewood, NJ) and 2.0 mg/ml dithioerythritol (Sigma Aldrich, St. Louis, MO) for 17 min at 37°C and then in 0.8 mg/ml type II collagenase (Worthington) for 12 min at 37°C. The digested segments were washed three times in ice-cold cell isolation solution and incubated on ice for 30 min. After this incubation period, vessels were triturated to liberate smooth muscle cells and stored in ice-cold cell isolation solution for use. Smooth muscle cells were used for electrophysiology or imaging within 6 h following isolation.

Electrophysiological Recording: Isolated smooth muscle cells were placed into a recording chamber (Warner Instruments, Hamden, CT) and allowed to adhere for 20 min at room temperature. Whole cell currents were recorded using an AxoPatch 200B amplifier equipped with an Axon CV 203BU headstage (Molecular Devices). Current data were collected and analyzed with pCLAMP 10.0 software (Molecular Devices, Sunnywale, CA). The patch electrodes (3-4 MΩ) were fabricated from 1.5-mm borosilicate glass capillaries. Smooth muscle cells were superfused at a rate of 2.0 ml/min with a solution containing (in mM) 145 NaCl, 5.4 KCl, 1.8 CaCl2, 1 MgCl2, 5 HEPES, 10 glucose; pH 7.4 (NaOH). Patch pipettes were filled with internal pipette solution contained (in mM) 145 KCl, 5 NaCl, 0.37 CaCl2, 2 MgCl2, 10 HEPES, 1 EGTA, 7.5 Glucose; pH 7.2 (KOH). All drugs were diluted in fresh bath solution and perfused into the

experimental chamber. Voltage-activated currents were filtered at 2 kHz and digitized at 10 kHz, and capacitative and leakage currents were subtracted digitally. Series resistance and total cell capacitance were calculated from uncompensated capacitive transients in response to 10 ms hyperpolarizing step pulses (5 mV), or obtained by adjusting series resistance and whole-cell capacitance using the Axopatch 200B amplifier control system. Standard recording conditions for BKCa were achieved by stepping in 10 mV increments from a holding potential of -60 to +80 mV. BK_{Ca} currents were expressed as current density (current divided by its capacitance).

Intracellular Ca^{2+} Imaging: Smooth muscle cells were plated in eight-well borosilicate cover-glass chambers (ThermoFisher Scientific) and incubated for 60 min in 5 μM fluo-4 AM (ThermoFisher Scientific), washed, and perfused with HBSS. The real time imaging was performed using an Olympus confocal laser-scanning microscope (Olympus, Tokyo, Japan) with a 40x numerical aperture oil immersion lens (with excitation at 488 nm and emission at 515 nm). All experiments were carried out at room temperature in HBSS. The effect of various agonists and inhibitors on intracellular Ca^{2+} level was obtained in paired experiments. In experiments with inhibitor, F13A (10 7 M) was added to the chamber for 5 min before addition of apelin (10-7 M). Smooth muscle cells were isolated from four animals (each animal on different day) and 2-3 cells were analyzed for each treatment from each animal.

Vascular Function Studies: Arterial rings (Cerebral: 80-100 μm and Coronary: 120-150 μm; 1.2 mm in length) were suspended in wire myographs (DMT, Aarhus, Denmark) for isometric tension recording. The myograph chambers were filled with PSS (5 ml), which was continuously aerated with 95% O2/5% CO2 and maintained at 37°C throughout the experiment. Cerebral arteries were stretched and normalized as described previously (Chapter 2). Coronary arteries were stretched to using DMT normalization guide and then allowed to stabilize for 30-40 min with

intermittent washings as described previously (chapter 3). Vessel reactivity was confirmed by evoking a response to KCl (60 mM). In some vessels, the endothelium was removed by gently rubbing the intimal surface with a human hair. The presence or absence of endothelium was confirmed by measuring relaxation in response to the endothelium-dependent vasodilators, acetylcholine (10^{-6} M) and bradykinin (10^{-7} M) in coronary and cerebral arteries respectively. Responses to the vasodilators used in this study were obtained in arterial rings contracted with 5-HT (10^{-7} M). Inhibitors were added to the myograph chamber 20 min prior to contraction with 5-HT and the inhibitors remained in contact with the tissues for the remainder of the experiment. Experiments with inhibitors were conducted in parallel with control rings taken from the same animal.

RT-qPCR: Freshly isolated arteries were immediately frozen in liquid nitrogen to collect arterial lysate. Arterial and primary cultured endothelial cell total RNA were isolated using an RNeasy Mini kit, according to the manufacturer's protocol (Qiagen, Germantown, MD). The concentration and purity of RNA was determined using a spectrophotometer (Nanodrop Technologies, Wilmington, DE). cDNA was synthesized using 50 ng of RNA and an iScript cDNA synthesis kit (Bio-Rad). A Sybr Green expression assay was used to determine expression of apelin, with β-actin used as a housekeeping gene (Bio-Rad). The following primers (synthesized by Invitrogen, Carlsbad, CA) were used:

Apelin gene – forward: 5'-GAGGAAATTTCGCAGACAGC-3'; reverse: 5'-CAGCGATAACAGGTGCAAGA -3'; β-actin – forward: 5'-GTCGTACCACTGGCATTGTG-3'; reverse: 5'-TCTCAGCTGTGGTGGTGAAG-3'. Real-time RT-PCR reaction conditions were 95°C for 10 min, followed by 40 cycles of 95°C for 10 s, 60°C for 20 s, and 72°C for 30 s.

Immunofluorescence Microscopy: Freshly isolated coronary and cerebral arteries were fixed in 10% formalin solution, processed and embedded in paraffin blocks. Paraffin blocks were sectioned at 5 μm and mounted onto ProbeOn Plus microscopic slides (ThermoFisher Scientific). Sections were fixed by heating at 60°C for 30 min. Nonspecific antibody binding was blocked with normal serum [10% w/v; in TBS] for 1 h at room temperature. Sections were incubated overnight at 4°C in 1% serum containing a primary antibody against apelin (Abcam, Cambridge, MA), smooth muscle actin (Santa Cruz Biotechnology) and/or PECAM-1 (Santa Cruz Biotechnology). For co-localization, double immunofluorescent staining was performed by incubating the tissue sections with more than one primary antibody at the same time. Detection of the primary antibodies against the apelin, smooth muscle actin and PECAM-1 was accomplished using Alexa Fluo-633 conjugated (donkey anti-rabbit IgG; Invitrogen, Carlsbad, CA), Alexa Fluor-488 (donkey anti-mouse IgG; Santa Cruz Biotechnology) and Alexa Fluor-555 (donkey anti-goat IgG; Santa Cruz Biotechnology) secondary antibodies, respectively. Rat lung tissue was used as positive control for apelin detection (Hosoya et al., 2000). All negative controls were incubated with 1% serum solution overnight followed by secondary antibodies. All dilutions and thorough washes between stages were performed using TBS containing Triton X-100 [0.3% (v/v)] unless otherwise stated. Sections were drained by blotting with filter paper, and a drop of mounting medium containing an anti-fade reagent (Vector Laboratories, Burlingame, CA) was added to the slides. Images of the sections were obtained using an Olympus confocal laser-scanning microscope (Olympus, Tokyo, Japan). The images were generated using Olympus FluoView FV300 (v. 4.3) confocal software.

Western Immunoblotting: Freshly isolated coronary and cerebral arteries were immediately frozen in liquid nitrogen. Tissues were homogenized in lysis buffer and supplemented

with a protease and phosphatase inhibitor cocktail (FabGennix International, Frisco, TX) at 4°C using an IKA Ultra-Turrax T8 homogenizer (IKA Works Inc., Wilmington, NC). Tissue homogenates were kept on ice for 10 min and then centrifuged at 10000g for 10 min. Supernatant was collected, and protein determination was performed using a Pierce BCA protein estimation kit (ThermoFisher Scientific, Waltham, MA). Aliquots of supernatant containing equal amounts of protein (40 μg) were separated on 7.5-10% polyacrylamide gel by SDS polyacrylamide gel electrophoresis, and proteins were electroblotted onto a polyvinylidene difluoride membrane (Bio-Rad Laboratories, Hercules, CA). Blots were blocked with 5% nonfat dry milk in Tris-buffered saline (TBS, pH 7.4) and incubated overnight at 4°C with a primary antibodies specific for Akt and phosphor-Akt using a dilution of (1:500) (Cell Signaling, Denver, MA). Membranes were washed three times for 10 min using TBS-Tween 20 and incubated with a horseradish peroxidase-linked secondary antibody (Cell Signaling). To ensure equal loading, the blots were analyzed for β-actin expression using an anti-actin antibody (Santa Cruz Biotechnology Inc.). Immuno-detection was performed using an enhanced chemiluminescence light detection kit (ThermoFisher Scientific).

Drugs: The following drugs were used: acetylcholine, diethylamine NONOate (DEA NONOate), sodium nitroprusside (SNP), diltiazem, 5-hydroxytryptamine (5-HT) and forskolin (Sigma Chemical, St. Louis, MO); iberiotoxin (Tocris, Ellisville, MO); apelin-13, and F13A (H-Gln-Arg-Pro-Arg-Leu-Ser-His-Lys-Gly-Pro-Met-Pro-Ala-OH trifluoroacetate salt) (Bachem, Torrance, CA). Drug solutions were prepared fresh daily, kept on ice, and protected from light until used. All drugs were dissolved in double-distilled water with the exception of forskolin, which was dissolved initially in DMSO prior to further dilution in double-distilled water. Drugs

were added to the myograph chambers in volumes not greater than 0.02 ml. Drug concentrations are reported as final molar concentrations in the myograph chamber.

Data Analysis: Relaxation responses are expressed as a percent of the initial tension induced by 5-HT (10-7 M). EC50 values (drug concentration that produced 50% of its own maximal response) were determined, converted to their negative logarithm, and expressed as -log molar EC50 (pD2). For Ca2+ imaging, amplitude of DAF-2 fluorescence was calculated by subtracting peak fluorescence intensity from basal fluorescence intensity. RT-qPCR data were analyzed to quantify relative gene expression by ΔCt relative to β-actin. Results are expressed as means ± SEM, and n refers to the number of animals from which blood vessels were taken, unless otherwise stated. Values were compared by Student's t-test or one-way ANOVA using Tukey's test as post-hoc analysis for paired or unpaired observations, as appropriate, to determine significance between groups. Values were considered significantly different when $p<0.05$.

Results

Electrophysiology Studies

Whole cell BK_{Ca} currents were recorded in freshly isolated smooth muscle cells from coronary and cerebral arteries. In cells isolated from coronary arteries, super perfusion of apelin (10^{-7} M, 5 min) had no inhibitory effects of BK_{Ca} channel current density, but further addition of iberiotoxin; (IBTx, 10^{-7} M, 5 min) caused a significant reduction in current density **(Figure 26A and 26B)**. Likewise, DEA NONOate (DEA, 10^{-5} M, 3 min) **(Figure 24E)** and NS1619 (10^{-5} M, 3 min) **(Figure 27B)**-induced currents were not attenuated in the presence of apelin **(Figure 26C and 27C)**, but were significantly inhibited by IBTx **(Figure 26D and 27D)** in coronary arterial smooth muscle cells. In contrast, apelin (10^{-7} M, 5 min) caused a significant reduction in BK_{Ca}

channel current density, in cerebral smooth muscle cells, induced by membrane depolarization **(Figure 28)** or DEA **(Figure 11)**.

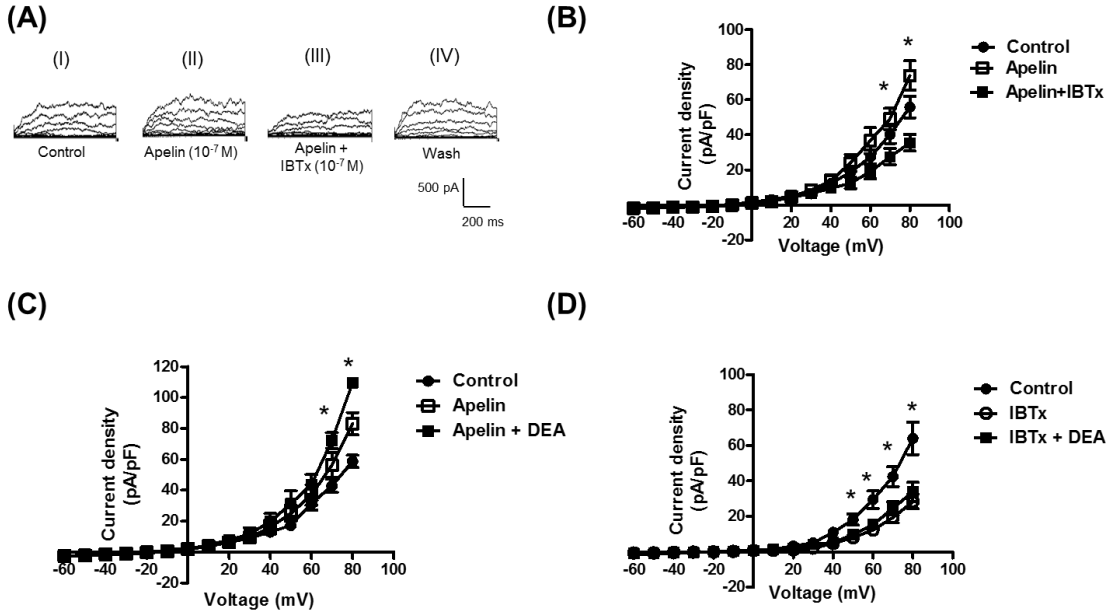

Fig. 26. Apelin does not inhibit BK_{Ca} channels currents in coronary arterial smooth muscle cells. Whole cell BK_{Ca} currents were recorded in freshly isolated vascular smooth muscle cells in response to successive voltage pulses of 800 ms duration, increasing in 10 mV increments from -60 mV to +80 mV with and without apelin (10^{-7} M) and/or Iberiotoxin (IBTx, 10^{-7} M). A.I - IV: Representative tracings depicting the sequential current recordings from a single smooth muscle cell I) control, in the presence of (II) apelin (10^{-7} M, 5 min) alone or (III) combined with IBTx (10^{-7} M, 5 min) and (IV) Wash; B-D: Summary I-V curve plots of BK_{Ca} currents at baseline (B) and after treatment with DEA (10^{-5} M), in the presence of (C) apelin and (D) IBTx (10^{-7} M). Values are represented as mean ± SEM (n=6). * $p<0.05$ vs. control current density.

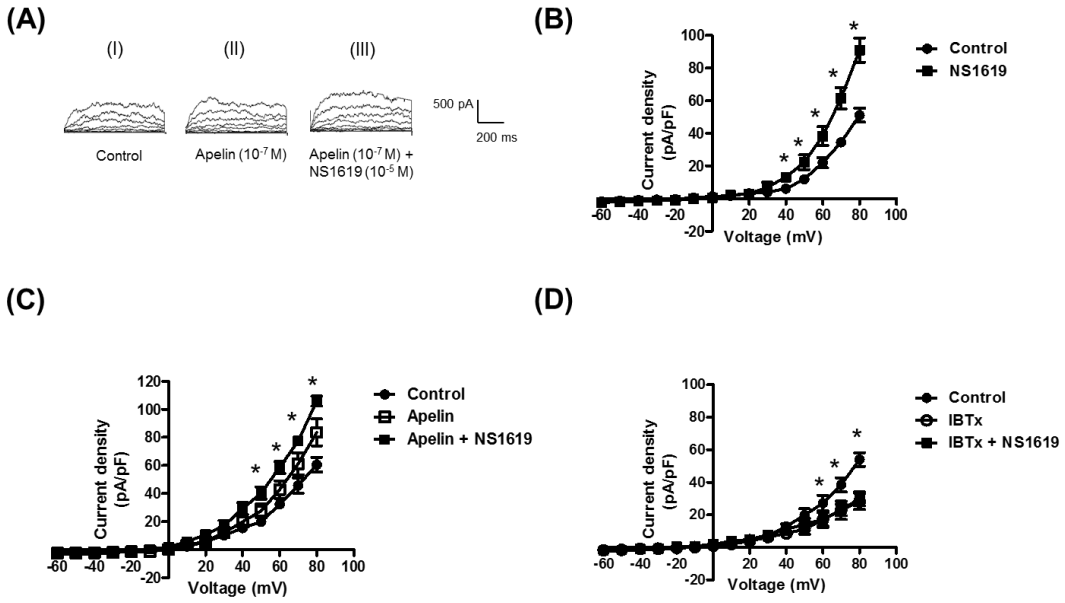

Fig. 27. Apelin has no inhibitory effects on BK_{Ca} channel currents-induced by NS1619.
Whole cell BK_{Ca} currents were recorded in freshly isolated vascular smooth muscle cells in response to successive voltage pulses of 800 ms duration, increasing in 10 mV increments from -60 mV to +80 mV with and without apelin (10^{-5} M) and/or Iberiotoxin (IBTx, 10^{-7} M). A (I – III): Representative tracings depicting the sequential current recordings from a single smooth muscle cell I) control, in the presence of (II) apelin (10^{-7} M, 5 min) alone and (III) along with NS1619 (10^{-5} M, 3 min); B - D: Summary I-V curve plots of BK_{Ca} currents at (B) baseline and after treatment with NS1619 (10^{-5} M), in the presence of (C) apelin (10^{-7} M) and (D) IBTx (10^{-7} M). Values are represented as mean ± SEM (n=6). * $p<0.05$ vs. control current density.

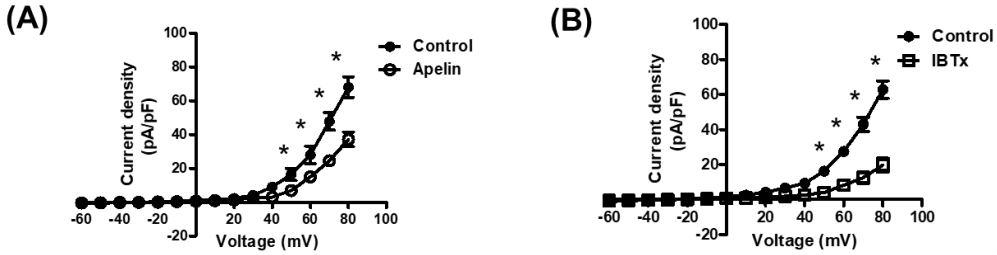

Fig. 28. Apelin inhibits BK_{Ca} channels currents in cerebral arterial smooth muscle cells.
Summary I-V curve plots of BK_{Ca} currents at baseline and in the presence of (A) apelin (10^{-7} M) and (B) IBTx (10^{-7} M) in cerebral arterial smooth muscle cells. Values are represented as mean ± SEM (n=6-7). * $p<0.05$ vs. control current density.

Functionality of APJ receptor

Intracellular calcium imaging was used to determine functionality of coronary and cerebral smooth muscle APJ receptor. Freshly isolated smooth muscle cells were stimulated with different concentrations of apelin (10^{-7} M and 10^{-6} M). Apelin (10^{-7} M) caused a strong rapid and transient signal in smooth muscle cells, isolated from both coronary and cerebral arteries, and fluorescent intensity was not affected by further increasing apelin concentration to 10^{-6} M. Likewise, bolus addition of apelin (10^{-6} M) caused an increase in fluorescence intensity. APJ receptor antagonist, F13A (10^{-7} M, 5 min) completely abolished apelin-induced increase in intensity; however, F13A by itself had no effect **(Figure 29)**.

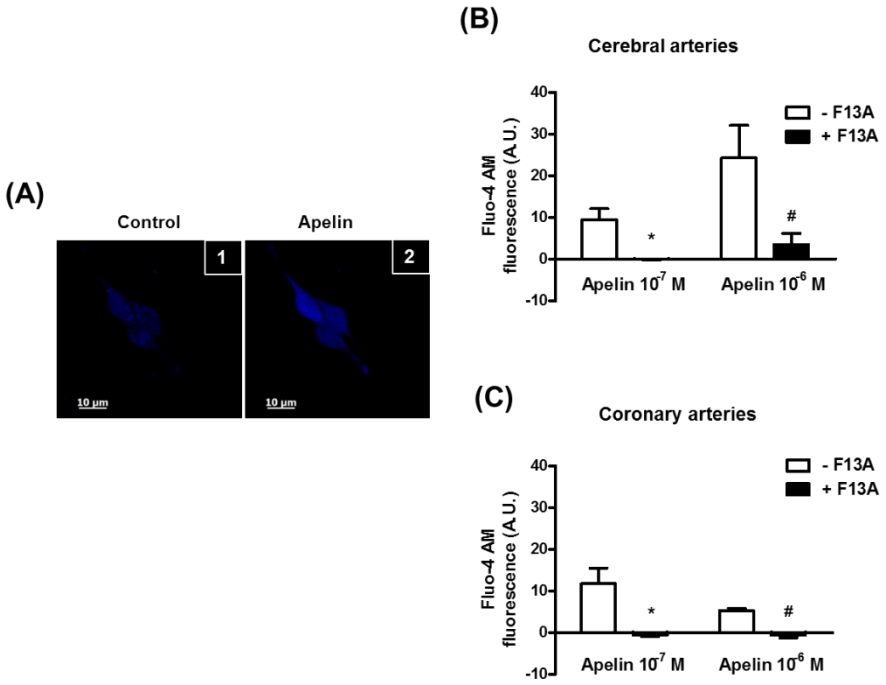

Fig. 29. Smooth muscle APJ receptor are functionally active.
(A) Representative images of Fluo-4 AM (1 µM) loaded freshly isolated smooth muscle cells (1) before and (2) after treatment of apelin (10^{-7} M). Bar graph representing increase in Fluo-4 AM fluorescence after exposure to apelin (10^{-7} M or 10^{-6} M) in the absence and presence of F13A (10^{-7} M) in (B) cerebral arterial and (C) coronary arterial smooth muscle cells. Amplitude of change in Fluo-4 AM fluorescence was calculated as the maximal fluorescence after agonist exposure corrected for baseline fluorescence. Values are represented as means ± S.E.M. (n = 4 animals, 5 - 15 total cells). * $p<0.05$ vs. apelin 10^{-7} M and $^{\#}$ $p<0.05$ vs. apelin 10^{-6} M as calculated by paired t-test.

Vascular Relaxation Studies

In coronary arterial segments contracted with 5-HT (10^{-7} M), nitric oxide donors DEA NONOate (DEA, 10^{-9} - 3 x 10^{-5} M) and sodium nitroprusside (SNP, 10^{-9} - 3 x 10^{-5} M) caused concentration dependent relaxations. Apelin (10^{-7} M) had no inhibitory effect on DEA (6.38 ± 0.20 vs. 6.15 ± 0.28 without and with apelin, n=5) and SNP (7.69 ± 0.15 vs.7.43 ± 0.27 without and with apelin, n=5)-induced relaxations **(Figure 30A and 30C)**, but IBTx caused a marked inhibition **(Figure 30B and 30D)**. Similarly, acetylcholine induced nitric oxide-cGMP dependent relaxation **(Figure 18A-B)**, was attenuated by IBTx, but apelin was without effect (pD2: 7.16 ± 0.17 vs. 7.38 ± 0.30, p>0.05, n=6) **(Figure 31A-B)**.

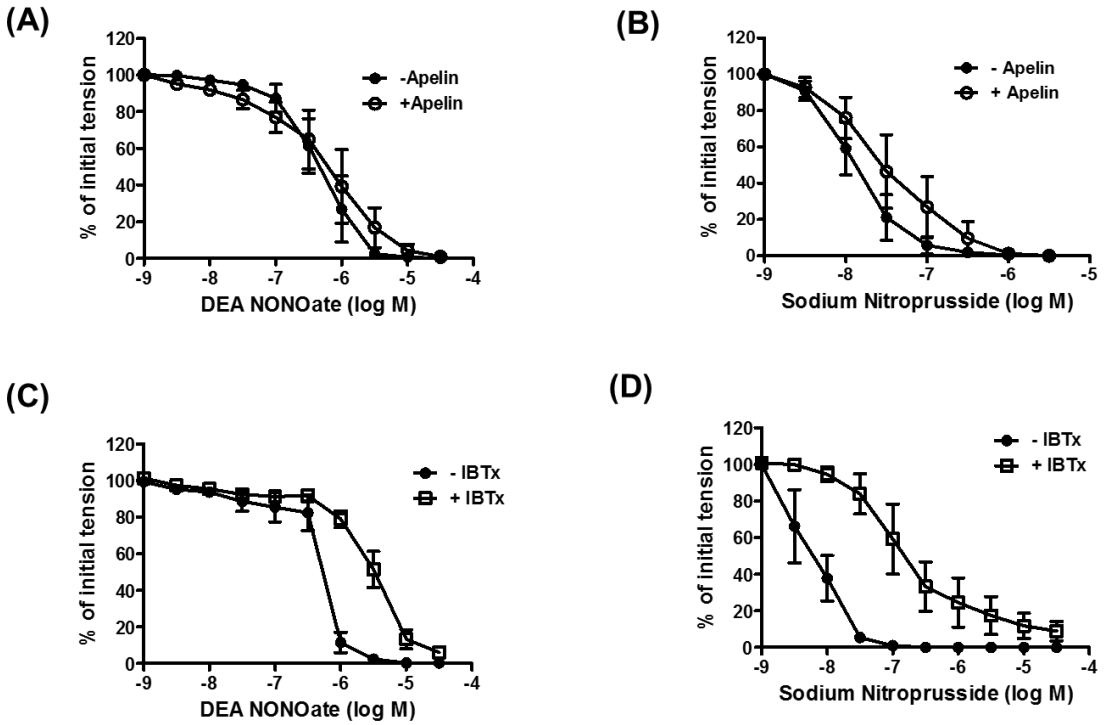

Fig. 30. Apelin does not inhibit nitric oxide donors-induced relaxations of coronary arteries. Log concentration-response curve for DEA NONOate (A and C) and Sodium nitroprusside (B and D) in producing relaxation of endothelium denuded coronary arteries in the absence and presence of apelin (10^{-7} M) or IBTx (10^{-7} M). Values are represented as mean ± SEM (n=4-6).

Then experiments were performed to evaluate effects of apelin on contractile response curve of 5-HT (10^{-9} - 3 x 10^{-5} M). In endothelium intact coronary arterial segments, apelin had no effect of contractile tone induced by 5-HT. However, apelin (10^{-7} M) caused a significantly leftward shift in the response to 5-HT in endothelium denuded arterial segments (pD2: 7.16 ± 0.17 vs. 7.38 ± 0.30, p>0.05, n=6) with no significant change in maximum contractile response **(Figure 31C-D)**. However, apelin had no effect on 5-HT -induced contractile response in cerebral arteries segments with or without endothelium.

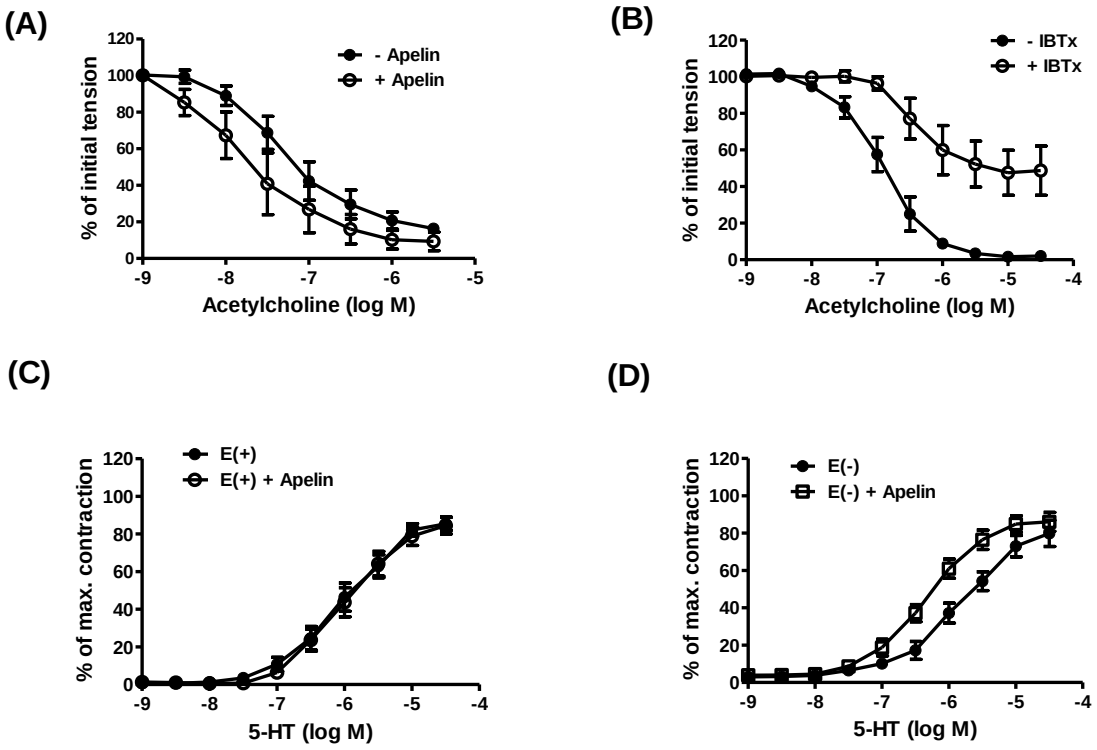

Fig. 31. Apelin does not impair acetylcholine-induced relaxation, but exacerbate 5-HT contractile response.
Log concentration-response curve for A-B) acetylcholine in producing relaxation of endothelium intact coronary arteries in the absence and presence of (A) apelin (10^{-7} M) or (B) IBTx (10^{-7} M); (C-D) 5-HT in producing vasoconstriction of endothelium (C) intact and (D) denuded coronary arteries in the absence and presence of apelin (10^{-7} M). Values are represented as mean ± SEM (n=6).

Effect of apelin on cAMP-induced response was evaluated using an adenylate cyclase activator, forskolin. Apelin had no inhibitory effects on forskolin (10^{-9} - 3 x 10^{-5} M)-induced concentration dependent relaxation of coronary arteries (pD2: 7.08 ± 0.31 vs. 7.12 ± 0.32 without and with apelin, n=6), but caused a rightward shift in the response in cerebral arteries (pD2: 6.94 ± 0.17 vs. 6.28 ± 0.15 without and with apelin, n=5), which was abolished in the presence of F13A **(Figure 32)**.

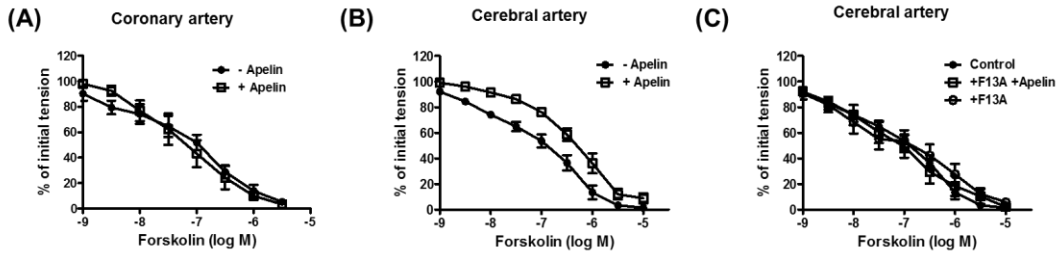

Fig. 32. Apelin impairs forskolin-induced relaxation of cerebral, but not of coronary arteries. Log concentration-response curve for forskolin in producing relaxation of endothelium denuded (A) coronary, and cerebral arteries in the absence and presence of (B) apelin (10^{-7} M) alone; or (C) with F13A (10^{-7} M). Values are represented as mean ± SEM (n=5-6).

Expression of Apelin

RT-qPCR and immunofluorescence confocal microscopy were used to determine expression and localization of apelin gene transcripts and protein respectively. **Figure 33A** shows expression of apelin gene transcript in coronary and cerebral arteries in comparison to rat lung tissue, which was used as a positive control (17). Likewise, apelin transcripts levels were also similar in primary endothelial cells cultured from coronary and cerebral arteries **(Figure 33B)**. Immunofluorescence staining showed localization of apelin in endothelial in both cerebral and coronary arteries **(Figure 33C)**. Moreover, apelin protein was also localized in smooth muscle in coronary arteries. Rat lung tissue demonstrated selective binding of apelin antibody on bronchial epithelium **(Figure 33C.7)**; inset showed non-specific binding of secondary antibody by itself.

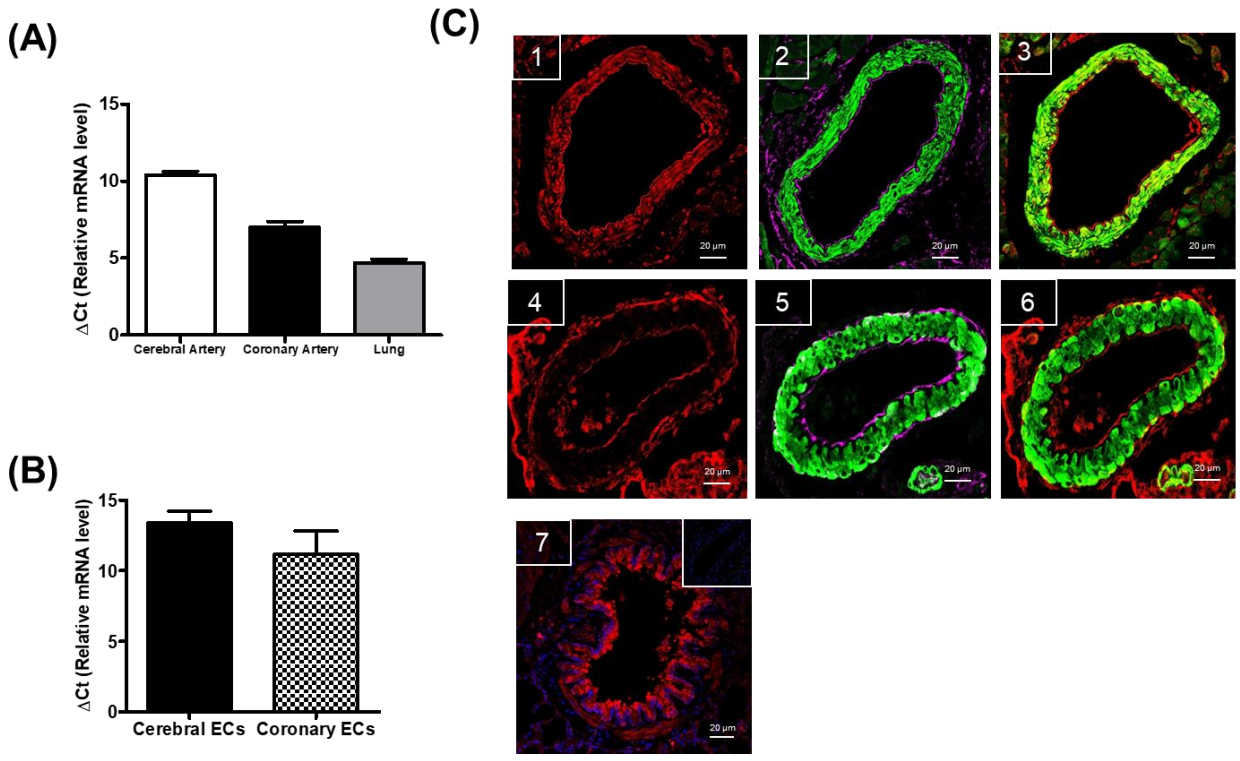

Fig. 33. Expression and localization of apelin.
Bar graph showing relative mRNA expression of apelin, represented as ΔCt values relative to β-actin in A) intact cerebral and coronary arteries and (B) primary endothelial cells cultured from cerebral and coronary arteries. Data are presented as mean ± SEM (n=4-6). (C) Representative immunofluorescence images of: 1 and 4: apelin (red fluorescence); 2 and 5: merged image showing endothelial cells (magenta fluorescence) with smooth muscle cells actin (green fluorescence); 3 and 6: merged image showing apelin co-localized areas in smooth muscle cells (yellow fluorescence) and endothelium (red fluorescence) in rat coronary artery (top panel) and cerebral artery (middle panel); and 7: apelin (red fluorescence) with nuclear staining (blue fluorescence) in rat bronchial epithelium (positive control); inset demonstrates a lack of staining after incubation of tissue with serum followed by the secondary antibody (negative control). The images are representative of those obtained from four different animals. Scale bar, 20 μm.

Effect of Apelin on PI3K/Akt Signaling Pathway

PI3K activity was detected by the ratio of phosphorylated Akt and total Akt using western blot in coronary and cerebral arteries. Apelin (10^{-7} M) treatment had no significant effect on PI3K activity in coronary arteries, as indicated by unchanged p-Akt/total Akt ratio **(Figure 34A-B)**. In cerebral arteries, apelin treatment stimulated time dependent increase in p-Akt level, which peaked at ~10 minute, indicating a two-fold increase in PI3K activity **(Figure 34C-D)**. These data suggest

that PI3K pathways are activated in response to apelin in cerebral arteries, but not in coronary arteries.

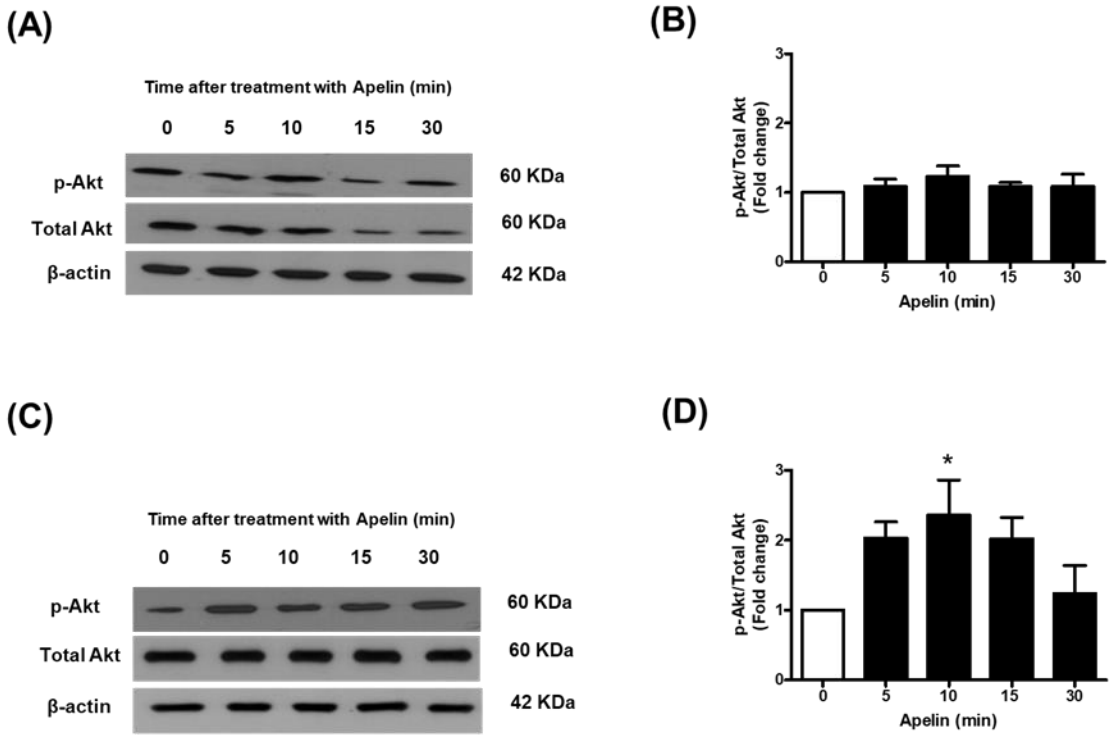

Fig. 34. Effect of apelin on PI3-kinase activity in coronary and cerebral arteries.
Phosphorylated and total Akt levels were measured in coronary (A-B) and cerebral (C-D) arteries after treatment with apelin (10^{-7} M) for durations indicated in the figure. A and C: representative blots were probed with anti-serine-phosphorylation of Akt (p-Akt) or anti-Akt (total) antibodies along with β-actin. B and D: Bar graphs summarizing the effect of apelin on PI3-kinase activity expressed as a ratio of p-Akt/Akt protein levels. Data are means ± SEM (n=4). * $p<0.05$ compared with non-stimulated control.

Discussion

The major findings of the present study are: 1) apelin does not inhibit BK_{Ca} currents and nitric oxide dependent relaxation of coronary arteries; and 2) functionally active smooth muscle APJ receptor participates in different signaling pathways between cerebral and coronary arteries to regulate vasomotor tone. These findings provide novel information about functional differences

in apelinergic signaling between cerebral and coronary arteries, which can help us in designing targeted apelin based therapeutics to enhance beneficial effects, while reducing the associated risk.

Vasoconstriction is known to be regulated by calcium release (63), MLC phosphorylation (64) and ion channels (65). APJ receptors are abundantly localized on vascular smooth muscle cells (30) and can cause vasoconstriction by modulating proteins (33) as well as ion channels (30). My previous data suggest that apelin alters vasomotor tone of cerebral arteries by impairing BK_{Ca} channel functions. Potassium ion channels are highly expressed throughout the vasculature including coronary arteries and are potential modulators for vessel diameter and reactivity. Hence, my first aim was to understand effect of apelin on BK_{Ca} channel currents in freshly isolated smooth muscle cells from coronary arteries. Surprisingly, apelin had no inhibitory effects on BK_{Ca} channel currents induced by membrane depolarization or by activators like nitric oxide donor or BK_{Ca} channel opener. However, IBTx caused significant inhibition of BK_{Ca} channel currents in the similar preparations. To further confirm these results using functional studies, effect of apelin was evaluated on exogenous and endogenous NO-induced relaxations and in line with the electrophysiology data, apelin had no inhibitory effects on NO-induced relaxation in coronary arteries.

These findings raised questions about functionality of APJ receptor and signaling events activated by apelin-APJ receptor in coronary arteries. Functionality of APJ receptor was evaluated using non-ratiometric analysis with intracellular calcium indicator dye, Fluo-4 AM. Apelin treatment caused a substantial increase in fluorescence intensity, which was abolished in the presence of F13A, confirming smooth muscle APJ receptor of coronary arteries are functionally active. APJ receptor are shown to be coupled with multiple G-protein subunits (32-34) and previous data showed involvement of pertussis toxin sensitive $G_{\alpha i/o}$ subunits involvement in apelin-

induced inhibitory effects on BK_{Ca} channels (30). Further, apelin is also shown to inhibit forskolin-induced cAMP formation via pertussis toxin sensitive $G_{\alpha i/o}$ subunits (131). In present study, I determined effect of apelin on forsokin-induced relaxation of coronary and cerebral arteries. In line with previous results (30), apelin inhibited forskolin-induced response in cerebral arteries, but not in coronary arteries.

Apelin-induced effects on vascular smooth muscle cells, including BK_{Ca} channel inhibition, are shown to be mediated by PI3K/Akt signaling pathways (30, 132, 133). Hence, I also evaluated effects of apelin on PI3K/Akt signaling pathways. The present results show that apelin has no effect on PI3K activity in coronary arteries, but significantly increases PI3K activity in cerebral arteries. These results altogether suggest activation of different signaling pathways in response to apelin between coronary and cerebral arteries. Further, I also determined expression and localization of apelin and in both cerebral and coronary arteries, apelin gene expression and localization were found similar as reported previously (17, 18, 78).

Interestingly, apelin-induced vasoconstriction response in aorta is shown to be mediated by PKC and MLC phosphorylation (64, 67). Although, I did not observe any inhibitory effects of apelin on BK_{Ca} channel functions and nitric oxide dependent relaxations, but intriguingly apelin enhanced 5-HT-induced contractile response of endothelial denuded coronary arteries, and this effect of apelin was absent in endothelium intact arterial segment or in cerebral arteries. A significant role of MLC phosphorylation and intracellular calcium has been shown in 5-HT induced contractile response in coronary arteries (134, 135). It is possible that apelin exacerbate 5-HT-induced contractile response by additive actions on MLC phosphorylation. Further studies in this direction can help in providing a comprehensive answer for the observed differences in apelin-induced response between cerebral and coronary arteries.

In summary, the present study suggests that apelin has different effects on smooth muscle BK_{Ca} channels between cerebral and coronary arteries. However, to provide a broader overview about effect of apelin in peripheral vasculature, further studies are required in other peripheral vascular beds, particularly in vascular beds where apelin is shown to increase PI3K/Akt activity (132, 133). Current findings along with others can help in developing apelin analogs with selective actions towards peripheral vasculature to produce beneficial cardiovascular response.

CHAPTER 5. SUMMARY AND CONCLUSIONS

Targeting apelinergic system for cardiovascular diseases provides many exciting opportunities. Apelin-APJ receptor signaling has beneficial effects in many cardiovascular and metabolic diseases including hypertension, myocardial infraction-reperfusion injury, pulmonary hypertension, obesity and diabetes. However, a cautionary evaluation of controversial reports, about different vasoactive response of apelin, is prerequisite. Rather than focusing on peripheral beneficial effects, a broader overview of apelin signaling in different vascular beds can help us in better understanding diverse response of apelin. The complex apelin-APJ receptor signaling makes apelinergic system a challenging target for therapeutic development; however, the enormous potential of apelin along with various novel beneficial effects demand for a thorough understanding about apelin-induced effects. Current literature provides several key, but incomplete information about apelin-signaling such as: 1) apelin has different effects on cerebral and peripheral system, but vascular effects are not studied thus far; 2) apelin is shown to have beneficial vascular effects in peripheral arteries, but these conclusions are made based on data from limited vascular beds. Moreover, the mediators and signaling cascade(s) involved in apelin-induced vasodilation are not yet determined; and 3) possible pathways or signaling events involved in the different effects of apelin between central and peripheral vasculature (if any) are not studied thus far.

Apelin and its analogs are currently being evaluated in multiple clinical trials for their therapeutic potential in pulmonary hypertension, myocardial infraction and coronary atherosclerotic heart disease (https://clinicaltrials.gov). Continuous efforts are made to design apelin analogs, but we still lack a comprehensive understanding about apelin signaling. Thus, the

present research was focused to determine apelin-induced vascular effects in cerebral arteries and compare them with coronary arteries.

The results of the present study for the first time demonstrate the presence of APJ receptor gene transcripts and protein in cerebral and coronary arteries. Immunofluorescence imaging show that APJ receptors are localized on both endothelial and smooth muscle cells of cerebral arteries and coronary arteries. Moreover, apelin itself has no effect on vasomotor tone of cerebral arteries. However, apelin inhibits NO-induced relaxation in cerebral arteries by inhibiting BK_{Ca} channels functions. BK_{Ca} channels are ubiquitously express on vascular smooth muscle cells and have an essential role in regulating membrane potential and hence, the vascular tone. BK_{Ca} channels are sensitive towards membrane depolarization and changes in intracellular calcium ion concentration. Activation of BK_{Ca} channels results into efflux of K^+ ions, bringing in hyperpolarization and vasorelaxation. BK_{Ca} channels are regulated by multiple factors including intracellular calcium, phosphorylation and oxidation state, and dysregulation of BK_{Ca} channel function is correlated with increased risk of vasospasm and ischemia. Hence, these findings raise a potential concern about risk of cerebral vascular dysfunction under conditions where plasma levels of apelin are elevated, such as diabetes or obesity.

Further, I evaluated vascular effects of apelin in coronary arteries and compared them with cerebral arteries. Interestingly, apelin causes endothelium dependent relaxation of coronary arteries and does not inhibit BK_{Ca} channel currents or functions in coronary arteries. Interestingly, functionally active smooth muscle APJ receptors are found to be participating in different signaling pathways between cerebral and coronary arteries. In cerebral arteries, apelin inhibits forskolin-induced cAMP mediated relaxation and results into an increase PI3K activity. In contrast, apelin has no inhibitory effect on forskolin response and/or PI3K activity in coronary arteries. These

heterogeneities in vascular effects of apelin between cerebral and coronary arteries provide novel mechanistic details, which can be utilized in designing apelin-based therapies.

Interestingly, apelin-induced relaxation of coronary arteries also has several novel and characteristic features: 1) apelin requires nitric oxide, but not cGMP to induce relaxation of coronary arteries; and (2) nitric oxide released in response to apelin can directly activate BK_{Ca} channels to mediate relaxation. Surprisingly, my results also suggest that nitric oxide generated in response to different stimuli (apelin vs. acetylcholine) has an ability to activate different signaling pathways. My data suggest that in contrast to apelin, acetylcholine causes relaxation via NO-cGMP-PKG dependent pathways in coronary arteries. This phenomenon may provide a paradigm shift as current literature suggest that nitric oxide can activate different signaling pathways in different vascular beds. However, for the first time, I am reporting that nitric oxide can participate in multiple signaling pathways in a single vascular bed.

The present research provides several new challenges and future directions. A logical extension would be to understand effects of endogenously released apelin on BK_{Ca} channel functions. Regulation and release of apelin in the circulation or surrounding tissue(s) are yet to be determined. It would be interesting to stimulate endogenous apelin release and evaluate its role in physiology and pathophysiology. My preliminary results in primary cultured cells isolated from cerebral arteries suggest that hypoxia causes time dependent increase in apelin gene expression, in both endothelial and smooth muscle cells **(Figure 35)**. Nevertheless, whether this increased gene expression correlates with increase in apelin release has yet to be determined. In addition, it is essential to understand impact of apelin-induced inhibitory effects in pathological conditions like hypertension, diabetes and obesity with higher plasma apelin levels. Moreover, determination of these inhibitory actions of apelin in human cerebral arteries can not only advance our knowledge,

but also help in devising apelin-based therapy. Another novel feature of present study that has high impact in future research; understands possible reasons for differences in nitric oxide response with different stimulus. A guanylate cyclase knockout animal model can be utilized to further characterize the phenomenon. Likewise, analysis of possible signaling mechanisms-activated in response to apelin in coronary arterial smooth muscle cells can provide a comprehensive understanding about heterogeneous effects between cerebral and coronary arteries. The present research also suggest the possibilities that multiple subtypes of APJ receptor exists in mammals. In fact, a recent study showed that response of apelin analog is not dependent on APJ receptor, giving possibilities of another cell surface receptor having affinity towards apelin and its analogs. Future research to answer these puzzling questions can provide better opportunities to target beneficial effects of apelin in human physiology and cardiovascular diseases.

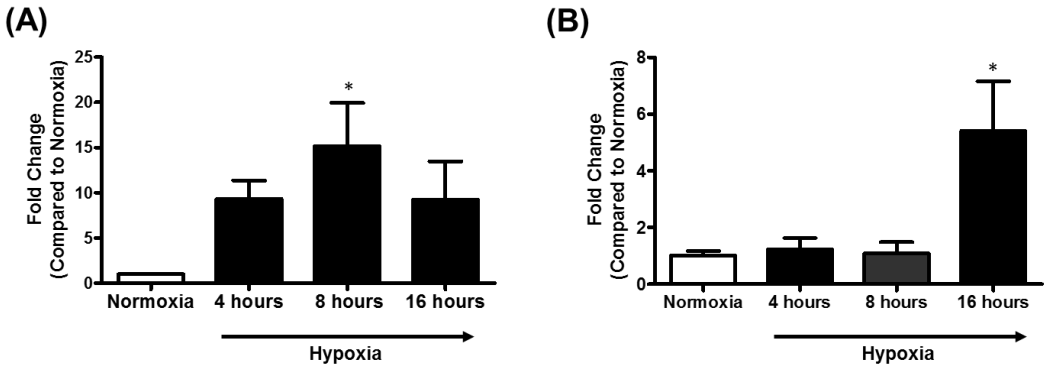

Fig. 35. Effect of hypoxia on apelin gene expression in primary cultured cells from cerebral arteries.
Bar graph representing fold change in apelin mRNA levels with the treatment of hypoxia (1% O_2) in primary cultured (A) endothelial cells; and (B) smooth muscle from cerebral arteries. Data are means ± SEM (n=3-5). * $p<0.05$ compared with Normoxia.

REFERENCES

1. E.J. Benjamin, M.J. Blaha, S.E. Chiuve, M. Cushman, S.R. Das, R. Deo, S.D. de Ferranti, J. Floyd, M. Fornage, C. Gillespie, C.R. Isasi, M.C. Jimenez, L.C. Jordan, S.E. Judd, D. Lackland, J.H. Lichtman, L. Lisabeth, S. Liu, C.T. Longenecker, R.H. Mackey, K. Matsushita, D. Mozaffarian, M.E. Mussolino, K. Nasir, R.W. Neumar, L. Palaniappan, D.K. Pandey, R.R. Thiagarajan, M.J. Reeves, M. Ritchey, C.J. Rodriguez, G.A. Roth, W.D. Rosamond, C. Sasson, A. Towfighi, C.W. Tsao, M.B. Turner, S.S. Virani, J.H. Voeks, J.Z. Willey, J.T. Wilkins, J.H. Wu, H.M. Alger, S.S. Wong, P. Muntner, C. American Heart Association Statistics, and S. Stroke Statistics. Heart Disease and Stroke Statistics-2017 Update: A Report From the American Heart Association. Circulation. 135:e146-e603 (2017).
2. M.P. Dubé, S. de Denus, and J.C. Tardif. Pharmacogenomics to Revive Drug Development in Cardiovascular Disease. Cardiovasc Drugs Ther. 30:59-64 (2016).
3. X.H. Yu, Z.B. Tang, L.J. Liu, H. Qian, S.L. Tang, D.W. Zhang, G.P. Tian, and C.K. Tang. Apelin and its receptor APJ in cardiovascular diseases. Clin Chim Acta. 428:1-8 (2014).
4. M.J. Kleinzand A.P. Davenport. Immunocytochemical localization of the endogenous vasoactive peptide apelin to human vascular and endocardial endothelial cells. Regul Pept. 118:119-125 (2004).
5. M.J. Kleinz, J.N. Skepper, and A.P. Davenport. Immunocytochemical localisation of the apelin receptor, APJ, to human cardiomyocytes, vascular smooth muscle and endothelial cells. Regul Pept. 126:233-240 (2005).
6. A.Z. Kaleaand D. Batlle. Apelin and ACE2 in cardiovascular disease. Current opinion in investigational drugs. 11:273-282 (2010).

7. A. Pauli, M.L. Norris, E. Valen, G.L. Chew, J.A. Gagnon, S. Zimmerman, A. Mitchell, J. Ma, J. Dubrulle, D. Reyon, S.Q. Tsai, J.K. Joung, A. Saghatelian, and A.F. Schier. Toddler: an embryonic signal that promotes cell movement via Apelin receptors. Science. 343:1248636 (2014).

8. S.C. Chng, L. Ho, J. Tian, and B. Reversade. ELABELA: a hormone essential for heart development signals via the apelin receptor. Developmental cell. 27:672-680 (2013).

9. X. Iturrioz, R. Alvear-Perez, N. De Mota, C. Franchet, F. Guillier, V. Leroux, H. Dabire, M. Le Jouan, H. Chabane, R. Gerbier, D. Bonnet, A. Berdeaux, B. Maigret, J.L. Galzi, M. Hibert, and C. Llorens-Cortes. Identification and pharmacological properties of E339-3D6, the first nonpeptidic apelin receptor agonist. FASEB journal : official publication of the Federation of American Societies for Experimental Biology. 24:1506-1517 (2010).

10. P. Khan, P.R. Maloney, M. Hedrick, P. Gosalia, M. Milewski, L. Li, G.P. Roth, E. Sergienko, E. Suyama, E. Sugarman, K. Nguyen, A. Mehta, S. Vasile, Y. Su, S. Shi, D. Stonich, H. Nguyen, F.Y. Zeng, A.M. Novo, M. Vicchiarelli, J. Diwan, T.D.Y. Chung, A.B. Pinkerton, and L.H. Smith. Functional Agonists of the Apelin (APJ) Receptor. Probe Reports from the NIH Molecular Libraries Program, Bethesda (MD), 2010.

11. D.K. Lee, V.R. Saldivia, T. Nguyen, R. Cheng, S.R. George, and B.F. O'Dowd. Modification of the terminal residue of apelin-13 antagonizes its hypotensive action. Endocrinology. 146:231-236 (2005).

12. P.R. Maloney, P. Khan, M. Hedrick, P. Gosalia, M. Milewski, L. Li, G.P. Roth, E. Sergienko, E. Suyama, E. Sugarman, K. Nguyen, A. Mehta, S. Vasile, Y. Su, D. Stonich, H. Nguyen, F.Y. Zeng, A.M. Novo, M. Vicchiarelli, J. Diwan, T.D. Chung, L.H. Smith, and A.B. Pinkerton. Discovery of 4-oxo-6-((pyrimidin-2-ylthio)methyl)-4H-pyran-3-yl 4-

nitrobenzoate (ML221) as a functional antagonist of the apelin (APJ) receptor. Bioorganic & medicinal chemistry letters. 22:6656-6660 (2012).

13. W. Xu, H. Yu, R. Ma, L. Ma, Q. Liu, H. Shan, C. Wu, R. Zhang, Y. Zhou, and H. Shan. Apelin protects against myocardial ischemic injury by inhibiting dynamin-related protein 1. Oncotarget. 8:100034-100044 (2017).

14. J. Hou, L. Wang, H. Long, H. Wu, Q. Wu, T. Zhong, X. Chen, C. Zhou, T. Guo, and T. Wang. Hypoxia preconditioning promotes cardiac stem cell survival and cardiogenic differentiation in vitro involving activation of the HIF-1alpha/apelin/APJ axis. Stem cell research & therapy. 8:215 (2017).

15. K. Tatemoto, M. Hosoya, Y. Habata, R. Fujii, T. Kakegawa, M.X. Zou, Y. Kawamata, S. Fukusumi, S. Hinuma, C. Kitada, T. Kurokawa, H. Onda, and M. Fujino. Isolation and characterization of a novel endogenous peptide ligand for the human APJ receptor. Biochem Biophys Res Commun. 251:471-476 (1998).

16. G.R. Pope, E.M. Roberts, S.J. Lolait, and A.M. O'Carroll. Central and peripheral apelin receptor distribution in the mouse: species differences with rat. Peptides. 33:139-148 (2012).

17. Y. Kawamata, Y. Habata, S. Fukusumi, M. Hosoya, R. Fujii, S. Hinuma, N. Nishizawa, C. Kitada, H. Onda, O. Nishimura, and M. Fujino. Molecular properties of apelin: tissue distribution and receptor binding. Biochim Biophys Acta. 1538:162-171 (2001).

18. S.L. Pitkin, J.J. Maguire, R.E. Kuc, and A.P. Davenport. Modulation of the apelin/APJ system in heart failure and atherosclerosis in man. Br J Pharmacol. 160:1785-1795 (2010).

19. D.K. Lee, R. Cheng, T. Nguyen, T. Fan, A.P. Kariyawasam, Y. Liu, D.H. Osmond, S.R. George, and B.F. O'Dowd. Characterization of apelin, the ligand for the APJ receptor. J Neurochem. 74:34-41 (2000).

20. S.L. Pitkin, J.J. Maguire, T.I. Bonner, and A.P. Davenport. International Union of Basic and Clinical Pharmacology. LXXIV. Apelin receptor nomenclature, distribution, pharmacology, and function. Pharmacol Rev. 62:331-342 (2010).

21. E.Y. Zhen, R.E. Higgs, and J.A. Gutierrez. Pyroglutamyl apelin-13 identified as the major apelin isoform in human plasma. Analytical biochemistry. 442:1-9 (2013).

22. J.J. Maguire, M.J. Kleinz, S.L. Pitkin, and A.P. Davenport. [Pyr1]apelin-13 identified as the predominant apelin isoform in the human heart: vasoactive mechanisms and inotropic action in disease. Hypertension. 54:598-604 (2009).

23. W. Wang, S.M. McKinnie, M. Farhan, M. Paul, T. McDonald, B. McLean, C. Llorens-Cortes, S. Hazra, A.G. Murray, J.C. Vederas, and G.Y. Oudit. Angiotensin-Converting Enzyme 2 Metabolizes and Partially Inactivates Pyr-Apelin-13 and Apelin-17: Physiological Effects in the Cardiovascular System. Hypertension. 68:365-377 (2016).

24. P. Yang, R.E. Kuc, A.L. Brame, A. Dyson, M. Singer, R.C. Glen, J. Cheriyan, I.B. Wilkinson, A.P. Davenport, and J.J. Maguire. [Pyr1]Apelin-13(1-12) Is a Biologically Active ACE2 Metabolite of the Endogenous Cardiovascular Peptide [Pyr1]Apelin-13. Frontiers in neuroscience. 11:92 (2017).

25. C. Vickers, P. Hales, V. Kaushik, L. Dick, J. Gavin, J. Tang, K. Godbout, T. Parsons, E. Baronas, F. Hsieh, S. Acton, M. Patane, A. Nichols, and P. Tummino. Hydrolysis of biological peptides by human angiotensin-converting enzyme-related carboxypeptidase. J Biol Chem. 277:14838-14843 (2002).

26. R. Gerbier, R. Alvear-Perez, J.F. Margathe, A. Flahault, P. Couvineau, J. Gao, N. De Mota, H. Dabire, B. Li, E. Ceraudo, A. Hus-Citharel, L. Esteoulle, C. Bisoo, M. Hibert, A. Berdeaux, X. Iturrioz, D. Bonnet, and C. Llorens-Cortes. Development of original metabolically stable apelin-17 analogs with diuretic and cardiovascular effects. FASEB journal : official publication of the Federation of American Societies for Experimental Biology. 31:687-700 (2017).

27. A. Murza, K. Belleville, J.M. Longpre, P. Sarret, and E. Marsault. Stability and degradation patterns of chemically modified analogs of apelin-13 in plasma and cerebrospinal fluid. Biopolymers. 102:297-303 (2014).

28. B.F. O'Dowd, M. Heiber, A. Chan, H.H. Heng, L.C. Tsui, J.L. Kennedy, X. Shi, A. Petronis, S.R. George, and T. Nguyen. A human gene that shows identity with the gene encoding the angiotensin receptor is located on chromosome 11. Gene. 136:355-360 (1993).

29. Y. Habata, R. Fujii, M. Hosoya, S. Fukusumi, Y. Kawamata, S. Hinuma, C. Kitada, N. Nishizawa, S. Murosaki, T. Kurokawa, H. Onda, K. Tatemoto, and M. Fujino. Apelin, the natural ligand of the orphan receptor APJ, is abundantly secreted in the colostrum. Biochim Biophys Acta. 1452:25-35 (1999).

30. A. Modgil, L. Guo, S.T. O'Rourke, and C. Sun. Apelin-13 inhibits large-conductance Ca2+-activated K+ channels in cerebral artery smooth muscle cells via a PI3-kinase dependent mechanism. PLoS One. 8:e83051 (2013).

31. W. Choe, A. Albright, J. Sulcove, S. Jaffer, J. Hesselgesser, E. Lavi, P. Crino, and D.L. Kolson. Functional expression of the seven-transmembrane HIV-1 co-receptor APJ in neural cells. Journal of neurovirology. 6 Suppl 1:S61-69 (2000).

32. I. Szokodi, P. Tavi, G. Foldes, S. Voutilainen-Myllyla, M. Ilves, H. Tokola, S. Pikkarainen, J. Piuhola, J. Rysa, M. Toth, and H. Ruskoaho. Apelin, the novel endogenous ligand of the orphan receptor APJ, regulates cardiac contractility. Circ Res. 91:434-440 (2002).

33. T. Hashimoto, M. Kihara, J. Ishida, N. Imai, S. Yoshida, Y. Toya, A. Fukamizu, H. Kitamura, and S. Umemura. Apelin stimulates myosin light chain phosphorylation in vascular smooth muscle cells. Arterioscler Thromb Vasc Biol. 26:1267-1272 (2006).

34. Y. Kang, J. Kim, J.P. Anderson, J. Wu, S.R. Gleim, R.K. Kundu, D.L. McLean, J.D. Kim, H. Park, S.W. Jin, J. Hwa, T. Quertermous, and H.J. Chun. Apelin-APJ signaling is a critical regulator of endothelial MEF2 activation in cardiovascular development. Circ Res. 113:22-31 (2013).

35. D.K. Lee, A.J. Lança, R. Cheng, T. Nguyen, X.D. Ji, F. Gobeil, S. Chemtob, S.R. George, and B.F. O'Dowd. Agonist-independent nuclear localization of the Apelin, angiotensin AT1, and bradykinin B2 receptors. Journal of Biological Chemistry. 279:7901-7908 (2004).

36. A. Drougard, A. Fournel, A. Marlin, E. Meunier, A. Abot, T. Bautzova, T. Duparc, K. Louche, A. Batut, A. Lucas, S. Le-Gonidec, J. Lesage, X. Fioramonti, C. Moro, P. Valet, P.D. Cani, and C. Knauf. Central chronic apelin infusion decreases energy expenditure and thermogenesis in mice. Sci Rep. 6:31849 (2016).

37. K.J. Clarke, K.W. Whitaker, and T.M. Reyes. Diminished metabolic responses to centrally-administered apelin-13 in diet-induced obese rats fed a high-fat diet. J Neuroendocrinol. 21:83-89 (2009).

38. A. Salcedo, J. Garijo, L. Monge, N. Fernández, A. Luis García-Villalón, V. Sánchez Turrión, V. Cuervas-Mons, and G. Diéguez. Apelin effects in human splanchnic arteries. Role of nitric oxide and prostanoids. Regul Pept. 144:50-55 (2007).

39. X. Cheng, X.S. Cheng, and C.C. Pang. Venous dilator effect of apelin, an endogenous peptide ligand for the orphan APJ receptor, in conscious rats. Eur J Pharmacol. 470:171-175 (2003).

40. J.C. Zhong, X.Y. Yu, Y. Huang, L.M. Yung, C.W. Lau, and S.G. Lin. Apelin modulates aortic vascular tone via endothelial nitric oxide synthase phosphorylation pathway in diabetic mice. Cardiovasc Res. 74:388-395 (2007).

41. F. Schinzari, A. Veneziani, N. Mores, A. Barini, N. Di Daniele, C. Cardillo, and M. Tesauro. Beneficial Effects of Apelin on Vascular Function in Patients With Central Obesity. Hypertension. 69:942-949 (2017).

42. A.G. Jappand D.E. Newby. The apelin-APJ system in heart failure: pathophysiologic relevance and therapeutic potential. Biochemical pharmacology. 75:1882-1892 (2008).

43. Y.X. Jia, Z.F. Lu, J. Zhang, C.S. Pan, J.H. Yang, J. Zhao, F. Yu, X.H. Duan, C.S. Tang, and Y.F. Qi. Apelin activates L-arginine/nitric oxide synthase/nitric oxide pathway in rat aortas. Peptides. 28:2023-2029 (2007).

44. W.K. Alderton, C.E. Cooper, and R.G. Knowles. Nitric oxide synthases: structure, function and inhibition. Biochem J. 357:593-615 (2001).

45. K.K. Griendling, R.M. Touyz, J.L. Zweier, S. Dikalov, W. Chilian, Y.R. Chen, D.G. Harrison, A. Bhatnagar, and S. American Heart Association Council on Basic Cardiovascular. Measurement of Reactive Oxygen Species, Reactive Nitrogen Species,

and Redox-Dependent Signaling in the Cardiovascular System: A Scientific Statement From the American Heart Association. Circ Res. 119:e39-75 (2016).

46. S.L. Archer, J.M. Huang, V. Hampl, D.P. Nelson, P.J. Shultz, and E.K. Weir. Nitric oxide and cGMP cause vasorelaxation by activation of a charybdotoxin-sensitive K channel by cGMP-dependent protein kinase. Proc Natl Acad Sci U S A. 91:7583-7587 (1994).

47. S.H. Francis, J.L. Busch, J.D. Corbin, and D. Sibley. cGMP-dependent protein kinases and cGMP phosphodiesterases in nitric oxide and cGMP action. Pharmacol Rev. 62:525-563 (2010).

48. V.M. Bolotina, S. Najibi, J.J. Palacino, P.J. Pagano, and R.A. Cohen. Nitric oxide directly activates calcium-dependent potassium channels in vascular smooth muscle. Nature. 368:850-853 (1994).

49. D.K. Mistry and C.J. Garland. Nitric oxide (NO)-induced activation of large conductance Ca2+-dependent K+ channels (BK(Ca)) in smooth muscle cells isolated from the rat mesenteric artery. Br J Pharmacol. 124:1131-1140 (1998).

50. R.A. Cohen and T. Adachi. Nitric-oxide-induced vasodilatation: regulation by physiologic s-glutathiolation and pathologic oxidation of the sarcoplasmic endoplasmic reticulum calcium ATPase. Trends Cardiovasc Med. 16:109-114 (2006).

51. C.W. Sun, J.R. Falck, H. Okamoto, D.R. Harder, and R.J. Roman. Role of cGMP versus 20-HETE in the vasodilator response to nitric oxide in rat cerebral arteries. Am J Physiol Heart Circ Physiol. 279:H339-350 (2000).

52. A.G. Japp, N.L. Cruden, D.A. Amer, V.K. Li, E.B. Goudie, N.R. Johnston, S. Sharma, I. Neilson, D.J. Webb, I.L. Megson, A.D. Flapan, and D.E. Newby. Vascular effects of apelin in vivo in man. J Am Coll Cardiol. 52:908-913 (2008).

53. C.J. Charles, M.T. Rademaker, and A.M. Richards. Apelin-13 induces a biphasic haemodynamic response and hormonal activation in normal conscious sheep. J Endocrinol. 189:701-710 (2006).

54. S. Kagiyama, M. Fukuhara, K. Matsumura, Y. Lin, K. Fujii, and M. Iida. Central and peripheral cardiovascular actions of apelin in conscious rats. Regul Pept. 125:55-59 (2005).

55. K. Tatemoto, K. Takayama, M.X. Zou, I. Kumaki, W. Zhang, K. Kumano, and M. Fujimiya. The novel peptide apelin lowers blood pressure via a nitric oxide-dependent mechanism. Regul Pept. 99:87-92 (2001).

56. S. El Messari, X. Iturrioz, C. Fassot, N. De Mota, D. Roesch, and C. Llorens-Cortes. Functional dissociation of apelin receptor signaling and endocytosis: implications for the effects of apelin on arterial blood pressure. J Neurochem. 90:1290-1301 (2004).

57. M. Seyedabadi, A.K. Goodchild, and P.M. Pilowsky. Site-specific effects of apelin-13 in the rat medulla oblongata on arterial pressure and respiration. Auton Neurosci. 101:32-38 (2002).

58. M. Hosoya, Y. Kawamata, S. Fukusumi, R. Fujii, Y. Habata, S. Hinuma, C. Kitada, S. Honda, T. Kurokawa, H. Onda, O. Nishimura, and M. Fujino. Molecular and functional characteristics of APJ. Tissue distribution of mRNA and interaction with the endogenous ligand apelin. J Biol Chem. 275:21061-21067 (2000).

59. Q. Zhang, F. Yao, M.K. Raizada, S.T. O'Rourke, and C. Sun. Apelin gene transfer into the rostral ventrolateral medulla induces chronic blood pressure elevation in normotensive rats. Circ Res. 104:1421-1428 (2009).

60. F. Yao, A. Modgil, Q. Zhang, A. Pingili, N. Singh, S.T. O'Rourke, and C. Sun. Pressor effect of apelin-13 in the rostral ventrolateral medulla: role of NAD(P)H oxidase-derived superoxide. J Pharmacol Exp Ther. 336:372-380 (2011).

61. T. Kitazono, F.M. Faraci, H. Taguchi, and D.D. Heistad. Role of potassium channels in cerebral blood vessels. Stroke. 26:1713-1723 (1995).

62. M. Feletou. Calcium-activated potassium channels and endothelial dysfunction: therapeutic options? Br J Pharmacol. 156:545-562 (2009).

63. A.G. Szent-Gyorgyi. Calcium regulation of muscle contraction. Biophysical journal. 15:707-723 (1975).

64. S.P. Driska, M.O. Aksoy, and R.A. Murphy. Myosin light chain phosphorylation associated with contraction in arterial smooth muscle. Am J Physiol. 240:C222-233 (1981).

65. K.S. Thorneloe and M.T. Nelson. Ion channels in smooth muscle: regulators of intracellular calcium and contractility. Can J Physiol Pharmacol. 83:215-242 (2005).

66. L.Y. Wang, D.L. Zhang, J.F. Zheng, Y. Zhang, Q.D. Zhang, and W.H. Liu. Apelin-13 passes through the ADMA-damaged endothelial barrier and acts on vascular smooth muscle cells. Peptides. 32:2436-2443 (2011).

67. X. Han, D.L. Zhang, D.X. Yin, Q.D. Zhang, and W.H. Liu. Apelin-13 deteriorates hypertension in rats after damage of the vascular endothelium by ADMA. Can J Physiol Pharmacol. 91:708-714 (2013).

68. H. Fukushima, N. Kobayashi, H. Takeshima, W. Koguchi, and T. Ishimitsu. Effects of olmesartan on Apelin/APJ and Akt/endothelial nitric oxide synthase pathway in Dahl rats with end-stage heart failure. J Cardiovasc Pharmacol. 55:83-88 (2010).

69. H.J. Chun, Z.A. Ali, Y. Kojima, R.K. Kundu, A.Y. Sheikh, R. Agrawal, L. Zheng, N.J. Leeper, N.E. Pearl, A.J. Patterson, J.P. Anderson, P.S. Tsao, M.J. Lenardo, E.A. Ashley, and T. Quertermous. Apelin signaling antagonizes Ang II effects in mouse models of atherosclerosis. J Clin Invest. 118:3343-3354 (2008).

70. T. Hashimoto, M. Kihara, N. Imai, S. Yoshida, H. Shimoyamada, H. Yasuzaki, J. Ishida, Y. Toya, Y. Kiuchi, N. Hirawa, K. Tamura, T. Yazawa, H. Kitamura, A. Fukamizu, and S. Umemura. Requirement of apelin-apelin receptor system for oxidative stress-linked atherosclerosis. The American journal of pathology. 171:1705-1712 (2007).

71. T. Peltonen, J. Napankangas, O. Vuolteenaho, P. Ohtonen, Y. Soini, T. Juvonen, J. Satta, H. Ruskoaho, and P. Taskinen. Apelin and its receptor APJ in human aortic valve stenosis. The Journal of heart valve disease. 18:644-652 (2009).

72. M. Seyedabadi, A.K. Goodchild, and P.M. Pilowsky. Differential role of kinases in brain stem of hypertensive and normotensive rats. Hypertension. 38:1087-1092 (2001).

73. A. Folino, P.G. Montarolo, M. Samaja, and R. Rastaldo. Effects of apelin on the cardiovascular system. Heart Fail Rev. 20:505-518 (2015).

74. R.E. Kälin, M.P. Kretz, A.M. Meyer, A. Kispert, F.L. Heppner, and A.W. Brändli. Paracrine and autocrine mechanisms of apelin signaling govern embryonic and tumor angiogenesis. Dev Biol. 305:599-614 (2007).

75. J. Ishida, T. Hashimoto, Y. Hashimoto, S. Nishiwaki, T. Iguchi, S. Harada, T. Sugaya, H. Matsuzaki, R. Yamamoto, N. Shiota, H. Okunishi, M. Kihara, S. Umemura, F. Sugiyama, K. Yagami, Y. Kasuya, N. Mochizuki, and A. Fukamizu. Regulatory roles for APJ, a seven-transmembrane receptor related to angiotensin-type 1 receptor in blood pressure in vivo. J Biol Chem. 279:26274-26279 (2004).

76. A.G. Japp, N.L. Cruden, G. Barnes, N. van Gemeren, J. Mathews, J. Adamson, N.R. Johnston, M.A. Denvir, I.L. Megson, A.D. Flapan, and D.E. Newby. Acute cardiovascular effects of apelin in humans: potential role in patients with chronic heart failure. Circulation. 121:1818-1827 (2010).

77. A.M. O'Carroll, S.J. Lolait, L.E. Harris, and G.R. Pope. The apelin receptor APJ: journey from an orphan to a multifaceted regulator of homeostasis. J Endocrinol. 219:R13-35 (2013).

78. A.D. Medhurst, C.A. Jennings, M.J. Robbins, R.P. Davis, C. Ellis, K.Y. Winborn, K.W. Lawrie, G. Hervieu, G. Riley, J.E. Bolaky, N.C. Herrity, P. Murdock, and J.G. Darker. Pharmacological and immunohistochemical characterization of the APJ receptor and its endogenous ligand apelin. J Neurochem. 84:1162-1172 (2003).

79. S.D. Katugampola, J.J. Maguire, S.R. Matthewson, and A.P. Davenport. [(125)I]-(Pyr(1))Apelin-13 is a novel radioligand for localizing the APJ orphan receptor in human and rat tissues with evidence for a vasoconstrictor role in man. Br J Pharmacol. 132:1255-1260 (2001).

80. A. Reaux, K. Gallatz, M. Palkovits, and C. Llorens-Cortes. Distribution of apelin-synthesizing neurons in the adult rat brain. Neuroscience. 113:653-662 (2002).

81. P. Yang, J.J. Maguire, and A.P. Davenport. Apelin, Elabela/Toddler, and biased agonists as novel therapeutic agents in the cardiovascular system. Trends Pharmacol Sci. 36:560-567 (2015).

82. S.T. O'Rourke, Vanhoutte P.M., and Miller, V. M. Biology of Blood Vessels: Vascular Pharmacology. In M.A.C. J. Loscalzo, and V. J. Dzau (ed.), Vascular Medicine, Little, Brown and Company, 2005, pp. 71-100.

83. G. Grande, E. Nilsson, and L. Edvinsson. Comparison of responses to vasoactive drugs in human and rat cerebral arteries using myography and pressurized cerebral artery method. Cephalalgia. 33:152-159 (2013).

84. A.L. Gonzales, G.C. Amberg, and S. Earley. Ca2+ release from the sarcoplasmic reticulum is required for sustained TRPM4 activity in cerebral artery smooth muscle cells. Am J Physiol Cell Physiol. 299:C279-288 (2010).

85. B. Erdös, A.W. Miller, and D.W. Busija. Impaired endothelium-mediated relaxation in isolated cerebral arteries from insulin-resistant rats. Am J Physiol Heart Circ Physiol. 282:H2060-2065 (2002).

86. C. Görlach and M. Wahl. Bradykinin dilates rat middle cerebral artery and its large branches via endothelial B2 receptors and release of nitric oxide. Peptides. 17:1373-1378 (1996).

87. J.L. Romine, S.W. Martin, N.A. Meanwell, V.K. Gribkoff, C.G. Boissard, S.I. Dworetzky, J. Natale, S. Moon, A. Ortiz, S. Yeleswaram, L. Pajor, Q. Gao, and J.E. Starrett. 3-[(5-Chloro-2-hydroxyphenyl)methyl]-5-[4-(trifluoromethyl)phenyl]-1,3,4-oxadiazol-2(3H)-one, BMS-191011: opener of large-conductance Ca(2+)-activated potassium (maxi-K) channels, identification, solubility, and SAR. J Med Chem. 50:528-542 (2007).

88. J.E. Brayden, J.M. Quayle, N.B. Standen, and M.T. Nelson. Role of potassium channels in the vascular response to endogenous and pharmacological vasodilators. Blood Vessels. 28:147-153 (1991).

89. E.A. Ashley, J. Powers, M. Chen, R. Kundu, T. Finsterbach, A. Caffarelli, A. Deng, J. Eichhorn, R. Mahajan, R. Agrawal, J. Greve, R. Robbins, A.J. Patterson, D. Bernstein, and

T. Quertermous. The endogenous peptide apelin potently improves cardiac contractility and reduces cardiac loading in vivo. Cardiovasc Res. 65:73-82 (2005).

90. C.M. Maragos, D. Morley, D.A. Wink, T.M. Dunams, J.E. Saavedra, A. Hoffman, A.A. Bove, L. Isaac, J.A. Hrabie, and L.K. Keefer. Complexes of .NO with nucleophiles as agents for the controlled biological release of nitric oxide. Vasorelaxant effects. J Med Chem. 34:3242-3247 (1991).

91. L.J. Ignarro, G. Cirino, A. Casini, and C. Napoli. Nitric oxide as a signaling molecule in the vascular system: an overview. J Cardiovasc Pharmacol. 34:879-886 (1999).

92. P.M. Vanhoutte, H. Shimokawa, M. Feletou, and E.H. Tang. Endothelial dysfunction and vascular disease - a 30th anniversary update. Acta Physiol (Oxf). 219:22-96 (2017).

93. J.E. Brayden and M.T. Nelson. Regulation of arterial tone by activation of calcium-dependent potassium channels. Science. 256:532-535 (1992).

94. M.T. Nelson and J.M. Quayle. Physiological roles and properties of potassium channels in arterial smooth muscle. Am J Physiol. 268:C799-822 (1995).

95. F.M. Faraci and D.D. Heistad. Regulation of the cerebral circulation: role of endothelium and potassium channels. Physiol Rev. 78:53-97 (1998).

96. B.D. Kyle, R.C. Mishra, and A.P. Braun. The augmentation of BK channel activity by nitric oxide signaling in rat cerebral arteries involves co-localized regulatory elements. J Cereb Blood Flow Metab:271678X17691291 (2017).

97. M. Yu, C.W. Sun, K.G. Maier, D.R. Harder, and R.J. Roman. Mechanism of cGMP contribution to the vasodilator response to NO in rat middle cerebral arteries. Am J Physiol Heart Circ Physiol. 282:H1724-1731 (2002).

98. A. Galvez, G. Gimenez-Gallego, J.P. Reuben, L. Roy-Contancin, P. Feigenbaum, G.J. Kaczorowski, and M.L. Garcia. Purification and characterization of a unique, potent, peptidyl probe for the high conductance calcium-activated potassium channel from venom of the scorpion Buthus tamulus. J Biol Chem. 265:11083-11090 (1990).

99. S.P. Olesen, E. Munch, P. Moldt, and J. Drejer. Selective activation of Ca(2+)-dependent K+ channels by novel benzimidazolone. Eur J Pharmacol. 251:53-59 (1994).

100. M. Holland, P.D. Langton, N.B. Standen, and J.P. Boyle. Effects of the BK_{Ca} channel activator, NS1619, on rat cerebral artery smooth muscle. Br J Pharmacol. 117:119-129 (1996).

101. G.G. Geary, D.N. Krause, and S.P. Duckles. Melatonin directly constricts rat cerebral arteries through modulation of potassium channels. Am J Physiol. 273:H1530-1536 (1997).

102. N. Satake, H. Oe, and S. Shibata. Vasorelaxing action of melatonin in rat isolated aorta; possible endothelium dependent relaxation. Gen Pharmacol. 22:1127-1133 (1991).

103. S. Doolen, D.N. Krause, M.L. Dubocovich, and S.P. Duckles. Melatonin mediates two distinct responses in vascular smooth muscle. Eur J Pharmacol. 345:67-69 (1998).

104. W. Wang, S.M. McKinnie, V.B. Patel, G. Haddad, Z. Wang, P. Zhabyeyev, S.K. Das, R. Basu, B. McLean, V. Kandalam, J.M. Penninger, Z. Kassiri, J.C. Vederas, A.G. Murray, and G.Y. Oudit. Loss of Apelin exacerbates myocardial infarction adverse remodeling and ischemia-reperfusion injury: therapeutic potential of synthetic Apelin analogues. J Am Heart Assoc. 2:e000249 (2013).

105. G.D. Barnes, S. Alam, G. Carter, C.M. Pedersen, K.M. Lee, T.J. Hubbard, S. Veitch, H. Jeong, A. White, N.L. Cruden, L. Huson, A.G. Japp, and D.E. Newby. Sustained

cardiovascular actions of APJ agonism during renin-angiotensin system activation and in patients with heart failure. Circulation Heart failure. 6:482-491 (2013).

106. J. Hata, K. Matsuda, T. Ninomiya, K. Yonemoto, T. Matsushita, Y. Ohnishi, S. Saito, T. Kitazono, S. Ibayashi, M. Iida, Y. Kiyohara, Y. Nakamura, and M. Kubo. Functional SNP in an Sp1-binding site of AGTRL1 gene is associated with susceptibility to brain infarction. Hum Mol Genet. 16:630-639 (2007).

107. I. Castan-Laurell, C. Dray, C. Attané, T. Duparc, C. Knauf, and P. Valet. Apelin, diabetes, and obesity. Endocrine. 40:1-9 (2011).

108. I. Castan-Laurell, M. Vítkova, D. Daviaud, C. Dray, M. Kováciková, Z. Kovacova, J. Hejnova, V. Stich, and P. Valet. Effect of hypocaloric diet-induced weight loss in obese women on plasma apelin and adipose tissue expression of apelin and APJ. Eur J Endocrinol. 158:905-910 (2008).

109. F. Soriguer, L. Garrido-Sanchez, S. Garcia-Serrano, J.M. Garcia-Almeida, J. Garcia-Arnes, F.J. Tinahones, and E. Garcia-Fuentes. Apelin levels are increased in morbidly obese subjects with type 2 diabetes mellitus. Obes Surg. 19:1574-1580 (2009).

110. L.B. Goldstein, C.D. Bushnell, R.J. Adams, L.J. Appel, L.T. Braun, S. Chaturvedi, M.A. Creager, A. Culebras, R.H. Eckel, R.G. Hart, J.A. Hinchey, V.J. Howard, E.C. Jauch, S.R. Levine, J.F. Meschia, W.S. Moore, J.V. Nixon, T.A. Pearson, A.H.A.S. Council, C.o.C. Nursing, C.o.E.a. Prevention, Council for High Blood Pressure Research, and a.I.C.o.Q.o.C.a.O.R. Council on Peripheral Vascular Disease. Guidelines for the primary prevention of stroke: a guideline for healthcare professionals from the American Heart Association/American Stroke Association. Stroke. 42:517-584 (2011).

111. M. Przewlocka-Kosmala, T. Kotwica, A. Mysiak, and W. Kosmala. Reduced circulating apelin in essential hypertension and its association with cardiac dysfunction. J Hypertens. 29:971-979 (2011).

112. P. Zhu, F. Huang, F. Lin, Y. Yuan, F. Chen, and Q. Li. Plasma apelin levels, blood pressure and cardiovascular risk factors in a coastal Chinese population. Ann Med. 45:494-498 (2013).

113. P. Atluri, K.J. Morine, G.P. Liao, C.M. Panlilio, M.F. Berry, V.M. Hsu, W. Hiesinger, J.E. Cohen, and Y. Joseph Woo. Ischemic heart failure enhances endogenous myocardial apelin and APJ receptor expression. Cell Mol Biol Lett. 12:127-138 (2007).

114. H. Pang, B. Han, T. Yu, and Z. Zong. Effect of apelin on the cardiac hemodynamics in hypertensive rats with heart failure. Int J Mol Med. 34:756-764 (2014).

115. W. Koguchi, N. Kobayashi, H. Takeshima, M. Ishikawa, F. Sugiyama, and T. Ishimitsu. Cardioprotective effect of apelin-13 on cardiac performance and remodeling in end-stage heart failure. Circ J. 76:137-144 (2012).

116. L.J. Ignarro, R.G. Harbison, K.S. Wood, and P.J. Kadowitz. Activation of purified soluble guanylate cyclase by endothelium-derived relaxing factor from intrapulmonary artery and vein: stimulation by acetylcholine, bradykinin and arachidonic acid. J Pharmacol Exp Ther. 237:893-900 (1986).

117. Y. Zhao, P.M. Vanhoutte, and S.W. Leung. Vascular nitric oxide: Beyond eNOS. J Pharmacol Sci. 129:83-94 (2015).

118. S.K. Sonkusare, A.D. Bonev, J. Ledoux, W. Liedtke, M.I. Kotlikoff, T.J. Heppner, D.C. Hill-Eubanks, and M.T. Nelson. Elementary Ca2+ signals through endothelial TRPV4 channels regulate vascular function. Science. 336:597-601 (2012).

119. S. Vázquez-Pérez, J. Navarro-Cid, N. de las Heras, E. Cediel, D. Sanz-Rosa, L.M. Ruilope, V. Cachofeiro, and V. Lahera. Relevance of endothelium-derived hyperpolarizing factor in the effects of hypertension on rat coronary relaxations. J Hypertens. 19:539-545 (2001).

120. M.R. Tschudi, L. Criscione, D. Novosel, K. Pfeiffer, and T.F. Lüscher. Antihypertensive therapy augments endothelium-dependent relaxations in coronary arteries of spontaneously hypertensive rats. Circulation. 89:2212-2218 (1994).

121. H.E. Tawfik, A.B. El-Remessy, S. Matragoon, G. Ma, R.B. Caldwell, and R.W. Caldwell. Simvastatin improves diabetes-induced coronary endothelial dysfunction. J Pharmacol Exp Ther. 319:386-395 (2006).

122. S. Shimizu, M. Nomoto, T. Yamamoto, and K. Momose. Reduction by NG-nitro-L-arginine of H2O2-induced endothelial cell injury. Br J Pharmacol. 113:564-568 (1994).

123. H.A. Kontos, E.P. Wei, J.T. Povlishock, and C.W. Christman. Oxygen radicals mediate the cerebral arteriolar dilation from arachidonate and bradykinin in cats. Circ Res. 55:295-303 (1984).

124. H. Miura, J.J. Bosnjak, G. Ning, T. Saito, M. Miura, and D.D. Gutterman. Role for hydrogen peroxide in flow-induced dilation of human coronary arterioles. Circ Res. 92:e31-40 (2003).

125. S. Roychowdhury, A. Luthe, G. Keilhoff, G. Wolf, and T.F. Horn. Oxidative stress in glial cultures: detection by DAF-2 fluorescence used as a tool to measure peroxynitrite rather than nitric oxide. Glia. 38:103-114 (2002).

126. X. Zhang, W.S. Kim, N. Hatcher, K. Potgieter, L.L. Moroz, R. Gillette, and J.V. Sweedler. Interfering with nitric oxide measurements. 4,5-diaminofluorescein reacts with dehydroascorbic acid and ascorbic acid. J Biol Chem. 277:48472-48478 (2002).

127. N. Nagata, K. Momose, and Y. Ishida. Inhibitory effects of catecholamines and anti-oxidants on the fluorescence reaction of 4,5-diaminofluorescein, DAF-2, a novel indicator of nitric oxide. Journal of biochemistry. 125:658-661 (1999).

128. N.W. Seidler, I. Jona, M. Vegh, and A. Martonosi. Cyclopiazonic acid is a specific inhibitor of the Ca2+-ATPase of sarcoplasmic reticulum. J Biol Chem. 264:17816-17823 (1989).

129. Z. Wang, D. Yu, M. Wang, Q. Wang, J. Kouznetsova, R. Yang, K. Qian, W. Wu, A. Shuldiner, C. Sztalryd, M. Zou, W. Zheng, and D.W. Gong. Elabela-apelin receptor signaling pathway is functional in mammalian systems. Sci Rep. 5:8170 (2015).

130. A. Reaux, N. De Mota, I. Skultetyova, Z. Lenkei, S. El Messari, K. Gallatz, P. Corvol, M. Palkovits, and C. Llorens-Cortès. Physiological role of a novel neuropeptide, apelin, and its receptor in the rat brain. J Neurochem. 77:1085-1096 (2001).

131. N. De Mota, Z. Lenkei, and C. Llorens-Cortes. Cloning, pharmacological characterization and brain distribution of the rat apelin receptor. Neuroendocrinology. 72:400-407 (2000).

132. C. Liu, T. Su, F. Li, L. Li, X. Qin, W. Pan, F. Feng, F. Chen, D. Liao, and L. Chen. PI3K/Akt signaling transduction pathway is involved in rat vascular smooth muscle cell proliferation induced by apelin-13. Acta Biochim Biophys Sin (Shanghai). 42:396-402 (2010).

133. H. Zhang, Y. Gong, Z. Wang, L. Jiang, R. Chen, X. Fan, H. Zhu, L. Han, X. Li, J. Xiao, and X. Kong. Apelin inhibits the proliferation and migration of rat PASMCs via the activation of PI3K/Akt/mTOR signal and the inhibition of autophagy under hypoxia. Journal of cellular and molecular medicine. 18:542-553 (2014).

134. P.H. Ratz and S.F. Flaim. Mechanism of 5-HT contraction in isolated bovine ventricular coronary arteries. Evidence for transient receptor-operated calcium influx channels. Circ Res. 54:135-143 (1984).

135. N. Katsumata, H. Shimokawa, M. Seto, T. Kozai, T. Yamawaki, K. Kuwata, K. Egashira, I. Ikegaki, T. Asano, Y. Sasaki, and A. Takeshita. Enhanced myosin light chain phosphorylations as a central mechanism for coronary artery spasm in a swine model with interleukin-1beta. Circulation. 96:4357-4363 (1997).

APPENDIX

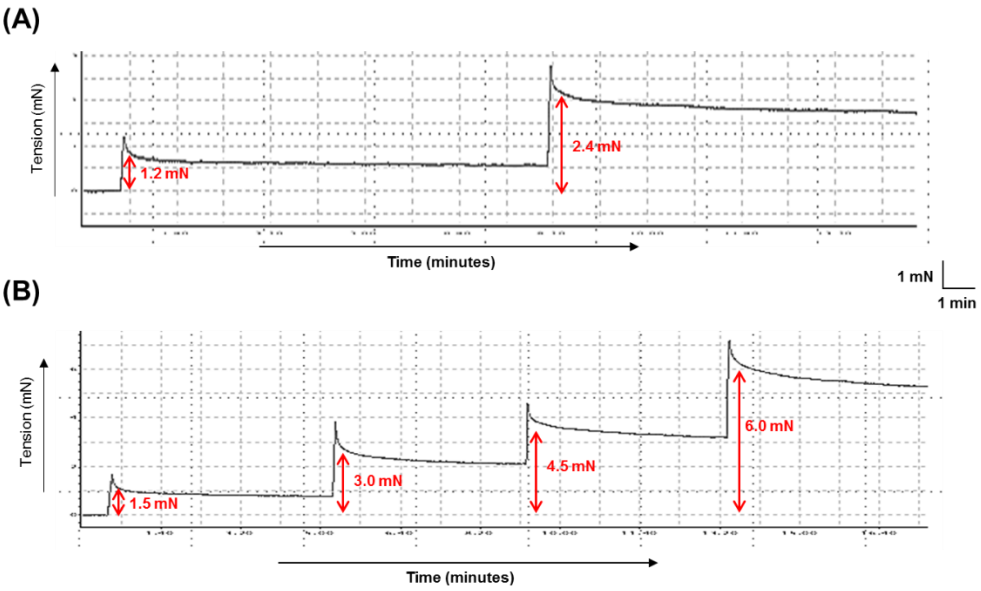

Fig. A1. Representative tracings from normalization protocol.
Representative original tracings showing arterial response to passive stretch during normalization of (A) cerebral and (B) coronary arteries.

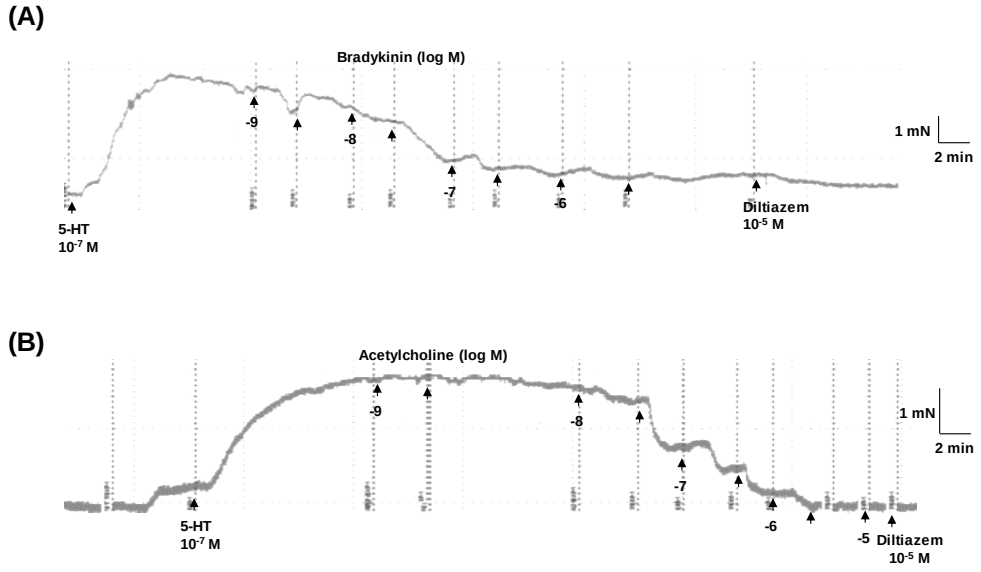

Fig. A2. Representative tracings for concentration response curves of bradykinin and acetylcholine.
Representative original tracings of isometric tension recordings from rat isolated arteries in response to cumulative addition of increasing concentrations of (A) bradykinin (cerebral arteries) and (B) acetylcholine (coronary arteries) followed by diltiazem (10^{-5} M).

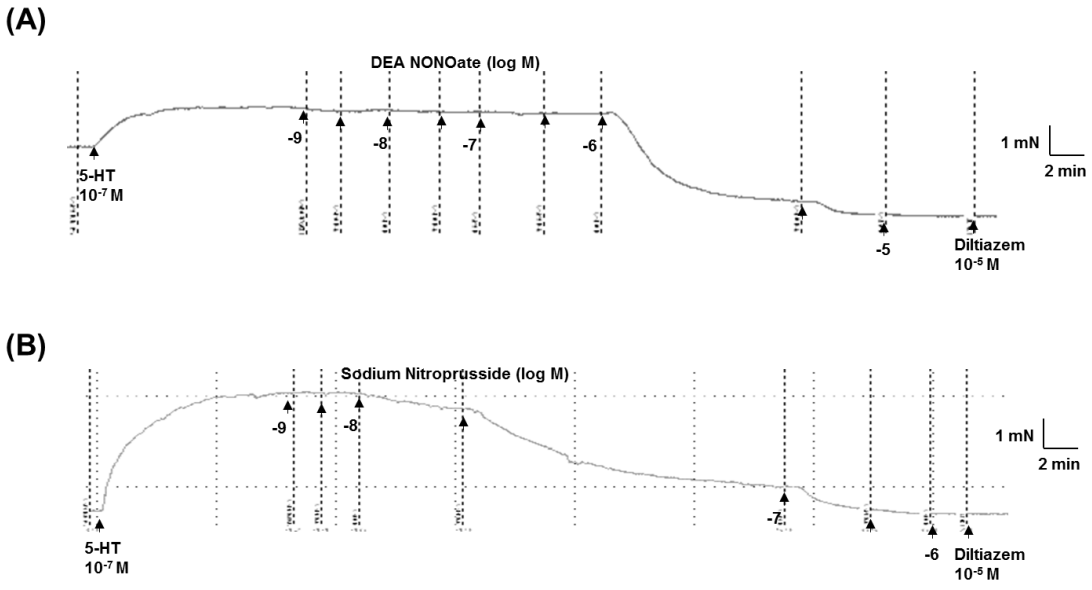

Fig. A3. Representative tracings for concentration response curves of DEA NONOate and sodium nitroprusside.

Representative original tracings of isometric tension recordings from rat isolated coronary arteries in response to cumulative addition of increasing concentrations of (A) DEA NONOate and (B) sodium nitroprusside followed by diltiazem (10^{-5} M).